FRACTURE TOUGHNESS, FLEXURAL STRENGTH AND FLEXURAL MODULUS OF NEW RESIN-COMPOSITE CAD/CAM BLOCKS

by

Iben Joseph Robert Lucsanszky

D.M.D., Laval University, 2010

A THESIS SUBMITTED IN PARTIAL FULFILLMENT OF

THE REQUIREMENTS FOR THE DEGREE OF

MASTER OF SCIENCE

in

THE FACULTY OF GRADUATE AND POSTDOCTORAL STUDIES

(Craniofacial Science)

THE UNIVERSITY OF BRITISH COLUMBIA

(Vancouver)

February 2019

The following individuals certify that they have read, and recommend to the Faculty of Graduate and Postdoctoral Studies for acceptance, a thesis/dissertation entitled:

Fracture toughness, flexural strength and flexural modulus of new resin-composite CAD/CAM blocks

submitted by Dr. Iben Lucsanszky in partial fulfillment of the requirements for

the degree of Master of Science

in Craniofacial Science

Examining Committee:

Dr. Dorin Ruse, Faculty of Dentistry
Supervisor

Dr. Ricardo Carvalho, Faculty of Dentistry
Supervisory Committee Member

Dr. Tom Troczynski, Faculty of Applied Science
Supervisory Committee Member

Dr. Christopher Wyatt, Faculty of Dentistry
Additional Examiner

Abstract

The commercialization of CAD/CAM resin-composite blocks (RCBs) has rapidly evolved while independent assessment of the mechanical properties has been scarce.

Objective: To determine and compare the fracture toughness (K_{IC}), flexural strength (σ_f) and modulus (E_f) of four commercially available RCBs and one lithium disilicate glass-ceramic CAD/CAM block, tested under dry and aged conditions.

Methods: Three dispersed-fillers (DF) RCBs, Cerasmart (CER), KZR-CAD-HR2 (KZR), and Camouflage Now (CAM), one polymer-infiltrated ceramic network (PICN) RCB, Vita Enamic (VE), along with Obsidian (OBS), a glass-ceramic block, were characterized. Blocks were cut into bars (10:1 span-to-thickness ratio) and 6x6x6x14mm prisms (n=25/group); half of the resin-composite (RC) specimens were aged in 37°C distilled water for 30 d before testing. σ_f and E_f were determined using a three-point bending test, whereas K_{IC} was determined through the notchless triangular prism specimen K_{IC} test. Fractured K_{IC} surfaces were characterized with a scanning electron microscope. Results were analyzed using Weibull statistics and two-way ANOVA, followed by Scheffé multiple means comparisons.

Results: With regards to σ_f, OBS>CER=KZR>CAM>VE and σ_f of RCs was lowered by ageing. VE was found to have the highest E_f among RCs (33.0 GPa), but was significantly lower than OBS (76.5 GPa); E_f was not affected by ageing. With regards to K_{IC}, KZR stood out among RCs with a

dry value of 1.4 MPa·m$^{1/2}$, which was significantly affected by ageing, while K_{IC} of the other DF RCs was not. OBS had the highest K_{IC} at 1.5 MPa·m$^{1/2}$.

Conclusions: Compared to PICN, DF RCBs exhibited significantly higher σ_f and lower E_f values, while for K_{IC}, only KZR was found to be superior. The tested glass-ceramic had higher σ_f, E_f and K_{IC} when compared to RCBs, with the exception of dry tested KZR that did not differ significantly for K_{IC}. Ageing had a deleterious impact on σ_f of all RCBs while its effect was not significant for E_f. With regards to K_{IC}, ageing significantly lowered the mean value for KZR while it increased for PICN. In light of the mechanical testing results, PICN seemed more promising than DF materials but did not surpass blocks made of lithium disilicate.

Lay Summary

The recent development of resin-composite blocks (RCBs) for computer aided design/computer aided manufacturing (CAD/CAM) has resulted in suitable characteristics that facilitated their incorporation in the digital field. Their excellent machinability, edge stability and reduced brittleness contributed to an increase in their usage and in the number of studies aiming to characterize them. However, due to the fact that development and commercialization occur rapidly, some new materials lack independent assessment of clinically relevant mechanical properties. Moreover, the effect of water ageing on their properties has rarely been assessed. Therefore, the aim of this study was to address this gap in knowledge and provide the clinician with a better understanding of the attributes and limitations of selected, commercially available, CAD/CAM RCBs.

Preface

All aspects of this project, including research, sample preparation, material testing, fractography, statistical analysis and dissertation writing, were accomplished exclusively with the collaboration of my supervisor, Dr. N. Dorin Ruse, from the Faculty of Dentistry who provided constant guidance and expertise. The research committee members were Dr. Tom Troczynski from the Department of Materials Engineering and Dr. Ricardo Carvalho from the Faculty of Dentistry. Ethics board approval was not required for this in-vitro study as no human or animal subjects or biohazardous materials were involved.

Table of Contents

List of Tables

List of Figures

List of Equations

List of Abbreviations

B3B – Ball-on-three-balls biaxial bending test

CAD/CAM – Computer aided design/Computer aided manufacturing

CAM – Camouflage

CER – Cerasmart

CNSR – Chevron-notched short rod

DC – Degree of conversion

DF – Dispersed fillers

FDP – Fixed dental prostheses

HP-HT – High-pressure and high temperature

IF – Indentation fracture

IPN – Interpenetrating network

IS – Indentation strength

KZR – KZR-CAD-HR2

NTP – Notchless triangular prism

PE – Pulse echo method

PICN – Polymer infiltrated ceramic network

PPR – Pre-polymerized resin

PS – Physiologic saline solution

RC – Resin-composite

RCB – Resin-composite block

RCT – Randomized controlled trial

SD – Standard deviation

SEM – Scanning electron microscopy

SENB – Single-edge notch beam

SEVNB – Single-edge-V-notched-beam

SCCG – Stress-induced subcritical crack growth

SiC – Silicon carbide

OBS – Obsidian

VE – Vita Enamic

3pb – 3-Point bending

4pb – 4-Point bending

List of Symbols

a– Crack length

α – Significance value

b– Specimen width

d – Displacement

D – Specimen diameter

δ – Difference of variation

E_f – Flexural modulus

E – Elastic modulus

E_m – Elastic modulus of the resin

GPa – Giga Pascal

i – Fracture load

K_{IC} – Fracture toughness according to linear elastic fracture mechanics

K – Stress intensity factor

m – Weibull modulus

MPa – Mega Pascal

N *or* n – Number of samples

L – Span

P – Load

P_f – Probability of failure

t – Specimen thickness

Tg – Glass transition temperature

μ – Mean

V_f – Volume fraction filler

V_m – Volume fraction matrix

W – Specimen length

W_c –Weibull characteristic value

wt – Filler weight

Y – Geometric factor

Y^*_{min} – dimensionless stress intensity coefficient factor minimum

Δ – Standardized difference

σ_f – Flexural strength

σ – Stress

σ_θ – Characteristic strength

σ_{appl} – Global stress in the specimen

Acknowledgements

Privileged are the students who can, even if only once in their academic path, receive the teaching of a professor animated by his passion. It was to my great benefit that I was able to meet Dr. Ruse, a mentor with exceptional qualities throughout the accomplishment of this project. His rigour, his critical spirit and especially his great generosity allowed me to profit from a high level of expertise while being always well supported and guided. His teaching style already encourages me to give back and hereby, I would like to express my deepest gratitude to him.

Besides my supervisor, I offer my most sincere appreciation to my committee members: Dr. Tom Troczynski and Dr. Ricardo Carvalho for their time and efforts in providing me with their constructive feedback.

I am also truly grateful to my sponsoring institution, the Canadian Armed Forces and the members of the Royal Canadian Dental Corps who believed in me and supported me towards the realization of my aspirations.

Finally, I would like to thank Vita Zahnfabrik, GC Corp., Yamakin Co., Ltd. and Glidewell Dental Laboratories for the donation of the tested materials.

Dedication

I would like to dedicate this master's thesis to my dear family, who has always inspired me and guided me to surpassing myself. Regardless of the many pitfalls encountered during this long journey back to school, it is with perseverance, hard work but especially by remaining united that we were able to overcome them. You have never stopped believing in me and have never asked for anything in return for your help. For all this I am eternally grateful to you.

Amelie, my valiant life teammate, I could never satisfy my aspirations without your daily help, your precious support and your limitless love. Know that your tireless positivism and constant sympathy made all the difference in the fulfillment of this quest. You are a model not only for our children but also for me.

To my children, Julia and Édouard, to whom I owe my sincerest apologies for all the hours that this work has stolen from us; never let your imagination and curiosity fade away.

Chapter 1: Introduction

With the expansion of computer aided design/computer aided manufacturing (CAD/CAM) technology in dentistry, the development of new restorative materials has increased significantly over the last years[1]. Subtraction technology has opened the door to different manufacturing processes, allowing for material production in an industrial environment with higher levels of control and reproducibility. Ceramic and resin-composite (RC) CAD/CAM milling blocks are available and can henceforth be machined chairside into good quality, digitally custom designed restorations. Although ceramic CAD/CAM blocks are still more commonly used clinically[2], the interest surrounding resin-composite blocks (RCBs) has recently been augmented due to their suitable characteristics, thus accelerating research (Figure 1) and commercialization[3]. On the one hand, their excellent machinability, edge stability and reduced brittleness palliated some of the disadvantages encountered with ceramic CAD/CAM blocks[4]. On the other hand, indirect restorations made from RCBs were not as negatively affected by polymerization contraction, light-curing variations and handling/manipulation inconveniences as those made from direct light-cured RC[5].

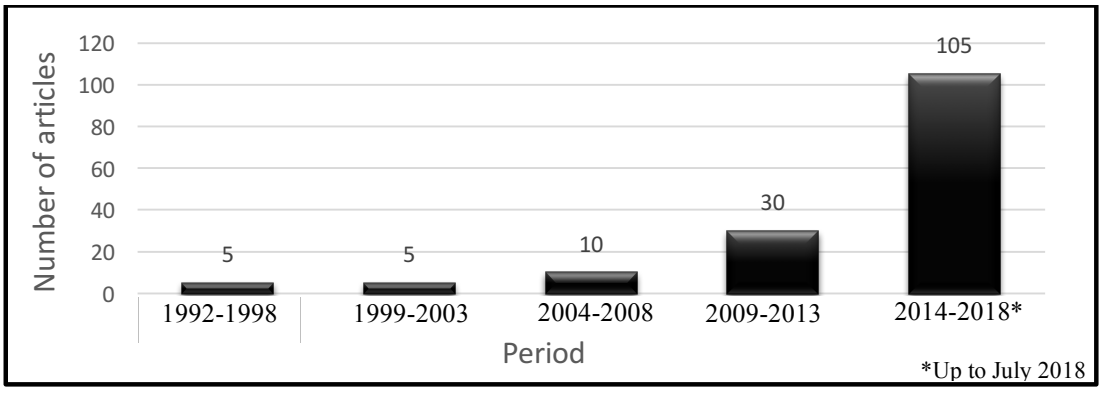

Figure 1: CAD/CAM RCB related articles (1992-2018; Pubmed search: "CAD-CAM AND resin composite*)

Many RCBs recently entered the market without having been clinically tested, yet received a seal from the manufacturer certifying that their product(s) meet clinical standards. Further, in an attempt to convince clinicians, different properties are put forward to promote a new material, where the misconception is that higher values necessarily mean a better material. While some companies may publish their internal data on material testing, many of them selectively or entirely fail to provide the exact material composition to protect against competition. This certainly adds limitations to independent research by restraining result interpretation and comparison.

Another consequence of the fast commercialization of RCBs is that it overpasses newly related publications and therefore independent available data, characterizing key properties identified as potential clinical indicators for success, remain scarce. This presents a major challenge for clinicians who wish to base the selection of new restorative materials on evidence. Clinical implications of in-vitro studies require a thorough analysis and any extrapolation must be carefully weighed. Material properties, although very pertinent, cannot directly predict clinical success and therefore in-vivo studies remain the ultimate validation method[6].

Unfortunately, clinical studies are complex, highly onerous in time and resources, require ethics approval and therefore are rarely realized before the implementation of a new material. The problem is compounded in that it appears their publication rate has considerably declined since 2007, representing less than 10% of the research activity in dentistry[7]. As multiple sources of variability may influence the outcome of a clinical trial, no consensus regarding a precise level of property values or required characteristics of a material exists that could guarantee its performance in challenging clinical situations. Conversely, it would be difficult to argue against some threshold value for a specific property under which a material would undeniably be considered unsatisfactory. In this regard, for light-cured RC materials, ISO 4049 set a minimal flexural

strength [σ_f, determined in 3-point bending (3pb)] of ≥ 80 MPa for an occlusal load bearing restoration and ≥ 50 MPa for other indications[8]. Nevertheless, these minimal requirements may appear too low for certain practitioners, especially for those who treat patients with parafunctional activities and heavy occlusal forces, engendering a certain degree of discomfort with the use of a new material.

Cognizant of this problem, manufacturers subject their new materials to a multitude of tests in order to characterize them (mostly physical properties) and to compare them to products already on the market that have demonstrated a satisfactory level of success. Despite the fact that material innovation is based on sound engineering principles and designs, this is not beyond reproach[6]. A stunning example occurred in 2015 when a dispersed filler (DF) RCB, called Lava-Ultimate (3M ESPE, USA), was found to be associated with a high debonding rate after only 5 years on the market, forcing the company to withdraw its recommendation for its use for crowns[9].

In light of the above, it would seem appropriate to adopt a prudent decision process that considers evidence that associates clinical predictability to certain properties. As suggested by Ferracane (2001), a logical approach would be to identify the most important cause of failure of a material and characterize its related properties with corresponding tests found to have clinical correlation[6].

Few authors have managed to identify debonding, bulk fractures and wear as the three most important negative outcomes in stress bearing restorations made of RCBs[10-12]. Although these prospective clinical studies only offer a short-term perspective, they are in accordance with those using direct light-cured RC, where restoration fracture was found to be the primary cause of failure in the first five years[13]. With long-term clinical evaluation of RCBs not being available yet, presumptions have to be based on studies made on the same class of material and for which fracture

and caries were found to be the most important causative factors for failure[14]. Moreover, the result of a meta-analysis demonstrated that the replacement cause of posterior direct RC restorations due to fracture approximated 5%, while about 12% showed appreciable signs of wear within a 10 year period[15]. Based on these estimations and considering the large number of restorations placed annually (800 million in 2015), 32 million restorations would need to be replaced due to fracture by 2025[16]. Without denying some degree of interpretation, variations and bias, these studies still provide some guidance toward some of the likeliest outcomes of restorations made from RCBs.

Several researchers have demonstrated evidence that clinical wear of restorations made from direct RC correlates with specific mechanical properties, such as σ_f, E_f and K_{IC}[17-19]. With the exception of E_f, this was corroborated in a recent systematic review by Heintze et al. (2017), who assessed the relationship between the laboratory mechanical parameters of RC restorations, wear and fracture in clinical trials. K_{IC} was found to have a moderately positive correlation with clinical fractures, and σ_f with clinical wear[16].

Compared to clinical studies, laboratory studies offer the advantage of a controlled environment that reduces the sources of variation of a tested material, potentially allowing for a more accurate characterization of the inherent properties of a material. As such, the determination of σ_f, E_f and K_{IC} of new RCBs appears justifiable and could be of clinical significance.

1.1 Computer Aided Design/Computer Aided Manufacturing (CAD/CAM)

Since its apparition, computer science and technology has evolved tremendously and, nowadays, it has invaded almost every sphere of our life. Dentistry is no exception; the pioneering work of Duret and Preston in the 1970s, followed by Moermann in the mid-1980s, led to the introduction of the first chairside CAD/CAM system, named Chairside Economical Restorations

of Esthetic Ceramic (CEREC). This system allowed for an intra-oral digital impression of a prepared tooth, the digital design of a restoration, its milling and insertion, all in one appointment. More than three decades later, the popularity surrounding CAD/CAM technologies has resulted in a wider range of marketed systems offering improved characteristics, such as user-friendly interfaces, better rapidity, accuracy and interoperability (opened access), to name only a few[20, 21]. Available materials for CAD/CAM use also increased, thus offering benefits related to industrial fabrication process[5].

Improvement of CAD/CAM systems has evolved around three main aspects: data acquisition, data processing and data manufacturing[1]. Intra and extra-oral acquisition equipment (camera, scanner) are usually optical and do not require contact probe technology, except for some extra-oral systems (coordinate measuring machines). Intra-oral systems operate under different types of imaging principle (triangulation, confocal microscopy, stereo photogrammetry, etc.) capable of producing a 3D virtual representation of a physical object with good quality. Digitization devices are associated with software algorithms for data processing. The CAD software is capable of designing restorations from preset design parameters while also allowing certain freedom for modifications/adjustments[22]. Data manufacturing operates through CAM software or numerical control, dedicated to generate a manufacturing process that automatically includes the configurations and parameters of the corresponding milling machine. This process is then transmitted to a multiaxial (3-5 axes) subtractive tool for the restoration to be fabricated[23, 24].

1.1.1 Chairside Workflow for Restorative Dentistry

The digital workflow in dentistry offers many options for clinicians and laboratory workers who want to incorporate CAM/CAM technologies into their practicum. Three types of production

chains are available: 1) Direct chairside, in which the entire process is digital (intra-oral digitizing, restoration design and milling); 2) Indirect production, in which the digitizing, restoration design and milling is outsourced to a laboratory or a production centre. This process requires conventional impressions and master cast fabrication before the digitalization can occur; 3) Semi direct process, which involves a chairside intra-oral digitalization and an outsourced designing and milling[22]. Figure 2 summarizes the workflow in digital restorative dentistry.

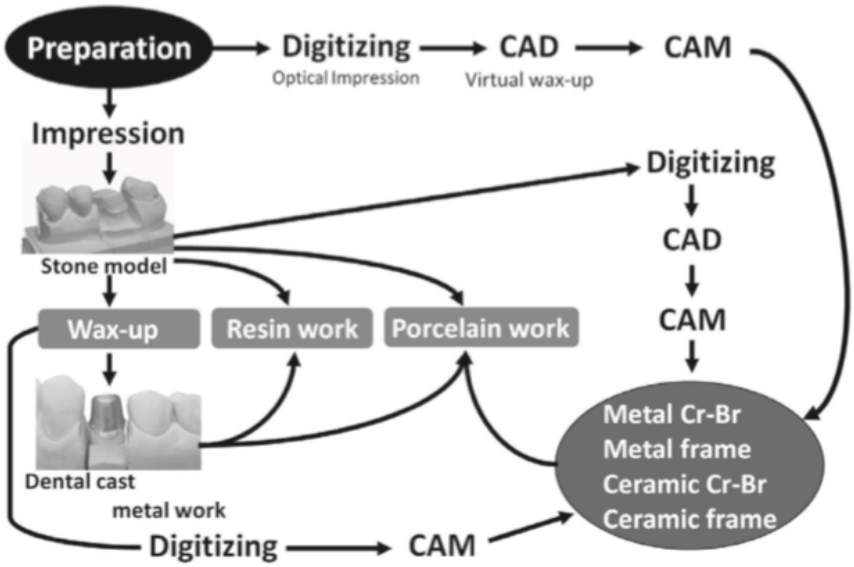

Figure 2: CAD/CAM digital workflow[25]

1.1.2 Clinical Advantages of CAD/CAM Restorative Technologies

Conventional dental restoration fabrication usually requires time, labour-intensive work and many technique-sensitive procedures that need to be accomplished by a highly skilled clinician and laboratory technician. The incorporation of CAD/CAM technologies in the fabrication chain has had the effect of easing some procedures, improving quality, efficiency, communication and, perhaps, lead to cost reduction[26]. Indirect restorations milled from CAD/CAM RCBs are a good example of such improvement as their quality (better homogeneity, reduced internal flaws, higher

degree of conversion - DC) and fabrication time are considered superior to the handmade light-cured RC indirect restorations, which are inevitably affected by air bubble incorporation and suboptimal light polymerization[5]. Therefore, it is not surprising that many dental laboratories have already adopted digital technologies in their production protocols[27].

Intra-oral scanning systems also offer a great deal of advantages. Real time scanning and impression visualization favours on-the-spot corrections of deficient sections. Compared to traditional impressions, this saves time, material and avoids the necessity of retaking a new impression. Digital impressions are generally preferred by the patient and are truly beneficial in cases of severe gag reflex or restricted mouth opening.

Moreover, multiple options such as pre-scan (scanning the entire mouth followed by prepared teeth only), teeth and gingival tissue colour display (using spectrophotometry technology) and tooth preparation analysis options (allowing for direct visualization and correcting the preparation) are available in the most current systems. As the modelling aspect is being conducted in a virtual environment, physical wear and tear of the stone cast is avoided. Archiving is also improved with digital technology as less physical space, depending on the selected workflow, is needed. The chairside aspect offers single visit restorations, to the benefit of the patient who avoids temporization and saves travel and wait time[28].

1.1.3 Clinical Limitations of CAD/CAM Restorative Technologies

Even though the acquisition cost of CAD/CAM systems seems to decrease with time, these systems are still considered expensive, which may cause practitioners to refrain from purchasing them. Moreover, they often have a steep learning curve and can quickly become outdated. Intra-oral scanners should be employed in a dry working environment and follow a strict scanning

strategy. Failing to adhere to these requirements may affect the quality of the impression[28]. Further, these scanners cannot record dynamic occlusion movements or centric relation other than centric occlusion or maximal intercuspation. Digital occlusion record accuracy is highly dependent on the amount of input data, with better results achieved with a scanning strategy and less captures[29, 30]. Doubts have been expressed with regards to the accuracy of full-arch impression, which may limit their use in full mouth rehabilitations[31]. The use of closed systems restrains interoperability between the different elements of the digital workflow. Chairside milling units usually offer 4-axis technology that cannot allow for undercut creation, compared to the more powerful laboratory 5-axis milling machines[28].

1.1.4 CAD/CAM Materials

CAD/CAM materials are either available as blocks for chairside use or as a puck for larger productions in a production centre or a dental laboratory. Only two categories of materials are available for CAD/CAM use: ceramic and RC[32]. As the main focus of this thesis is on the latter category of material, ceramic will only be addressed for comparative purposes.

1.1.4.1 Resin-Composite Dental Material

In 1962, Bowen revolutionized the world of dental polymers when he created a restorative resin-based composite material using Bis-GMA as a durable cross-linked polymer matrix in conjunction with an organic silane coupling agent to chemically link reinforcing filler particles to the matrix[33]. Since then, the desire to solve the negative clinical effects related to their use, thereby improving the properties of this new class of material, has propelled the introduction of many innovations. Among the most notable, the content, type, size and shape of the reinforcing filler

have been extensively developed and adjusted with a trend toward decreasing their size, thus improving surface polishing, wear resistance and many other properties[33]. Matrix formulations have also been developed from the traditional but still successful methacrylate-based molecules to create of completely different molecules with the aim of reducing polymerization shrinkage, lowering viscosity, reducing internal stress and improving biocompatibility[33, 34]. The mode of polymerization and, by extension, the nature of the incorporated initiator molecules has evolved from self-curing to visible light-curing systems that improve colour stability, working time and manipulation[35].

1.1.4.1.1 Composition

A composite consists of a mixture of at least two different substances, insoluble in each other that form a combination exhibiting specific advantageous properties where an individual component taken separately would be unserviceable[36]. In dentistry, RC materials are composed of three different components: the filler, the polymerizable resin and the coupling agent.

1.1.4.1.1.1 Filler Particles

The role of filler particles in RC materials is crucial and varies from enhancing the modulus of elasticity and other mechanical and physical properties, providing radiopacity, thermal expansion and workability control, reducing polymerization contraction by reducing the amount of resin fraction as well as decreasing water sorption[33].

The composition of reinforcing filler particles used in RC materials can be inorganic (ceramics or glass-ceramics or glasses), organic and composite. Inorganic fillers are related to the chemistry of silicon (Si) and are generally composed of ground glass, colloidal silica or pyrogenic

silica, such as borosilicate, fused quartz, aluminum silicate, lithium aluminum silicate, zinc glass, etc. However, quartz has been forsaken due to difficulties encountered in particle size reduction, low polishing and high abrasiveness properties. These materials are advantageous in the sense that they can be bounded to the polymer matrix with a silane coupling agent forming a Si-O-Si bond, thus providing strength to the mixture. Other heavy elements, such as barium (Ba), strontium (Sr), zirconium (Zr) and ytterbium (Y), may also enter as oxides in the composition of glass filler and improve radiopacity, wear resistance and optical properties[37].

Organic fillers refer to aggregated fumed silica nanoscale particles that are embedded in a resin matrix, cured and subsequently pulverized to form so-called pre-polymerized resin (PPR) fillers. This process, which led to the creation of "microfilled" composites, was initially developed to increase the volume fraction filler (V_f) of small size particles limited by the high mixture viscosity, considering the crucial role that the V_f plays in the development of good mechanical and physical properties[33]. In contrast with the microfill RC, also using nano sized or fine particles (0-100 nm), the recent nanofilled or nanohybrid composites use a different pyrolytic process to obtain colloidal silica particles that can be individually coated with a silane agent, thus limiting their agglomeration and their negative impact on the viscosity. This process also allowed improvement in optical properties, polishability and to reach a filler loading superior to 60%. With a trend in decreasing the size of the biggest particles, recent hybrid composites combine both microfine (0.1 to 10 μm) ground glass particles containing heavy metals and fine colloidal silica particles, which results in improved surface smoothness, wear resistance and mechanical properties[33].

Composite fillers refer to the organically-modified-ceramic (ORMOCERS) which combine the organic structure of a polymer to an inorganic oxide at the molecular level[37]. Minor other possible constituents, such as pigments, antioxidants, inhibitors, preservatives and

antimicrobials, can enter in the composition of RC materials. The capacity to increase the filler content highly depends on the viscosity of the mixture, which also increases with smaller size particles due to an augmentation in the total surface area that needs to be "covered" or wet by the resin. As a consequence, a theoretical packing fraction limit exist depending on the particle size distribution. Figure 3 illustrates this relationship, at room temperature, with a maximal V_f of 74% achievable with spherical particles.

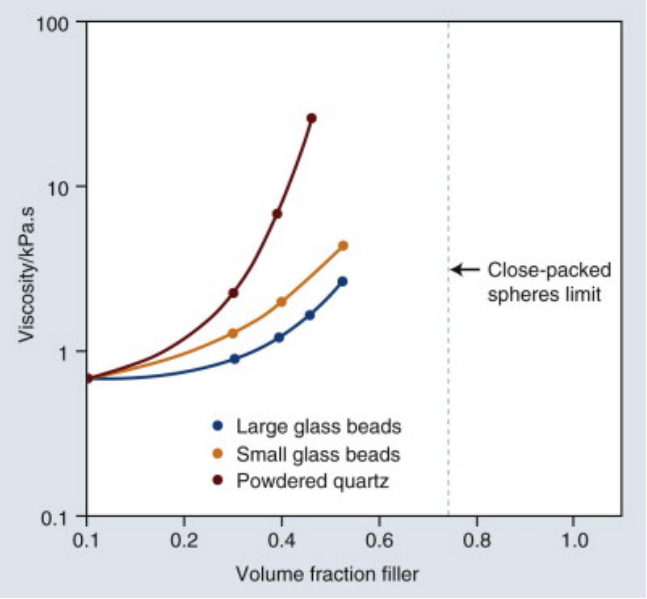

Figure 3: Viscosity (log scale) as a function of the V_f for different filler size[33]

Interestingly, a recent study by Randolph et al. (2016) noted the possibility of RC material to surpass this theoretical limit with V_f values up to 82%. This was achieved mainly by varying the size and shape as well as by using discrete silanized nano sized particles[38]. Generally, the concentration of filler in a composite material ranges between (30-70)% by volume and (50-85)% by weight[33]. However, because of the presence of heavy elements, the weight can vary tremendously and therefore fails to reflect the filler content. Substantial research concerning filler

shape has led to the development a wide range of spherical, fibers or flake shaped particles with different impacts on the material properties and handling characteristics[39, 40].

1.1.4.1.1.1.1 Classification

Randolph et al. (2016) also observed that mechanical and physical properties, particularly the elastic modulus and solvent sorption, better suit the filler content as opposed to the particle size. Therefore, they suggested a classification system for composite type based on the inorganic filler content, dividing the different materials into ultra-low fill, low fill and compact fill containing nano and micrometer scale particles (Figure 4)[38].

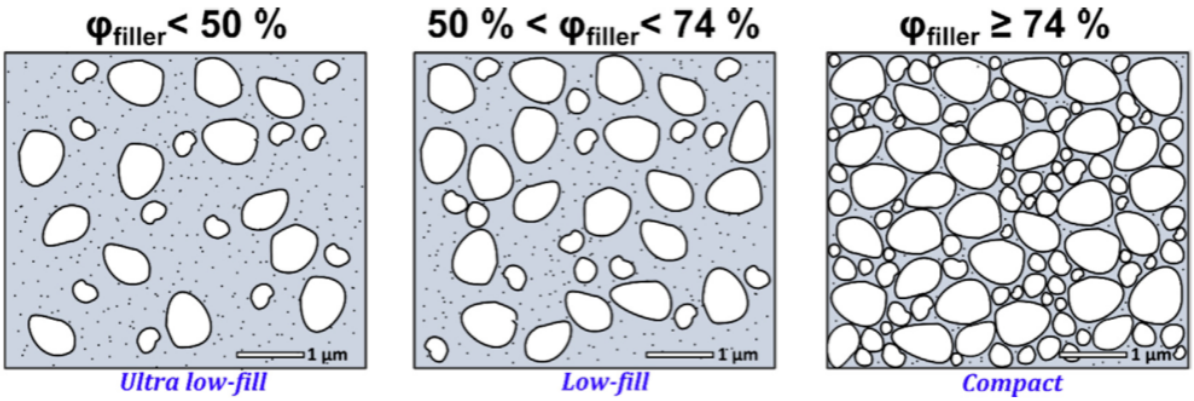

Figure 4: Classification based on inorganic filler content[38]

Although practical in terms of handling characteristics, this classification system appears oversimplified and does not reflect the filler composition or filler specificities such as PPR and morphology. Interestingly, an older classification by Willems et al. (1992) also based on the filler content, also includes the filler size and morphology and PPR fillers. However, this classification was based on the available product at the time and does not reflect improvements that have

occurred since then[41]. Moreover, Ferracane (2011) has provided an intelligible summary of the chronological development of RC filler groups based on their size, including the underlying rationale (Figure 5)[35].

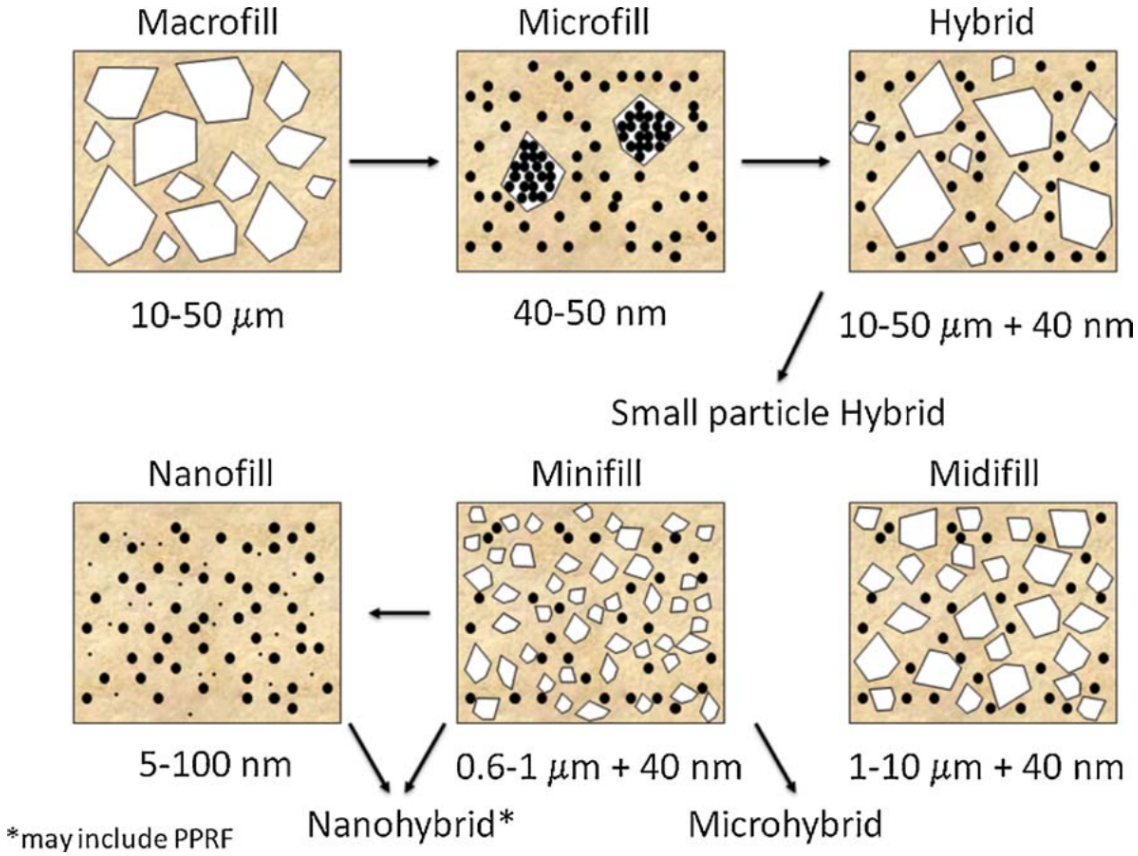

Figure 5: Chronological development of RC groups based on filler size[35]

1.1.4.1.1.2 Resin Phase

The resin phase is composed of liquid monomers capable of free-radical polymerization and form a highly-cross-linked polymer network that acts as a strong and rigid structural skeleton supporting embedded fillers. Although multiple types of monomers exist, the most currently used

are still the conventional ones composed of a blend of aromatic and/or aliphatic dimethacrylate monomers such as 2,2-bis[4-(2-hydroxy-3-methacryloyloxypropoxy)phenyl]propane (Bis-GMA), 1,6-bis, 2,2-bis-(4-(2-methacryloxyethoxy)phenyl)propane (Bis-EMA), urethane dimethacrylate (UDMA) and triethyleneglycol dimethacrylate (TEGDMA)[33, 39]. The chemical structures of these molecules are illustrated in Figure 6.

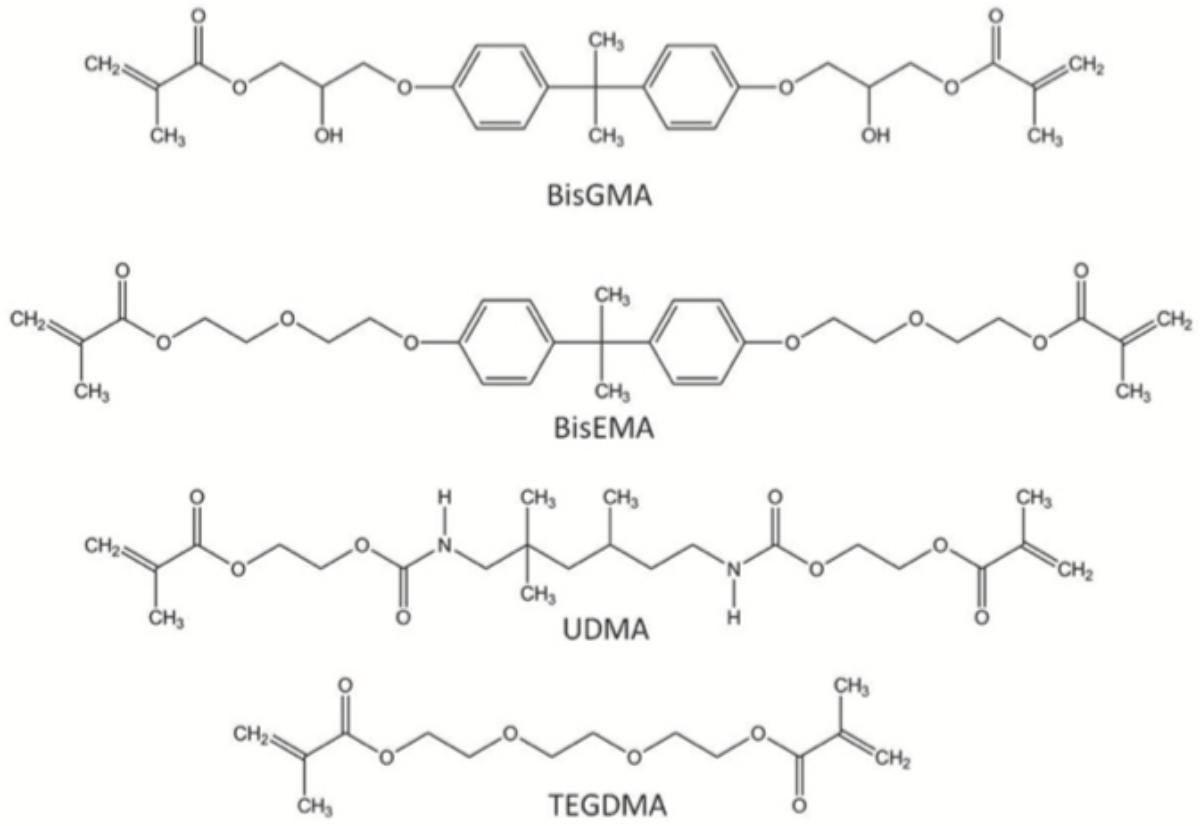

Figure 6: Structural molecule of the most common composite monomers[42]

Restorative materials using base monomer, such as Bis-GMA, Bis-EMA and UDMA, generally achieve good mechanical properties, rapid polymerization and low shrinkage.

Conversely, their use results in a rather low degree of methacrylate conversion which can lead to a higher level of unreacted monomers and associated leaching-related concerns. Moreover, they come in highly viscous solutions which limit particle incorporation. Hence, low-viscosity reactive diluent, such as TEGDMA, is often mixed with the base monomer to enable higher filler content.

As Klapdohr and Moszner (2005) mentioned, the selection of the monomers has a significant influence on the reactivity, viscosity and polymerization contraction of the paste, as well as the mechanical properties and water uptake of cured composites[37]. The desire to improve properties of conventional formulation, notably with regard to shrinkage stress, has led to substantial research surrounding monomers and many new formulations have been proposed[39]. Among the most promising, ring opening monomers, such as siloranes, have shown reduced volumetric shrinkage, better reliability in storage condition and similar mechanical properties compared to methacrylate based monomers[43].

1.1.4.1.1.3 Coupling Agents

Coupling agents are molecules capable of forming covalent attachments to the reinforcing filler and the matrix, thus strongly binding both components together. In other words, they are bifunctional surface-active molecules capable of adhering to the surface of a filler particle and to co-polymerize with the monomers of the resin matrix. Coupling agents are crucial for stress distribution between the high-modulus fillers and the more flexible matrix, thus enhancing the clinical performance of RC. Moreover, they also provide a hydrophobic environment that minimizes water sorption. Although many different coupling agents have been developed over time, the most commonly used are organosilane-based, such as the 3-methacryloxypropyltrimethoxysilane (MPTS). In the presence of water, organosilane molecules

hydrolyze to ultimately form (–Si–O–Si–) bonds with the filler surface. This reaction is illustrated in Figure 7.

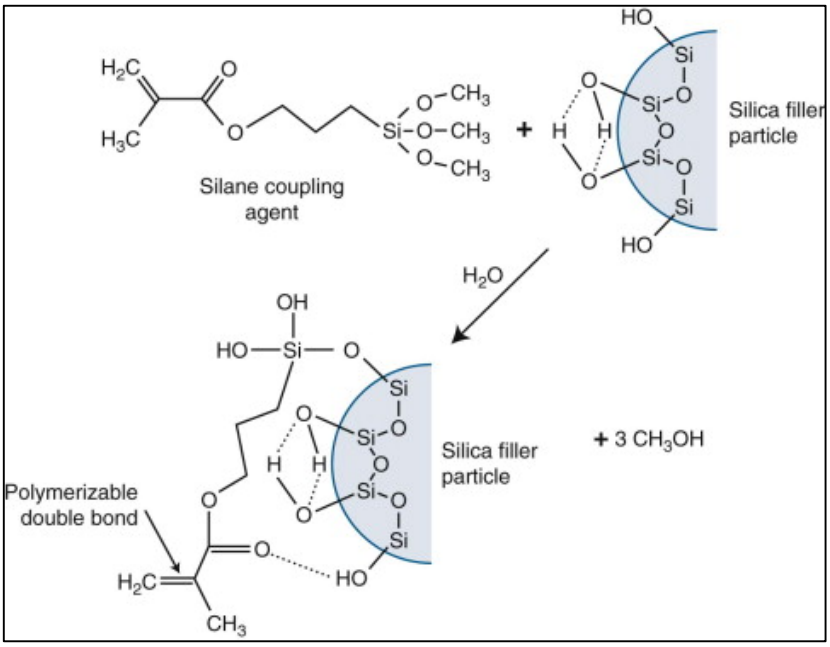

Figure 7: Silanization reaction[33]

1.1.4.1.1.4 Influence of Composition on Mechanical Properties

For a RC restorative material to be able to structurally resist the high posterior occlusal forces over a long period of time, good mechanical properties are required. Several factors related to the three main ingredients in their composition have been found to have different levels of influence. More specifically, factors such as the filler content, size, type and shape, the efficiency of the coupling agent and the nature of the matrix and DC are contributory to the σ_f, E_f and K_{IC} properties of a material[44].

From the macrofill composition of the late 1970s to the recent micro and nano-hybrid RC materials, an evolution has occurred, making fillers an important aspect in the material development. The volume percentage of embedded filler in a matrix, V_f, is considered one of the

most important aspects that impacts the mechanical properties of a composite and many authors concentrated their research trying to find an optimum formulation[45, 46]. In a study by Ilie and Hickel (2009) that measured and compared the σ_f, E_f, diametric tensile and compressive strength of 72 different products (hybrid, nano-hybrid, micro-filled, packable, ormocer-based and flowable composites, compomers and flowable compomers), V_f was found to have the highest influence on the measured properties[8]. Other filler characteristics, such as the dimension of the filler (length, width and thickness) and their orientation, were also important contributing factors[38, 40]. It has been postulated that K_{IC} values may be negatively affected by irregularly shaped particles with sharp angles causing stress concentration and crack precipitation[47]. Moreover, Kim et al. (2002) demonstrated that the filler morphology influenced V_f and the σ_f, E_f and hardness of RC, with round-shaped fillers obtaining a superior result compared to irregularly-shaped ones[48]. Spherical particles seemed to improve packing and mechanical stress distribution compared to irregular particles. In fact, an exponential relationship has been established between the V_f of spherical particles and the modulus of elasticity of a RC material, where significance was attained beyond 60% (Figure 8)[41].

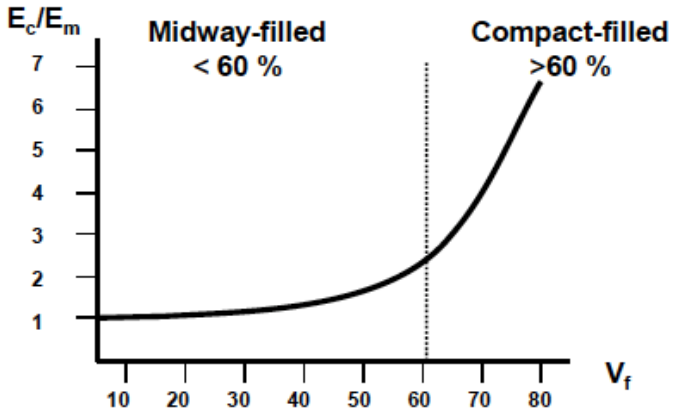

Figure 8: Elastic modulus as a function of volume fraction filler[41]

Furthermore, the existence of such a correlation allowed the calculation of the modulus of elasticity of a composite, based on composition and the modulus of the constituents, with the Rule of Mixture's formula, elaborated in 1929 by Reuss and Angew:

$$E_c = \frac{1}{(V_f/E_f) + (V_m/E_m)}$$

Equation 1: Rule of mixture for elastic modulus of RC materials[49]

Where E_c is the elastic modulus of the RC material; E_m the elastic modulus of the resin; E_f the elastic modulus of the filler; V_m the volume fraction of the resin; and V_f the volume fraction filler.

From an elastic modulus standpoint, increasing the V_f past 60% may sound logical as this would result in higher values. However, this effect is not equivalent towards other mechanical properties. As Ilie and Hickel (2009) noted, filler incorporation beyond 60% of the total volume had a deleterious effect on σ_f and K_{IC}[8, 50]. Dense filler incorporation seems to favor high viscosity, improper mixing, and the incorporation of flaws and defects, all of which can act as stress concentrators and facilitate crack initiation[50]. Hence, as many authors observed, K_{IC} increased with the filler content until a critical value at around 57% was reached and subsequently decreased beyond 65%[48, 50].

The modulus of elasticity has also been found to be exponentially and negatively affected by an increasing volume of voids[8]. Since it represents an important structural parameter that characterizes the level of stiffness or rigidity of a material and relates directly to elastic deformation (i.e., non-permanently), low modulus values will be more likely to cause restoration deformation under masticatory stress and lead to premature failure. Hence, a successful restorative material should aim to reach modulus values that correspond to the hard tissue it intends to replace.

Generally, the modulus of elasticity of restorative RC materials ranges from 15 GPa to 25 GPa while it is approximately 18 GPa and 80 GPa for dentin and enamel, respectively[36, 40]. This observation certainly argues in favour of developing a material with higher E_f, closer to enamel and possibly with anisotropic properties. However, stiffer materials are usually more brittle and thus less tough.

Strength can be defined as the stress required to achieve the limiting value of strain that the material can bear. In other words, it is the maximum strain that a material can support before breaking under a recorded stress. Usually, the higher the modulus of the matrix is, the greater the strength will be[36].

The load transferring effect from the matrix to the reinforcing of the filler depends on the capacity of the silane coupling agent to fulfill its role. Failure to provide proper bonding would be equivalent to having voids or no fillers in the polymeric matrix[36]. The quality of salinization and the amount of silane absorbed on the filler surface is expected to affect chemical bonding between the components and therefore, the mechanical properties[51, 52]. An incomplete filler coverage would result in an inadequate bonding to the matrix, a non-uniform filler distribution, an increase in viscosity and thus, lower mechanical properties such as σ_f and E_f [53, 54]. Conversely, an excess of silane would also lead to a decrease in mechanical properties[51]. Moreover, Ferracane et al. (1987) observed that in the presence of an optimal filler/matrix adhesion, cracks seemed to propagate in the matrix and around the particles as opposed to the interface, thus increasing the surface area and required energy. This observation conferred some importance to matrix properties in K_{IC}. However, other toughening mechanisms related to the filler particles, such as crack pinning, crack bowing, crack blunting and crack deflection, may occur as a result of suboptimal interfacial bonds and cause fracture energy increase[50, 55].

The influence of the polymeric matrix on the mechanical properties is somehow considered secondary in comparison to that of the fillers, but still plays a role. Hence, at a given V_f, size and geometry, material properties would be influenced by the chemistry of the resin phase[38, 56]. The nature of the monomer has an influence on the degree of conversion (DC) and polymer flexibility. The DC refers to the percentage of carbon-carbon double bonds that have been converted to single bonds during the polymerization reaction that lead to polymer formation. Generally, light cured materials composed of Bis-GMA resin achieve a DC of 50% to 60%[33]. Obtaining a high DC is important for strength, stiffness and wear resistance properties, to name only a few, although it has not been proven to be significant for K_{IC}[50, 55, 56].The use of TEGDMA in traditional dimethacrylate composites increases molecular mobility and therefore DC, but also reduces the elastic modulus, glass transition temperature (T_g) and increases volume shrinkage and stress[39]. The extent of volumetric contraction depends on the V_f, the monomer size and concentration and the extent of the polymerization reaction. Polymerization shrinkage is an important aspect of RC that can lead to marginal leakage of a RC restoration[35, 37]. As Lovell et al. (2001) observed, the polymerization conditions seemed to have little effect on a material properties other than through the change in the DC. However, a small change in DC can have a pronounced effect on the mechanical properties, especially the modulus of elasticity[57].

The optimization of the above-mentioned characteristics drives the industry to develop better products, but composite formulation should rather be seen as a compromise where obtained benefits are traded against inconveniences. For this reason, multiple formulations exist to offer a wide range of different properties and textures, tailored to specific needs.

1.1.4.1.1.5 Influence of Water-Ageing on Mechanical Properties

As observed by Ferracane in 1998[58] and others, the effect of a solvent, such as water, on RC materials has considerable impact on their mechanical properties. While many studies have identified a reduction in K_{IC}[58, 59], σ_f[60-62], tensile strength[63], elastic modulus[64, 65], wear[66] and hardness[62] in water storage conditions that vary from a few weeks up to two years, some studies have also revealed contradictory results[67, 68]. This phenomenon appears to be complex and may be related to a multitude of influencing factors, including testing methods.

The specific composition of a RC material affects the water sorption and desorption diffusion coefficient. While the size of the particles and their distribution have some effect, the volume fraction of non-absorbent filler is expected to reduce, in direct proportion, the overall absorption of water[36]. The nature of the filler may also have some impact as it was observed that some of the glass of some fillers may undergo hydrolysis due to stress-corrosion, thus weakening the material[69, 70].

One of the most critical degrading factors relates to the bonded interface between the filler and the resin. In fact, the Si-O-Si covalent bonds between the glass-filler and silane-based coupling agent are subject to hydrolysis, i.e. a diffusion rate-dependent process enhanced by stress that leads to the breakdown of the chemical link. In the case of a deficient or degraded bond, water can be held in the interstices, thus increasing the total water absorption and the plasticizing effect. Since salinization results in an improvement of mechanical properties of a RC material by assuring stress transfer between the filler and the matrix, the deterioration of this structure certainly has the opposite effect[71]. Also, it has been hypothesized that a suboptimal coupling may facilitate crack propagation under stress conditions and consequently lower K_{IC} [58].

The nature of the monomer, the composition and the DC also affect the water diffusion coefficient of the resin matrix[72]. When absorbed, water has a plasticizing effect that facilitates matrix chain drawing, thus relieving internal stress and making the matrix more flexible. For some products, this may result in an apparent increase in mechanical properties. However, longer exposure may lead to matrix swelling and cross-linked degradation, resulting in a decrease in mechanical properties[59]. As Asaoka and Hirano (2003) observed, water sorption is also influenced by the temperature, immersion time, surface condition, stress and water volume, while the dissolution of resin components is rather influenced by the water sorption, DC, immersion-time, temperature and stress[72]. Figure 9 shows variations in weight percentage of 2 mm and 3 mm discs immersed in distilled water as a function of immersion time until saturation is reached.

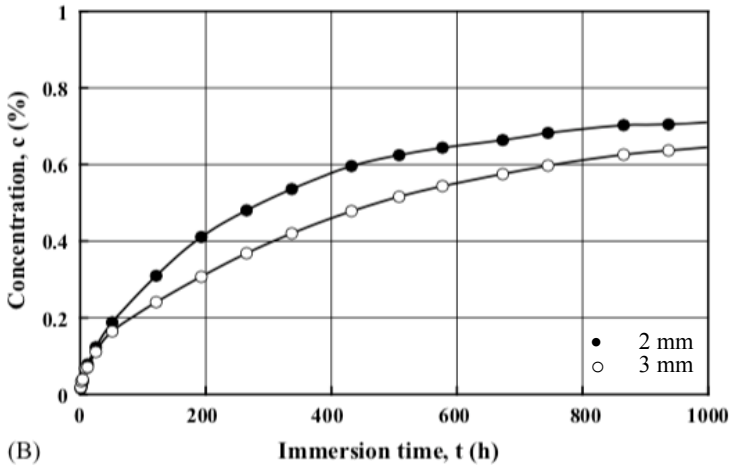

Figure 9: Mass (%) variation as a function of immersion (H_20) time of different RC discs thickness[72]

Mechanical properties of RC materials, especially K_{IC} and σ_f, can be lowered as a consequence of micro crack growth and enucleation when subject to environments causing

degradation and ageing. In this regard, Drummond (2008)[59] provided a summary of the possible causes leading to these changes:

1) Chemical breakdown by hydrolysis;
2) Chemical breakdown by stress induced effects due to material swelling and applied stress;
3) Chemical composition changes by leaching;
4) Precipitation and swelling phenomena causing voids and cracks; and
5) Loss of strength due to corrosion.

1.1.4.1.2 Resin-Composite Blocks

1.1.4.1.2.1 History and Commercialization

The first CAD/CAM RCB to enter the market was the Paradigm MZ100 in 1997[73]. Its composition was similar to the successful direct light-curing RC Z100 but its combined heat, light and pressure polymerization industrial manufacturing process was different and resulted in modest improvement in mechanical properties. At the time, an increase in the general acceptance of CAD/CAM technology, combined with a higher esthetic demand and decrease in the use of metal-containing restorations, motivated 3M ESPE (Maplewood, USA) to develop a RCB for CEREC. Even though ceramic blocks were providing superior mechanical properties, some disadvantages, such as the need for firing procedures, hydrofluoric acid for bonding, high opposing dentition abrasiveness and characteristics brittleness, contributed to the development of RCBs. Indications for this material were limited only to single unit crowns, inlays, onlays or veneers[74].

Nearly a decade later, in 2008, a company called Creamed GmbH & Co. (Marburg, Germany) released its industrial DF "hybrid glass ceramic", called Ambarino High Class[75]. The manufacturer claimed to have developed a complex multi-step manufacturing process that

included a special "hardening" and milling blocks tempering technique combined with a specific selection of raw materials to reach superior mechanical properties. Boldly, they marketed their product as being suitable for three unit fixed dental prostheses (FDP).

Only a few years after that, 3M ESPE (Maplewood, USA) developed its highly marketed Lava Ultimate[9] block, fabricated with a high temperature polymerization manufacturing process that resulted in improved properties compared with Paradigm MZ100. Designated by the manufacturer as "Resin Nano Ceramic", emphasis was put on its combination of nano-sized ceramic particles and resins along with its proprietary manufacturing process that supposedly resulted in a new material that could combine the advantages conferred by its constituents taken separately. Therefore, they promoted their material as being allegedly superior to glass-ceramic and light-cured RC and issued a 10 year warranty. This material benefited from a strong advertising campaign that was potentiated by the emerging trend in dentistry favouring CAD/CAM technology. Soon, interest towards Lava Ultimate was also transposed to research and it resulted in its inclusion in many in-vitro studies where mechanical properties were often compared to other materials[2, 4, 76-78]. However, as mentioned earlier, the company published a statement in 2015 to exclude recommendations for its use as full coverage crowns due to a higher than anticipated debonding rate[9]. Interestingly, this drawback has intensified research regarding bonding properties of RCB materials but has not hindered similar materials from entering the market.

The year 2013 was marked by the commercialization of a very different kind of RCB, a polymer-infiltrated ceramic-network (PICN), named Vita Enamic[79] (Vita Zahnfabrik) in which the manufacturing process used a combination of high temperature and high pressure (HT-HP) polymerization. The concept of having a pre-sintered ceramic substructure infiltrated with a polymer is based on the glass-infiltrated ceramic named In-Ceram by Vita Zahnfabrik (Bad

Säckingen, Germany) and was patented by Giordano in 1997. However, the product never emerged due to residual internal stress caused by polymerization contraction. In 2011, Sadoun resolved the issue by developing a HT-HP manufacturing process[5]. Compared to the available industrial DF RCBs, Vita Enamic contains a higher percentage of ceramic per volume, 80% for Vita Enamic versus ~70% for the Lava Ultimate[4]. It is unique in that it has a E_f similar to that of dentin[80] and its mechanical properties seem less affected by water storage[2, 4].

The same year, 2013, two other RCBs, Polyglass Blank[81] and Crystal Ultra[82], entered the Korean and U.S. markets, respectively. Manufactured by Vericom Co., Ltd. (Gyeonggi-do, South Korea), Polyglass Blank was marketed as a next generation "hybrid ceramic" block suitable for crowns, inlays, onlays and veneers. In reality, it can be classified as an industrial DF containing approximately 80% ceramic fillers by weight, similar to other materials of the same category. Its manufacture was described as using a "high density and high dispersion" process but did not provide any information regarding the mode of polymerization, the matrix composition or the type of ceramic filler.

Crystal Ultra was introduced by Dental Laboratory Milling Supplies and promoted by Digital Dental (Scottsdale, USA). The material's given name is rather confusing as it is mentioned in the premarket notification as being composed of an interpenetrating network of glass-ceramic and polymer, but its marketing names are "hybrid nanoceramic" or "ultra nanoceramic". The filler content was established at 70% (*wt*) of glass-ceramic fillers but not much information with regards to the filler composition, matrix constituents or manufacturing/polymerization process was made available. The manufacturer also marketed its product as being the first and only material that can be used for hybrid implant denture without a bar and provided customers with one case report without follow-up. Its "shock absorption" property was promulgated as a stress reducer on teeth

and implants, although no scientific evidence exists to document whether it is beneficial or not. Crystal Ultra was also marketed as an "advanced hybrid ceramic" by the dental laboratory company Knight Dental Group (Oldsmar, USA) under NanoCera's name[83].

In 2014, according to Shofu Dental, a legal health insurance reform in Japan had the effect of enhancing the expansion of CAD/CAM systems. This certainly contributed to motivate Japanese dental companies to develop their own RCBs and two new products joined the market the same year: KZR-CAD-HR[84] by Yamakin Co., Ltd., (Kochi, Japan) and Cerasmart[85] by GC Corporation (Tokyo, Japan). KZR-CAD-HR is a HT-HP industrial DF RCB composed of a mixture of ceramic clusters, submicron and spherical nano particles embedded in a UDMA and TEGDMA polymer matrix. Also included in the KZR-CAD-HR was the company's previous ceramic cluster filler technology, called TWiNY, the cornerstone of their successful indirect RC material also named TWiNY. The final material was marketed as a "hybrid ceramic" with similar restorative indications as for Paradigm MZ100.

Cerasmart was introduced the same year by GC Corporation. Marketed as a "hybrid nano ceramic", it consisted of an industrial DF RCB polymerized under high temperature. Contrary to KZR-CAD-HR, Cerasmart was approved by Health Canada and is actually available in Canada. Once again, the manufacturer highlighted the allegedly force absorbing and impact dispersion properties of this new material, obtained from a matrix composition and homogenous distribution of the embedded filler. Restorative recommendations were made for anterior and posterior crowns, inlays, onlays and veneers. Similar to other RCBs, blocks were made available in different colours and with different mandrel options for multiple milling systems. Opalescence and fluorescence characteristics were publicized as supposedly close to natural tooth characteristics. A minimally

invasive preparation requirement was also claimed, even if the proposed guidelines were the same as for a complete glass-ceramic crown.

In 2015, Yamakin marketed its second generation RCB, the KZR-CAD-HR2[86]. Improvements were obtained regarding abrasiveness and polishing properties by controlling the homogeneity of the ceramic cluster filler, while previously claimed mechanical properties were maintained. Furthermore, fluoride particles (700 nm) were added to the filler content, aiming at the benefits of fluoride ion release. To our knowledge, it is the only RCB that offers this characteristic. Whether this represents a true benefit, considering that fluoride may leach under ageing conditions causing material degradation, remains unclear.

The same year, Shofu Inc., (Kyoto, Japan) made a partnership with Sirona Dental Systems (Bensheim, Germany) and released the Block HC[87] that was adapted to be milled from the CEREC unit. Again, marketed as a last generation "hybrid ceramic", Block HC was, in reality, an industrial DF containing approximately 61% by weight of a mixture of silica powder, micro fumed silica and zirconium silicate (also present in Shofu's Ceramage direct restorative RC material) embedded in a UDMA and TEGDMA polymer matrix. Interestingly, Block HC was the first RCB to offer a colour gradient, composed of two layers, for improved esthetic results.

In 2016, Brillant Crios[88] from Coltene (Altstätten, Switzerland) entered the market as a reinforced composite bloc for the CAD/CAM grinding process. Its true classification relies on its composition and manufacturing process. As it is composed of 51% by volume and 71% by weight of barium glass, silica particles and pigments (ferrous oxide and titanium oxide) as fillers embedded in a heat polymerized methacrylate matrix, it falls in the industrial DF RCB category. Interestingly, Brillant Crios was the material that recommended the most minimal preparation for veneers, with 0.3 mm at the margin. For the cementation procedure, the manufacturer

recommended their adhesive, containing MDP monomer (10-methacryloyloxydecyl dihydrogen phosphate), instead of using a silane primer.

Luxacam composite,[89] from DMG Chemisch-Pharmazeutische Fabrik GmbH (Hamburg, Germany), was also commercialized in 2016. Although this material is a DF RCB containing 70% silicate glass particles by weight, very little information was made available with regards to its other constituents and manufacturing process.

The year 2017 was even more prolific with regards to new materials. While some companies improved their old materials, others released new ones. Vita Zahnfabrik and Yamakin Co., Ltd. developed a shade gradient version of their previous RCB, the Vita Enamic multicolor[90] and KZR-CAD-HR2 GR[86], respectively. To achieve the gradient, Yamakin Co., Ltd used a "simultaneous injection layering method" of three different colour pastes that are injected in a mold and subsequently polymerized. Vita Enamic multicolour has eight gradient shades but the manufacturing process is not available. Their composition and properties remained unchanged. Polyglass Blank, which was initially commercialized in 2013 in South Korea, entered the USA market in 2017 under a different name: Mazic Duro[91]. Although it looked like a new material, its advertisement was very similar as are its components and properties.

Little information was available regarding the constituents (matrix and fillers) of the newest materials (Table 1), such as the Nacera Hybrid[92] from Doceram Medical Ceramics GmbH (Dortmund, Germany), Camouflage Now[93] from Glidewell Laboratories (Newport Beach, California, USA), Katania Avencia block[94] from Kuraray Noritake Dental (Tokyo, Japan), Grandio Blocks[95] from Voco (Cuxhaven, Germany), Brava Blocks[96] from FGM Produtos Odontológicos (Joinville, Brasil) and Estelite Block[97] from Tokuyama Dental (Kamisu, Japan). However, they can all be classified as industrial DF CAD/CAM RCBs.

Tetric CAD[98] was released in 2017 by Ivoclar Vivadent AG (Schaan, Liechtenstein). This RCB can be classified as a DF containing 51% by volume of barium glass filler, silicon dioxide, pigments and additives, embedded in a polymeric matrix formed by the mixture of four different methacrylate monomers (Bis-GMA, Bis-EMA, TEGDMA, UDMA). Surprisingly, the manufacturer published its associated scientific documentation. However, no real distinctive feature could be observed in comparison with other materials of the same family. It offered the same indications and recommendations with regards to the minimal thickness as other DF RCBs.

Table 1: Worldwide commercially available CAD/CAM RCBs

Item (marketed year)	Filler classi-fication	Manufacturer	Matrix	Filler (*wt*%), [V_f%]	Mechanical properties	
					σ_f (MPa)	E_f (GPa)
Paradigm MZ100 (1997)	DF	3M ESPE	BisGMA TEGDMA	Ultrafine zirconia-silica ceramic particles of spherical shape: 0.6μm (85), [64.2][99]	145	12
Ambarino High Class (2008)	DF	Creamed GmbH & Co.	Bis-GMA UDMA BDDMA	Inorganic silicate glass fillers: 0.8 μm average size and width 0.2-10.0 μm (70), pigments	175	10
Lava Ultimate (2012)	DF	3M ESPE	Bis-GMA, UDMA Bis-EMA, TEGDMA[100]	SiO_2: 20nm, ZrO_2: 4-11nm, aggregated ZrO_2/SiO_2 cluster (80)[2], [~65][101]	204[2]	12.8[2]
Vita Enamic (2013)	PICN	Vita Zhanfabrik	UDMA TEGDMA	Glass-ceramic sintered network (86), [75][5]	150-160	30
Polyglass blank (2013)	DF	Vericom	Bis-GMA TEGDMA	Silica: 10 nm, barium glass: 500 nm, zirconia: 1 μm, (77)[102]	213	10
Crystal Ultra (2013)	DF	Dental Laboratory Milling Supplies	--------	Glass ceramic fillers (70)	175	10
NanoCera (2014)	DF	Crystal Ultra, Knight dental group	--------	Glass ceramic fillers (70)	175	10
Cerasmart (2014)	DF	GC Corp.	Bis-MEPP UDMA, DMA[2]	Silica: 20nm, barium glass: 300nm, (71)[2], [55][101]	231[2]	7.5[2]
KZR-CAD-HR (2014)	DF	Yamakin Co., Ltd	UDMA, TEGDMA	SiO2: 20nm, aggregated SiO_2-Al_2O_3-ZrO_2: 200-600nm, ceramic cluster: 1-6μm, (74)[103]	------	------
KZR-CAD-HR2 (2015)	DF	Yamakin Co., Ltd	UDMA, TEGDMA	SiO_2: 20nm, aggregated SiO_2-Al_2O_3-ZrO_2: 200-600nm, ceramic cluster: 1-20μm, fluoride filler: 700nm, (~74)	235	------
Bloc HC (2015)	DF	Shofu	UDMA TEGDMA	Silica powder, micro fumed silica, zirconium silicate (61)[2]	191[2]	9.5[2]
Brillant Crios (2016)	DF	Coltene	Methacrylate	SiO_2: <20 nm, barium glass: < 1.0 μm, inorganic pigments (ferrous oxide or titanium dioxide), (71), [51]	198	10.3

Item (marketed year)	Filler classi-fication	Manufacturer	Matrix	Filler (*wt*%), [V_f%]	Mechanical properties	
					σ_f (MPa)	E_f (GPa)
LuxaCam Composite (2016)	DF	DMG Chemisch-Pharmazeutische Fabrik GmbH	--------	Silicate glass filler (70)	------	------
Mazic Duro (2017)	DF	Vericom	Bis-GMA TEGDMA	Silica:10 nm, barium glass: 500 nm, zirconia: 1 µm, (77)[102]	213	10
Vita Enamic multicolor (2017)	PICN	Vita Zhanfabrik	UDMA TEGDMA	Glass-ceramic sintered network (86), [75][5]	150-160	30
Nacera Hybrid (2017)	DF	Doceram Medical Ceramics GmbH	--------	----------	175	9.9
KZR-CAD-HR2 GR (2017)	DF	Yamakin Co., Ltd	UDMA TEGDMA	SiO_2 filler: 20nm, aggregated SiO_2-Al_2O_3-ZrO_2: 200-600nm, ceramic cluster 1-20µm, fluoride filler 700nm, (~74)	235	------
Grandio Blocks (2017)	DF	Voco GmbH	--------	(86)	------	~18
Katana Avencia Block (2017)	DF	Kuraray Noritake Dental	UDMA TEGDMA[104]	Aluminum oxide filler: 20nm, silica filler light anhydrous silicic acid: 40nm (62)[104]	265	18
CAMouflage Now (2017)	DF	Glidewell Laboratories	---------	----------	------	------
Tetric CAD (2017)	DF	Ivoclar Vivadent	Bis-GMA, Bis-EMA TEGDMA, UDMA	Barium glass filler: < 1.0 µm (64), silicon dioxide: < 20 nm (7.1), additive and pigments (0.5), [51]	273.8	10.2
Estelite Block (2017)	DF	Tokuyama Dental	UDMA TEGDMA	Silica powder, silica-zirconia filler	------	------
Brava Block (2018)	DF	FGM Produtos Odontológicos	---------	Glass ceramic filler: 40-500 nm (72-82), [55-60]	~159	------

Table is based on manufacturers' data when available and on referenced authors.
PICN: polymer-infiltrated ceramic-network; DF: dispersed fillers; BisGMA: bisphenol A diglycidyl ether dimethacrylate; TEGDMA: tri[ethylene glycol] dimethacrylate; UDMA: urethane dimethacrylate; BDDMA: butanediol dimethacrylate; Bis-EMA: ethoxylatedbisphenol A dimethacrylate; Bis-MEPP: 2,2-Bis(4-methacryloxypolyethoxyphenyl)propane; DMA: dimethacrylate, SiO_2: silica; Al_2O_3: alumina; CaO: calcium oxide; Na_2O: sodium oxide; K2O: potassium oxide; B_2O_3: boron trioxide; ZrO_2: zirconia; $[SiO4]^{4-}$: silicates; *wt*%: filler weight percentage; V_f%: volume fraction filler percentage.

1.1.4.1.2.2 Advantages and Limitations of RCBs

1.1.4.1.2.2.1 Milling Characteristics

Compared to CAD/CAM ceramic blocks, RCBs are easier to mill because they are considerably softer. Hence, more restorative units can be produced with the same set of burs and in a shorter amount of time[4]. They are less costly and do not require any firing procedure after milling. In 2007, Tsitrou et al. established a correlation between the brittleness characteristics of a material and the chipping factor and concluded that a high brittleness index for products, such as ceramics, could result in a higher rate of compromised margination in minimally invasive preparation restorations[105]. Conversely, the edge stability of RCBs was considered superior because they had a brittleness index and chipping factor lower than ceramics. Consequently, they can be safely milled in lower thickness for a minimally invasive preparation as less damage and chipping is expected at the margination[105, 106]. Another advantage over the "classical" light-cured indirect restorations is that they can be produced in one appointment, reducing treatment time.

1.1.4.1.2.2.2 Bonding Properties

RCBs can also be repaired with a direct RC material without needing to use hydrofluoric acid (HF) etching, except for Vita Enamic. When indicated, RC repairs should be encouraged because a total replacement can be traumatic for the pulp and result in unnecessary removal of dental structure; moreover, long-term evidence surrounding the success of this method is available[107]. Composite repair of feldspathic ceramic restorations generally produces inferior esthetic results due to differences in the optical properties and ageing susceptibility of the composite that causes colour to change overtime[4, 108]. The bond strength of RCBs rely predominantly on mechanical interlocking rather than on a chemical bond because the amount of

unreacted monomer at the surface of the material is low as is the amount of exposed glass-ceramic particles available for silanisation[3, 109]. Although this assertion is true for industrial DF RCBs, PICN materials seem to behave differently because they contain a higher V_f of glass-ceramic network, which can be silanated[109]. Surprisingly, a study that compared the microtensile bond strength of different resin cements on CAD/CAM ceramics and RCBs revealed higher results for the RCBs[110]. However, reservations exist regarding the interpretation of such tests; the stress generated during testing as well as the underrepresentation of the bonded surface areas may be important sources of bias[111, 112].

1.1.4.1.2.2.3 Biocompatibility

It is recognized that monomers used in RC materials can induce a multitude of adverse effects on human cells[113]. Sources of free-monomer can be either from incomplete polymerization or from degradation over time and contain low and high molecular weight molecules, photoinitiators and free radicals.[114] However, due to an improved manufacturing process, RCBs are considered more biocompatible than light-cured RC because they release less monomer[5, 115]. Their DC and volume fraction of fillers (especially for PICN materials) being higher, they have a smaller quantity of unreacted monomers and a higher cross-linking density. This contributes to minimizing long-term degradation. Also, because they are not light-cured, they do not release any photoinitiators[114, 116, 117]. Conversely, the recent work of Hussein et al. (2017) has revealed a superior level of cytotoxicity for RCBs compared to conventional RC materials, although no monomer elution was observed with the former. The authors argued that the cytotoxic effect may come from the elution of different constituents such UV stabilizers, photoinitiators or particles that was not detected by the experiment[118].

1.1.4.1.2.2.4 Optical Properties

Along with colour, translucency is an important feature to achieve optimal esthetics. Although the overall optical properties of RCBs are inferior to glass-ceramic materials[4], they still exhibit a good potential in terms of translucency. The inner structure and composition highly influence the refractive index and therefore the light transmission. Some DF RCBs have shown better translucency compared to lithium disilicate, leucite glass-ceramic and PICN materials[119]. However, other studies have contradictory results with other DF materials and different shades[120]. Characterization by staining methods or veneering with direct light-cured RC material can be added, but this may affect the mechanical properties and be lead to higher wear rates[5]. The vast majority of available RCBs are monochromatic with the exception of three products offering a colour gradient, Shofu Block HC, KZR-CAD-HR2 GR, and Vita Enamic multicolour. Whether the gradient blocks carry different properties per layers needs to be determined. Colour stability also being important for esthetics, Stawarczyk et al. (2016) found that regardless of the storage medium, RCBs showed higher discolouration rates compared to lithium disilicate[119]. Moreover, tooth brushing had a superior deleterious impact on surface gloss on PICN compared to glass-ceramic[121].

1.1.4.1.2.2.5 Mechanical Properties

The industrial manufacturing process of RCBs results in better homogeneity, a higher degree of conversion, reduced flaws and internal defects, making them more reliable, with improved mechanical properties compared to traditional light-cured indirect restorations. In addition, RCBs generally have lower σ_f, E_f, hardness and K_{IC} compared to glass-ceramics/ceramic, even if the K_{IC} value of the latter is considered low[4].

A new marketing trend from the manufacturer of CAD/CAM RCBs is to promote the "shock absorption" or "stress distribution" or "biomimetic" properties of their products. Using nature as a role model, they developed relatively low E_f materials that could hypothetically mimic the resilience of the periodontal ligament in an implant-supported case or the masticatory stress distribution of the dentin/enamel complex. Available evidence that supports this concept is scarce and consists of in-vitro and FEA studies[122-125]. Petrini et al. (2013) developed a biomimetic ceramic/polymer composite with anisotropic characteristics, similar to natural dentin. The authors argued that anisotropy is an important feature of light transmission and mechanical properties and, therefore, that a material could benefit from having E_f similar to dentin rather than the actual ceramic which is much stiffer, harder, more brittle and abrasive[126]. According to Coldea et al. (2013), PICN materials may allow for a more uniform stress distribution of the occlusal forces because they have E_f close to dentin and RC luting cement[125]. This assertion was mainly based on the work of Ichim et al. (2007)[127] and Ausiello et al. (2004)[128]. Also, it is worth mentioning that PICN materials have a higher E_f compared to DF RCBs, which, themselves, are generally lower than dentin but higher than direct RC[125, 127]. This may add to the uncertainty around the benefit of achieving relatively low E_f materials, especially considering that all commercially available CAD/CAM RCBs are DF except one. Moreover, this concept appears somewhat questionable because it fails to replicate the combinative properties of different structures (dentin and enamel) by dissociating them and replicating the properties of only one of them. Interestingly, Lawson et al. (2016) attributed the Lava Ultimate high debonding rate to hoop stresses and microseparation at the crown/tooth interface, caused by elastic flexure of the crown under occlusal loading[76]. The fact that this phenomenon has not been reported for PICN materials is noteworthy. Nevertheless, further research is required to determine the impact of material flexure on bonding properties.

1.1.4.1.2.2.6 Restorative Indications

Manufacturers claim that RCBs are suitable for permanent crowns, implant-supported crowns, inlays and onlays. Although a few prospective clinical trials revealed adequate results for inlays and onlays, the other indications have not been studied yet. Moreover, few RCB manufacturers have claimed suitability of their materials for long-term multi-unit fixed dental prostheses. However, since no in-vitro or clinical studies published on this topic could be found, a careful analysis of this particular application is recommended. In 2007, Studart et al. published two very interesting studies that analyzed cyclic fatigue in water of multi-unit FDPs made of different materials and connector diameters. They suggested that high mechanical strength materials like zirconia are more suitable for a multi-unit FDP for long-term applications. The indication for lithium disilicate was a three unit FDP with proper connector size[129, 130]. From a mechanical standpoint, even if RCBs exhibit lower E_f and therefore are less brittle, they are inferior to zirconia and lithium disilicate in terms of σ_f and K_{IC}. Hence, their suitability for permanent multi-unit FDP is questionable.

1.1.4.1.2.3 Classification

RCBs are often classified by their manufacturers with a misleading designation that does not reflect their material properties. Indeed, “hybrid ceramic”, “nano-hybrid”, “ultra nano-ceramic” and “resin nano-ceramic” are but a few examples of marketing-oriented names that may suggest a material that can offer the best of ceramic and composite properties. In reality, even if RCBs were significantly improved by their manufacturing process, polymerization mode, matrix and filler constituents and microstructure, they remain RC materials[5].

1.1.4.1.2.3.1 Manufacturing Process

As a starting point for classifying indirect RC materials, the manufacturing process can either be qualified as traditional or industrial. Traditional refers to a direct RC material that is adapted and polymerized extra-orally by hand to obtain a restoration which would further be bonded to a tooth. Although this technique is costlier and requires multiple appointments, it has the advantage of significantly reducing the polymerization contraction compared to a direct RC restoration in terms of volumetric change[131,132]. This can significantly reduce stress at the tooth-restoration interface, micro-leakage and interfacial gaps associated with premature failure[132, 133]. Moreover, indirect RC restorations are polymerized in laboratory environments which allow the use of different post-cure techniques such as light, heat or pressure, which contribute to relaxing internal stress and increasing DC, leading to improved mechanical properties[133] and biocompatibility as the amount of unreacted monomers is reduced[114]. Traditional indirect restorations are also subject to manipulation errors that can also have a deleterious effect. The incremental insertion can lead to voids and internal defects as well as non-ideal light-curing parameters associated with the type and age of the source, usage (distance, cleanliness, angulation), irradiation time, material composition, shade and age, thickness and optical properties[36, 134]. As a consequence, a reduced degree of conversion and/or inhomogeneous polymerization can lead to internal stress and reduced overall material properties[5].

CAD/CAM expansion in dentistry has favoured the manufacturer to develop industrially processed materials for indirect restorations ready for insertion after milling. Classified as industrial CAD/CAM RCBs, their manufacturing process offers the benefit of better controlling the homogeneity of the material and the polymerization process, which results in a material

containing fewer flaws and internal defects[119]. Some companies add an additional quality control for the internal homogeneity of their materials through x-ray radiation (Yamakin Co., Ltd). Another aspect that contributes to their high-performance is that the manufacturing process allows for a superior filler content compared to direct composite materials, since manipulation becomes less of a concern and thus a higher viscosity can be managed before polymerization[5].

1.1.4.1.2.3.2 Microstructure

The microstructure of industrial RCBs can be categorized as being either DF or PICN. The DF consist of a mixture of different types and sizes of silanated fillers embedded in a methacrylate-based matrix similar to that of direct composite materials. PICN materials consist of a glass-ceramic network, usually pre-sintered, that has been silanated by capillary action and then infiltrated with a resin matrix[5]. In fact, the vast majority of commercialized industrial CAD/CAM RCBs are DF except one, Vita Enamic, which is a PICN.

1.1.4.1.2.3.3 Polymerization Mode

The polymerization of DF materials occurs predominantly under a heat process except for the first available RCB, Paradigm MZ100, which was light-cured. The influence of matrix composition and filler constituents, size, volume content and its coupling with the matrix is also linked to the polymerization parameters (light, heat, pressure, curing time, etc.). Finding the right parameters that give optimal results is very challenging. Urethane dimethacrylate (UDMA) and tri-ethylene glycol dimethacrylate (TEGDMA) are often found to be the matrix foundation of new RCBs and two main reasons can explain this observation. Manufacturers try to avoid Bis-GMA because of its association with an estrogenic effect due to BPA release following the long-term

degradation of the composite[135] and because of the different properties obtained from these molecules as a matrix. UDMA is less viscous than Bis-GMA, has a relatively high molecular weight and produces a larger number of covalent bonds when polymerized. Moreover, urethane-based materials were found to have superior mechanical and physical properties[99]. TEGDMA co-monomer is commonly used as a diluent because of its lower molecular weight and lower viscosity that helps in filler incorporation and allows a higher DC[136].

The combination of HP-HT as a polymerization vector is capital in the fabrication of PICN materials. Prior to achieving the first PICN, multiple attempts to use a heat-curing process demonstrated internal stress and were clinically unserviceable[5]. Polymerization occurs very differently under combined HT and HP compared to only HT. On the one hand, HP contributes to slowing the molecular movement, decreasing the intermolecular distance and free volume and slowing the curing process[137]. On the other hand, HT restores the molecular mobility, necessary for the cross-linking reaction to occur[138]. Much research has shown that this combined process resulted in an improved matrix density and a decreased number of defects and with smaller sizes. The degree of cross linking was found to be higher and less unreacted monomer was present, resulting in better mechanical properties and biocompatibility[99, 137-139]. Some authors have emitted the hypothesis that HP reduces the polymerization contraction because molecules get closer together during chemical bond formation, which may result in internal stress reduction[138].

1.1.4.1.2.3.4 Fillers

The addition of filler particles to a resin matrix is well known to reinforce the properties of a RC material, but it also affects the viscosity and handling properties that are of critical importance for direct applications. However, this aspect becomes less essential with RCB materials due to the

milling process and therefore, a higher initial viscosity can be achieved up to a certain point where filler addition causes the incorporation of defects. DF RCBs contain a wide range of particles of different size, shape (discrete, cluster, network, etc.), composition and content per volume that strongly influence the material's mechanical, physical, biological and chemical properties. Although DF RCBs could be classified by filler size similar to direct light-cured RC (Figure 5, p.13), this information is often not available (Table 1, p.30-31), which limits the elaboration of such classification without further laboratory investigation. The structural network filler that composes PICN RCB is truly innovative and therefore, such material cannot be classified according to the filler size. However, according to Randolph et al. (2016)'s classification (Figure 4, p.12), PICN materials could fall in the "compact" filled category while DFs should be considered as "low" filled.

1.1.4.1.2.4 Clinical Implications

A summary of the available prospective clinical studies performed with CAD/CAM RCBs is provided in Table 2. The first conclusion that can be drawn from this literature search is that the number of clinical studies is very scarce. Three clinical reports presented interesting indications for the use of RCBs in full mouth comprehensive treatment of severely worn and eroded dentition[140], generalized amelogenesis imperfecta[141] or for restoration of primary teeth[142]. Although low in terms of evidence weight, these studies may provide the clinician with additional tools/minimally invasive restoration techniques or even trigger further clinical research.

In addition, four short term (1-3 years) prospective clinical trials were found. To our knowledge, Fasbinder et al. (2005) are the first authors who published a clinical trial that included millable RCBs. Indeed, they fabricated, inserted and assessed 40 CAD/CAM RC (Paradigm

MZ100, 3M ESPE) and 40 CAD/CAM porcelain (Vita Mark II, Vita Zahnfabrik) inlays in 43 patients over a 3-year period. Both materials performed similarly, although, surprisingly, RC inlays showed a significantly better colour match[143]. The authors used a U.S. Public Health Service (USPHS) index to clinically assess the restorations. Another study by Vanoorbeek et al. (2010) comparing 200 CAD/CAM RC (n = 59) and ceramic (n = 141) full coverage layered restorations luted intraorally in 130 patients showed survival and success rates of 87.9% and 55.6% for RC and 97.2% and 81.2% for all-ceramic crowns. At 3 years, the main cause of failure was restoration loosening and poor wear resistance. Early in-vivo complications related to RC crowns incited the authors to modify their study protocol to only perform ceramic crowns. Unfortunately, the material's names were not published, which limits the result analysis[12]. The study realized by Schepke et al. (2016) consisted of a case series within a RCT where 50 single implant-supported crowns made of an industrial DF material (Lava-Ultimate) were bonded on two different designs of zirconia abutments, inserted intra-orally in 50 patients and followed for 12 months. Surprisingly, the uncompromised survival rate of RC crowns was as low as 14% and the major failure was debonding (80%) and catastrophic failure (6%)[11]. Through a conventional/digital protocol, Zimmermann et al. (2017) milled 42 industrial DF RC (Lava-Ultimate) partial crowns (29 molars and 13 premolars) that were beforehand silica-coated with the Cojet system (3M ESPE, USA), silanated and adhesively bonded intraorally with a RC cement (Variolink II). The clinical evaluation followed the FDI World Dental Federation guidelines and recalls were made at baseline, 12 and 24 months. The success rate at 12 months was 95% and 85.7% at 24 months and the main causes of failure were debonding and fracture. Further, the surface gloss was significantly reduced at 24 months.

Table 2: Summary of clinical studies implicating RCBs

Author	Study design	Sample size	Intervention	Outcome
Fasbinder et al. (2005)[143]	Prospective clinical 3-years trial	43 patients	80 inlays, 40 RC and 37 porcelain were cemented intra-orally with an adhesive resin cement. With a follow-up period of 3 years, two examiners reassessed the restorations according to the US. Public Health Service index.	No significant difference was noted regarding the performance of resin-based and ceramic inlays.
Schepke et al. (2016)[11]	Case series within a RCT	50 patients	50 Lava Ultimate implant-supported crowns were digitally fabricated and bonded either on a customized or stock zirconia abutment. The study had a 12 months' follow-up period.	The uncompromised survival rate of RC crowns was 14% at 1 year. The major cause of failure was debonding (80%) and catastrophic failure (6%).
Vanoorbeek et al. (2010)[12]	Prospective clinical 3-years trial	130 patients	200 RC (59) and ceramic (141) full coverage restorations were fabricated and luted intraorally. A veneered material, leucite or direct RC was added on the respective milled coping. The names of the tested materials were not mentioned.	Inferior number of RC crowns were fabricated due to early complications. At 3 years, survival and success rates of RC were 87.9% and 55.6% while 97.2% and 81.2% for all-ceramic crowns respectively. Main causes of failure for RC were restorations loosening and poor wear resistance.
Zimmermann et al. (2017)[10]	Prospective clinical 2-year trial	32 patients	42 Lava-Ultimate partial crowns (29 molars and 13 premolars) were bonded intraorally.	Success rate at 12 months was 95% and 85.7% at 24 months. Main failure causes were debonding and fracture.

None of the above-mentioned studies had a similar design, which makes any comparison difficult. Drawing any conclusions is even more challenging because of the presence of multiple sources of bias, mainly related to the operator, design, materials, site and patient[144]. More precisely, differences in fabrication techniques (digital technology, milling system, etc.), tooth preparation geometry, thickness of the material, material selection (PICN vs DF RCBs), type and pool of restoration (ex: inlays vs crowns), type of abutment (tooth structure or implant abutments), bonding protocol, type of cement, demography (heterogeneity, genetic, etc.), intra-oral conditions (hygiene IQ, occlusion, pH, thermal variations, etc.), clinical assessment and guidelines may explain the variation in the results. Moreover, experimental designs, which can be classified as longitudinal or cross-sectional, short-term (1-5 years) or long-term (5-20 years) and university-based or practice-based research networks may influence the clinical performance assessment and resultant validity. Although more valuable, large scale, longitudinal and long-term studies are generally difficult to perform and therefore rarer. Consequently, it is thought that many smaller prospective studies that balance funding, statistical design needs and patient availability with a careful risk-analysis determination and that aim for larger pools of patients and longer periods of evaluation may help determine the baseline clinical outcome of a material[7, 144].

Nevertheless, it was interesting to see that two separate studies that included Lava-Ultimate reported a higher than expected debonding rate, which concurs with the manufacturer's decision to retract crowns as an indication for use[9]. Perhaps this explains the recent increase in the number of in-vitro studies related to bonding strength of RCBs. In this regard, it is important to reiterate that the in-vitro often seen goal to achieve a 20 MPa bond strength has never been validated in-vivo[7]. Moreover, many manufactured RCBs (Table 1, p.30) have not been properly assessed clinically, which adds to the colossal and endless mandate for research.

From another perspective, it would seem appropriate to look at the outcome of previous clinical studies that compared traditional direct versus indirect RC or ceramic restorations. Having improved properties over the former, one could expect RCBs to have at least similar or improved performance. In a systematic review examining the longevity of direct and indirect traditional RC restorations in permanent posterior teeth, da Veiga et al. (2016) could not find any significant difference, regardless of the materials, technique or type of restoration (inlays and onlays)[133]. This is interesting considering the polymerization contraction issues and inferior degree of conversion, subgingival behaviour and mechanical properties associated with direct restorations using RC materials[5, 6, 35]. Perhaps some explanation lies in the preparation parameters that are usually more conservative, as obtaining divergent walls is not necessary[145]. Conversely, direct composite restorations with a higher number of surfaces were associated with a higher failure rate, the main reasons being caries and fractures[13, 146]. Many factors (improvement in bonding, material and technique) can explain why RC has become the material of choice for posterior class I and II direct restorations, promoting a minimal intervention shift in dentistry[145]. However, the literature is less conclusive with regards to the restoration of a large size cavities and the material of choice, although a slight tendency towards ceramics was observed[147-149]. Often, feldspathic ceramic restorations were compared with traditional indirect RC restorations which, unfortunately, do not reflect current applications. Indeed, different outcomes would be expected for recent higher-performance glass-ceramic/ceramic and RC, such as lithium disilicate and CAD/CAM RCBs, which offer improved properties. In a systematic review and meta-analysis that included 5811 restorations, Morimoto et al. (2016) observed a superior survival rate for glass-ceramic restorations (95%) compared to feldspathic (92%) at 5 years. The main cause of failure was fractures/chipping at 4%[147]. Nevertheless, when comparisons are made, one should consider equalizing as much as

possible the influencing factors to reduce the amount of variation and bias. The history of success and significantly larger number of studies available on glass-ceramic/ceramic materials should also have an impact on any clinical decision-making.

Another aspect that was apparent in the case reports was that RCBs, especially PICN, seemed to be the material of choice for preparation-free/minimally invasive rehabilitation cases among patients affected by gastroesophageal reflux disease (GERD), bulimia nervosa, amelogenesis imperfecta, bruxism and dental erosion[141, 150, 151]. Indeed, reduced risks of pulp irritation can truly be beneficial but often come at the price of a very sensitive technique[152]. However, there is a lack of data analyzing the behaviour of ultra-thin ceramic and RC overlays or occlusal veneers[153]. Even though Schlichting et al. (2011) observed a superior fracture resistance for ultra-thin non-retentive posterior occlusal veneers made of RCBs compared to lithium disilicate under high loads, their in-vitro study could not truly reflect the genuine intra-oral condition. Therefore, whether these materials can live up to expectations remains uncertain. Nevertheless, the concept of minimally invasive preparation using ceramic restorations is not a new one and has already proven to be advantageous[154, 155]. Further studies are required to see if the same concepts can be transposed to RCBs.

1.2 Biomaterial Characterization

As part of a development cycle, every material should be extensively tested prior to being used intraorally[36]. However, despite the wide range of available laboratory tests/procedures to characterize many properties (mechanical, physical, chemical and biological), many of them lack validation, are technically very sensitive and prone to errors or do not correlate with clinical realities. Selecting meaningful properties and proceeding with adequate testing is not an easy task

and investigators must attempt to integrate useful/applicable engineering design models with clinical evidence[156].

Fractures and wear have been clinically identified by many authors as important causes of failure of RC restorative materials[16]. Therefore, the characterization of corresponding mechanical properties is a sound starting point for comprehending these clinical issues. Fortunately, the Academy of Dental Materials has recently reviewed and critically appraised methods to determine fractures, deformation and wear resistance in order to provide guidelines to researchers. More specifically, each testing method has been subcategorized according to its related property, where both property and methods were ranked in priority of measurement relevance. The ranking was based on convenience, applicability and supportive evidence. Strength, elastic modulus, K_{IC}, fatigue, indentation hardness, wear abrasion (three-body) and attrition (contact/two-body) were considered the most meaningful mechanical properties to characterize[157]. These recommendations were also in accordance with those stated earlier by Ferracane[6]. However, as part of this project, only the first three will be further elaborated. With respect to the testing methods, 3pb and tensile were ranked first out of four and 4-point bending (4pb), biaxial flexural, impact, transverse impact and shear punch were ranked second for strength characterization. Recommended tests for elastic modulus determination were 4pb and tensile (ranked first out of four) and subsequently 3pb (ranked second). Finally, the single-edge notch beam (SENB) test was ranked first out of three for K_{IC} while double torsion, chevron-notch short rod (CNSR) and compact tension ranked second[157].

Dental material testing often requires specific instrumentation and/or custom fabricated apparatus (jigs, holders, etc.) to accommodate for the relatively small quantities of available material. This is especially true with regards to CAD/CAM RCB materials, which usually come in fully cured and ready-to-use (18 x 12 x 14) mm size blocks. This makes cutting necessary for

sample fabrication and dimensions are limited by the dimensions of the block. Moreover, it requires test miniaturization, such as span and sample size reductions seen in the 3pb σ_f test. Unfortunately, this miniaturization cannot be made for every test and even though feasible for 3pb, it poses the risk of amplifying some intrinsic problems related to the test, such as positioning errors, friction and wedging effect, to name only a few. Investigators should be aware of these limitations and precautions should be taken to minimize their effects on test validity[158]. The notchless triangular prism (NTP) test for K_{IC} represents a useful application for small size samples.

1.2.1 Strength

Strength is a useful mechanical property for a restorative material because it helps anticipate whether a prosthesis will fulfill its intended function over an extended period of time. The strength of a material can be defined as the necessary stress capable of causing either a specified amount of plastic deformation (yield strength) or fracture (ultimate strength) once the elastic stress limit (proportional limit) has been surpassed. With brittle materials, such as RC, the amount of plastic deformation is expected to be minimal and the material will fracture rather than deform plastically under stress. Strength is not an inherent property of a material, so values will vary according to a sample's geometry, size, composition, the employed tests and stressing rate. As Wendler et al. (2016)[158] stated: "strength data is a window into the nature of the microstructure, residual stresses and defect size, type and distribution in the material." The deleterious role of these internal or surface flaws will lead to stress concentration, crack formation and tensile rupture under stress, thus altering the strength results. Flaw size distribution can be statistically calculated (with Weibull statistics) and a larger stressed surface or tested volume is likely to contain critical size flaws that can cause crack precipitation. RC are weaker in tension than in compression,

making tensile or σ_f meaningful properties. Tensile properties are influenced by multiple testing parameters such as speed, specimen preparation and fixture grip, making tensile tests difficult to control and standardize. This has led investigators toward simpler tests such as the 3pb and 4pb test[157].

1.2.1.1 3-Point Bending Test

The 3pb test is used to determine σ_f of a material by recording the stress-to-fracture of a bar specimen placed on two rollers separated by a defined span and subsequently centrally loaded with a single roller, at a determined cross-head speed. While a specimen is being bent, the upper portion of the specimen is being compressed, the middle portion undergoes shear forces and the lower portion is put under tension where a crack will initiate and propagate causing fracture (Figure 10).

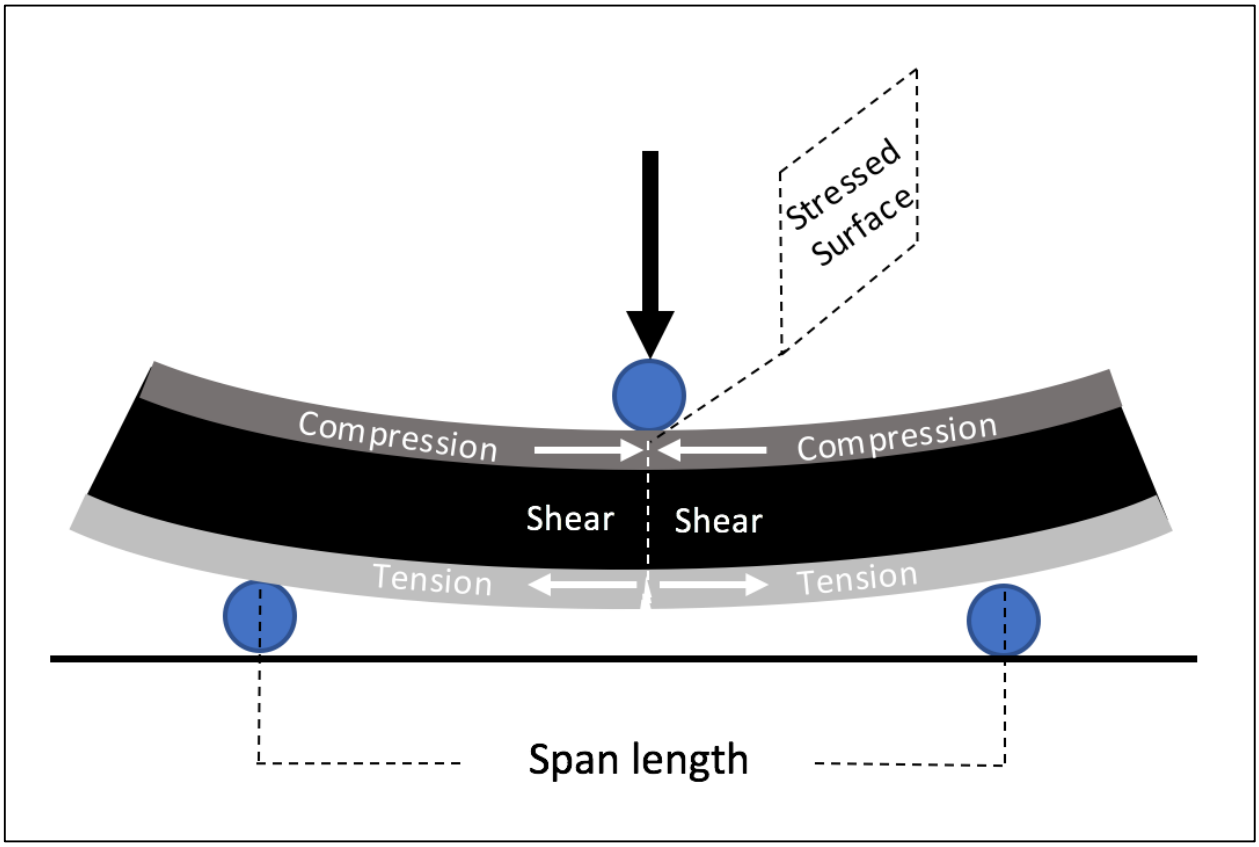

Figure 10: 3-Point bending test

The 3pb test is advantageous in that it tends to reproduce the loading condition that is expected to occur in the oral cavity. Indeed, both the anatomy and neuromuscular system govern the mechanics of the masticatory apparatus and, ultimately, the way forces are transmitted to the tooth structure and/or the restorative material. As a result, simple axial loading is rarely encountered and rather a combination of compressive, shear and tensile forces occurs[157]. According to the ISO 6872, 3pb is a low-cost test that allows standardization and small sample size testing with a span as short as 12 mm. Moreover, it allows for calculation of E_f by using a tangent to the slope of the load-deflection curve. σ_f has been moderately correlated with the clinical wear of posterior RC restorations but not with bulk fracture[16].

Some limitations of the σ_f test are related to its sensitivity to edge integrity and surface defects that are created during sample preparation, as well as to the ability to execute a perfect alignment. The 4pb test is even more sensitive to flaws because it stresses a volume as opposed to a slice, like in 3pb test (where the slice is directly under the central loading roller). Therefore, the 4pb test usually gives lower strength values compared to the 3pb test. However, the 3pb test poses the risk that the fracture does not occur directly under the applied force. This may lead to important result variations. E_f values obtained from bending tests (3pb and 4pb) have proven to be less sensitive than σ_f and no significant differences were identified between both tests for the former property. Moreover, a minimum of a 10:1 span to thickness ratio has been advocated, as well as the use of a rigid loading frame with a low compliance jig/holder/testing machine to limit external stress absorption[157]. The use of fractography with this type of test is limited because the flaw or defect that led to fracture can be difficult to identify.

1.2.2 Flexural Modulus

The modulus of elasticity is a critical property that is dictated by a material's microstructure and the interatomic bonds between its constituents. More specifically, it is a measure of a material's resistance to be elastically deformed, i.e. non-permanently, when a stress is applied. Graphically, it is represented by the ratio of the elastic stress to the elastic strain, i.e. the slope of the linear part of the stress-strain curve. The elastic modulus is also a constant and, therefore, is not affected by the cumulative stress (elastic or plastic) in a material. As mentioned earlier, multiple tests are available for measuring the modulus of elasticity but flexure tests are the most commonly used, mainly for convenience reasons.

1.2.3 Fracture Mechanics

Fracture toughness is an intrinsic material property which characterizes the material's ability to withstand unstable crack propagation from a pre-existing flaw when loaded under tension[159]. Contrary to strength, K_{IC} is independent of the material geometry and testing specimens have an artificially introduced crack of known dimensions. The theoretical concept of fracture mechanics was initiated by Inglis who discovered that stress concentration in a loaded material occurs at the flaw's tip and increases with defect length and sharpness. Griffith further developed Inglis' idea when he employed an energy approach that balanced the stored elastic energy during loading and the surface energy needed for the creation of two new surfaces during crack propagation. However, his model was valid for brittle or linear-elastic materials. Irwin, on the other hand, incorporated a dissipative term to Griffith's equation as he realized that additional energy was required for surfaces to form in ductile material due to the presence of plastic deformation around the crack tip and under loading conditions[50, 160]. He also termed the stress intensity factor, *K*, a parameter independent of the material, representing the stress field around a sharp crack in linear-elastic material. This has led to the Griffith-Irwin fracture mechanics equation:

$$K = Y\sigma_{appl}\sqrt{\pi a}$$

Equation 2: Stress intensity factor formula

Where *Y* is the geometric factor; σ_{appl} is the global stress in the specimen; and *a* represents the crack length.

When K exceeds a critical value leading to unstable crack propagation, the subscript c is added to the stress intensity factor, leading to the fracture toughness parameter, K_C, an inherent material property. Also, because a crack can propagate as a result of different modes of loading, the formula for stress intensity factor will vary accordingly and a subscript Roman numeral that corresponds to the selected mode will be added to the parameter K_C[161]. Mode-I refers to tensile or opening force, mode-II to shear or sliding force and mode-III to torsional or tearing force (Figure 11)[162]. Hence, K_{IC} characterizes the critical stress intensity factor value for crack growth in linear-elastic materials, such as RC or ceramics, under tensile loading.

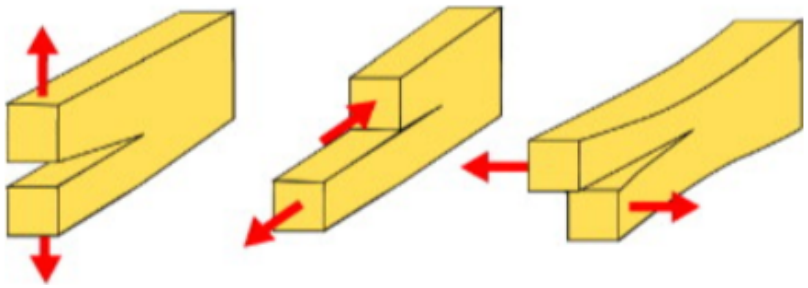

Figure 11: Mode of loading defined by Irwin[162]

Mechanical failure of a material is always associated with a crack-initiation/crack-propagation process and, therefore, K_{IC} characterization represents a useful tool to compare a material's performance in laboratory and possibly, in clinical conditions[159]. Indeed, a few studies identified K_{IC} as a clinically relevant mechanical parameter that correlates with the fracture of restorations made of RC materials[16, 163].

Many different techniques measuring K_{IC} exist, although no standard regarding which specimen design is the most appropriate for CAD/CAM RCB material has been defined yet. The selection of the testing method should be based on factors which influence the results, such as the

testing environment, the loading rate, the method to initiate the crack and its length, the notch depth ratio, the crosshead speed, the test geometry and the testing method itself[16, 161]. This puts emphasis on the need for investigators to understand the benefits and limitations of the test method they employ and the necessity to master the sample fabrication process.

1.2.3.1 Notchless Triangular Prism (NTP) Specimen Test

The NTP was developed by Ruse et al. in 1996 as a novel and convenient approach to determine K_{IC} and interfacial K_{IC} of diverse dental materials and dental-related adhesive interfaces. The configuration of its specimen and holder assembly was designed to reproduce the parameters of the already validated chevron-notched short rod (CNSR) test, but to limit the inherent difficulties and sources of error related to sample preparation (especially when small and brittle) of the latter. Another improved feature of the NTP over the CNSR test resided in the rigidity of the sample holder (E = 210 MPa) which limited the elastic energy stored in the system. This feature most probably contributed to a high level of control that led to the obtainment of specimens with an arrested crack following an unstable propagation. The dimensionless stress intensity factor, an essential feature, was calculated from the NTP configuration along with the extrapolation of data from Bubsey et al. (1982)[164]. Moreover, the results obtained for the NTP test were found to correlate with those obtained from other K_{IC} methodologies[4, 165, 166] thus adding to the validity of this method that has been endorsed by prominent researchers[162, 167].

The NTP test first consists of the preparation of equilateral prism specimens (6 x 6 x 6 x 12) mm or (4 x 4 x 4 x 12) mm with the use of a set of custom fabricated jigs (cutting, grinding/polishing, molding or aligning/bonding). Specimens are subsequently mounted into a customized holder, made of two halves, with the help of a customized mounting jig. This jig is

advantageous in the sense that it allows the use of a spacer to standardize the gap between the two halves and centralize an incorporated defect of a defined size (100 μm) from where the crack will initiate. Once the assembly is completed, samples are loaded in tension by a testing machine at a defined crosshead speed. An image representation and a comprehensive description of the NTP test methodology is provided in the methodology section of this thesis (p. 69). Table 3 provides a list of the advantages and limitations related to the NTP test.

Table 3: Advantages and limitations of the NTP test

Advantages	Limitations
- Sample size approximates clinical situations - Reduces surface flaws introduced in the sample as compared with the CNSR method and fabrication is easier - Enables testing of very small and brittle materials and of low K_{IC}, i.e. < 1 MPa·m$^{1/2}$ - Avoidance of embedding of tooth tissues for interfacial K_{IC} adhesive tests - Simplicity and reproducibility of testing conditions by means of the specimen holder configuration and mounting jig - Controlled environment for crack propagation - Known crack propagation direction and defect size that facilitate fractography - Versatility: allows for K_{IC} and interfacial K_{IC} characterization	- Requires careful and time consuming sample preparation with custom fabricated jigs - Sensitive alignment for interfacial adhesive testing - Requires a minimum length of 12 mm - Requires good edge integrity without chipping - Difficult defect introduction with hard material - Sample may slide from the holder during testing if not griped firmly enough

Chapter 2: Specific Aim

The objective of this project was to determine and compare σ_f, E_f and K_{IC} of four commercially available CAD/CAM RCBs and one glass-ceramic/ceramic block. Respective selected products were HT Enamic Universal (VITA, Germany), which is a modified polymer-infiltrated ceramic interpenetrating network (PICN), KZR-CAD HR2 (Yamakin, Japan), Cerasmart (GC, Japan) and Camouflage (Glidewell Dental Laboratories, USA), which are DF RC materials, and Obsidian (Glidewell Dental Laboratories, USA), a novel lithium disilicate glass-ceramic block. Half of the RC specimens were subjected to ageing conditions in order to replicate their possible alteration by an in-vivo environment.

2.1 Null Hypotheses

- **H_{01}:** There are no significant differences between the different materials regarding their σ_f, E_f and K_{IC} properties.
- **H_{02}:** Ageing in 37 °C water for 30 d does not have any effect on the tested mechanical properties of the different RC materials.

Chapter 3: Materials and Methods

3.1 Tested Materials

Table 4 provides a list of the four RC and the lithium disilicate CAD/CAM blocks that were included in this study. The rationale behind the selection of the different materials was mainly in their distinctive microstructure (PICN versus DF RC), novelty on the market and lack of characterization of their mechanical properties. All the materials are new and commercially available in Canada except KZR-CAD-HR2, a product from Japan, not yet approved by Health Canada and exclusively advertised as a fluoride ion releaser. Obsidian[168], a newly developed glass-ceramic material, was selected to allow for its characterization and comparison with RCBs materials, considering the popularity of lithium disilicate material for CAD/CAM restorations and associated clinical success. Unfortunately, manufacturers provided only limited information with regards to their materials' V_f, constituents and manufacturing process, especially for Camouflage. OBS' constituents were obtained through the material's safety data sheet (Figure 12).

Chemical Name & Components	CAS #'s	Weight %	
		Min.	Max.
Silicon Dioxide (SiO_2)	7631-86-9	50	58
Lithium Oxide (Li_2O)	12057-24-8	10	20
Germanium Dioxide (GeO_2)	1310-53-8	1	10
Potassium Oxide (K_2O)	12136-45-7	2	6
Phosphorous Pentoxide (P_2O_5)	1314-56-3	2	4
Aluminum Oxide (Al_2O_3)	1344-28-1	2	4
Zirconium Dioxide (ZrO_2)	1314-23-4	2	4
Pigments		0	10

Figure 12: OBS constituents[169]

Table 4: Tested materials

Microstructure Classification	CAD/CAM block (Shade)	Manufacturer	Code	Matrix	Filler (size), [*wt*%]	Lot	Illustration
PICN	Vita Enamic (0M1-HT)	Vita Zahnfabrik H. Rauter GmbH & Co., Bad Säckingen, Germany	VE	UDMA TEGDMA	Glass-ceramic sintered network [86], V_f%: 75	50920	
DF	Cerasmart (A2HT)	GC Corp., Tokyo, Japan	CER	Bis-MEPP UDMA DMA	Silica (20 nm), barium glass (300 nm) [a] [71], V_f%: 55	1509032	
	KZR-CAD-HR2 (A2L)	Yamakin Co., Ltd., Osaka, Japan	KZR	UDMA TEGDMA	SiO_2 (20nm), aggregated SiO_2-Al_2O_3.ZrO_2 (20-60 µm) cluster (1-6 µm) [a], fluoride particles (700 nm), [74]	01101501	
	Camouflage (A2LT)	Glidewell Dental Laboratories, Newport Beach, USA	CAM	----	----	----	
Lithium disilicate glass-ceramic	Obsidian (A2)	Glidewell Dental Laboratories, Newport Beach, USA	OBS	----	Crystalline lithium silicate and lithium phosphate	16-279-0946	

Material characteristics were obtained from manufacturer's data when available; a: Data obtained from Lauvahutanon et al., (2017)[103]
PICN: polymer-infiltrated ceramic network; DF: Dispersed fillers; UDMA: urethane dimethacrylate; TEGDMA: triethyleneglycol dimethacrylate; Bis-MEPP: 2,2-Bis(4-methacryloxypolyethoxyphenyl)propane; DMA: dimethacrylate; SiO_2: silica; Al_2O_3: alumina; ZrO_2: zirconia;

3.2 Sample Size Calculation

A power analysis, according to Lehr's equation (Equation 3), was first performed to determine the required sample size (n) for each of the investigated mechanical properties. Calculations were based on the mean results of a similar study by Thornton and Ruse[170] with a significance value set at $\alpha = 0.05$ and a power of 80%. A clinically relevant difference among the group's performance was established at 15%.

Rule of Thumb

The basic formula is

$$n = \frac{16}{\Delta^2},$$

where

$$\Delta = \frac{\mu_0 - \mu_1}{\sigma} = \frac{\delta}{\sigma}$$

Equation 3: Lehr's basic Rule of Thumb[171]

In the above equation, Δ represents the standardized difference and was obtained from the targeted difference between means over the standard deviation (SD), δ/σ. The following represents values that were used to determine the appropriate sample size to reach statistical significance:

- σ_f: mean of 114.81 MPa, SD of 12.94 MPa, $\Delta = 1.33$, $n = 9$
- E_f: mean of 29.20 GPa, SD of 3.03 GPa, $\Delta = 1.45$, $n = 8$
- K_{IC}: mean of 0.93 MPa·m$^{1/2}$, SD of 0.10 MPa·m$^{1/2}$, $\Delta = 1.40$, $n = 9$

Considered brittle material, the ability of RC and ceramic to resist fracture under stress is influenced by the presence of intrinsic flaws of different size. Since larger size imperfections are

not normally distributed in a Gaussian curve and are more likely to precipitate failure, Weibull statistics should be applied with the following probability of failure formula:

$$P_f = 1 - \exp\left[-\left(\frac{\sigma - \sigma_u}{\sigma_\theta}\right)^m\right]$$

$$P_f(\sigma_i) = \frac{i - 0.5}{N}$$

Equation 4: Failure probability equation[172]

where *i* represents the fracture load and *N* the total number of specimens in the tested group. Quinn and Quinn, 2010[172] mentioned that for dental material strength testing, $n > 20$ provides reasonable confidence limits and a small risk of bias. However, in order to increase the statistical robustness of this study, an $n = 25$ per group was selected. This means that 2% of additionally tested specimens would be weaker than the first datum while 98% would be weaker than the strongest recorded value.

3.3 Experimental Design

The experimental design is illustrated in Figure 13. The values for σ_f and E_f were obtained from the same 3pb test. While σ_f was the highest recorded stress before specimen fracture, E_f was calculated based on the slope of the linear portion of the stress/strain curve obtained during load application. All RC groups were tested under dry and aged conditions, while the ceramic groups were only tested dry. Ageing was performed in distilled water at 37 °C for 30 d. The determination of the ageing period was based on the work of Asaoka and Hirano (2003) who determined the time required to saturate RC disks of different thicknesses immersed in distilled water (Figure 9, p.22)[72].

Distilled water was preferred as an ageing medium to limit any additional variables such as may be found with artificial saliva, thus facilitating interpretation of results without additional confounding factors. For each RC material, 50 bars and 50 NTP were fabricated while only 25 of each were required for OBS. Hence, 18 groups were formed with a total number of 450 samples. Groups were identified according to the material code followed by the condition (example.g.: VEdry, VEaged, CERdry, etc.). OBS was the only material that needed to be crystallized before testing and, according to the manufacturer, no oversizing of the sample is required.

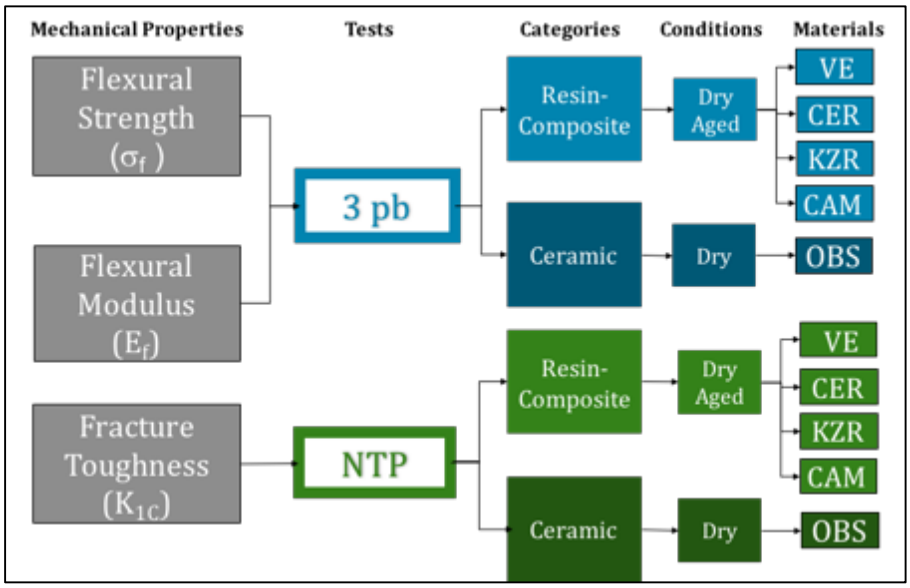

Figure 13: Experimental design

3.4 Specimen Preparation

3.4.1 Bars

For each material, blocks were first removed from their packaging box and inspected for any irregularities. Next, they were fixed with sticky wax (Kerr, Romulus, USA) on a metal cutting holder to have their milling stem removed from the blocks (Figure 14-A). Plain blocks were

subsequently glued longitudinally on the same holder and with the help of the translating arm, precisely cut into multiple 1.2 mm thick pieces (Figure 14-B). To limit cutting flaws, each side was polished (Figure 14-C) under water using a 600-grit silicon carbide (SiC) abrasive disk (Buehler, Lake Bluff, USA) and a digital caliper (Fowler, Sylvac, Switzerland) was used to determine final dimensions. Following the same fixation method, longitudinal 2 mm sections of all pieces stacked together were performed. Two-sided tape was placed beforehand on each side of the stack for holding purposes and to collect detached bars (Figure 14-D).

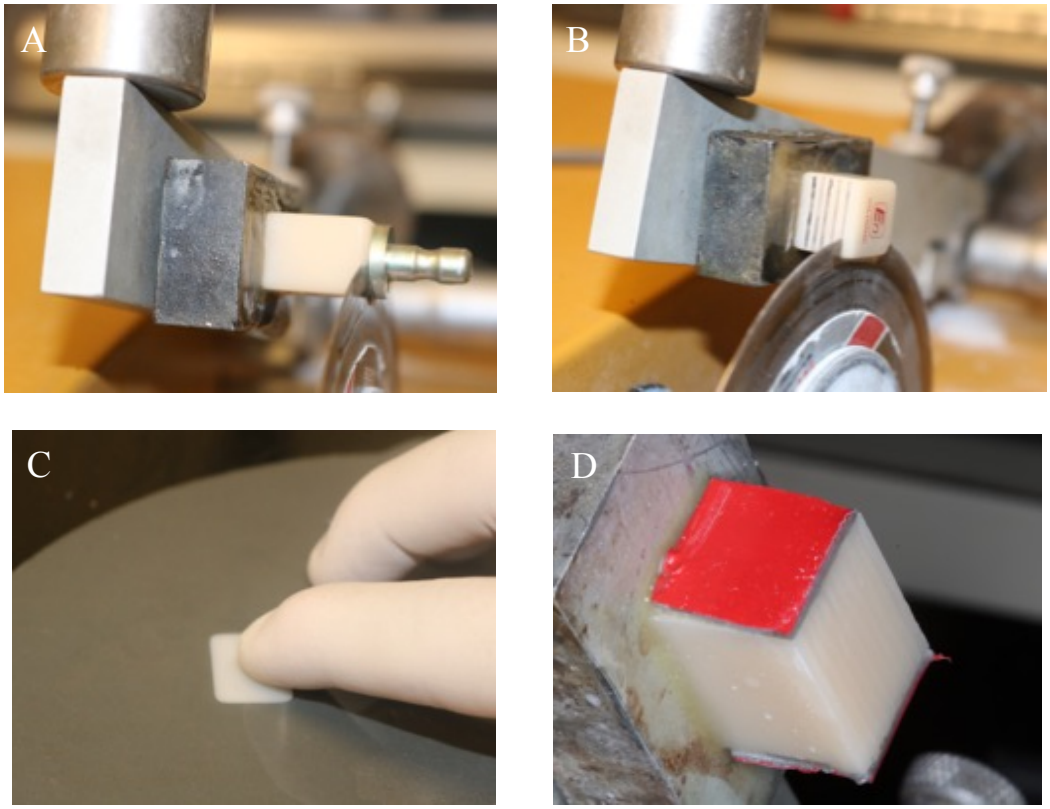

Figure 14: Bar specimen preparation

All sections were made with the constant rotation of a low speed Isomet saw (Buehler, Lake Bluff, USA) under cooling water and with a 0.014″ MK-303 Professional lapidary blade (MK Diamond Products, Inc., Torrance, USA) (Figure 15). Careful attention was paid to avoid

utilizing the same lapidary blade, used to cut the milling stem, for material sections. Also, as the first cut served to equalize and adjust the samples to the lapidary blade orientation, no specimen that resulted from its cut was kept.

Figure 15: Isomet saw and Lapidary blade

All bar specimens had the final dimension of (1.2 x 2 x 18) mm (Figure 16). A thickness to span ratio no greater than 1:10 needed to be respected because of the power character attributed to the thickness variable in the σ_f formula for the 3pb test (Equation 5 p.68). The bar material extended beyond the supports by at least 10%.

Figure 16: Bar specimens

3.4.2 Prisms

To optimize the sample production, plain blocks were first cut longitudinally in half (Figure 17-A). Pieces were then adhered with the same two-sided tape, as previously mentioned, to a custom-fabricated jig (UBC Faculty of Dentistry, Vancouver, Canada) that allow 60˚ angle cuts in different orientations (Figure 17-B). Obtained prisms were wet ground and polished to their final dimensions using a custom grinding/polishing jig (UBC Faculty of Dentistry, Vancouver, Canada) and SiC 320 and 600-grit abrasive disks under the constant water irrigation on a Metaserv wheel grinder (Buehler, Lake Bluff, USA) (Figure 17-C, D).

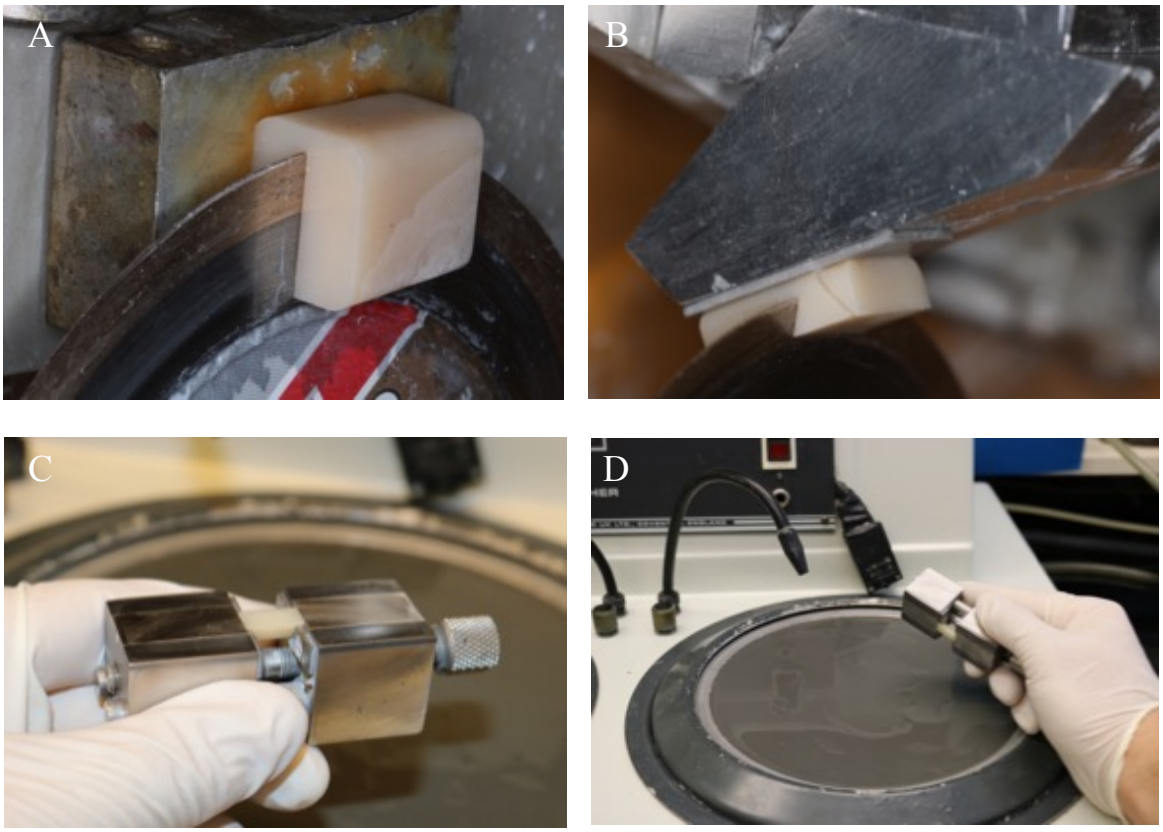

Figure 17: Prism specimen preparation

The final dimensions of the prism specimens (Figure 18) were (6 x 6 x 6 x 14) mm which was 2 mm longer than the minimum length required by the specimen holder testing device. This allowed proper holding of the prisms without the effect of any variations in the minimal length.

Figure 18: Prism specimens

3.4.3 Crystallization

All OBS samples were crystallized at 820 °C in an Ivoclar Programat P500 furnace (Ivoclar Vivadent, Amherst, USA), following the manufacturer's recommendations (Figure 19-A, B). Figure 20 illustrates the program manually entered in the furnace. Special attention not to influence or accelerate the cooling rate was taken, therefore the honeycomb firing tray with the samples on top was only removed several minutes after the crystallization process. No staining or glazing was applied and therefore, no additional firing was carried out.

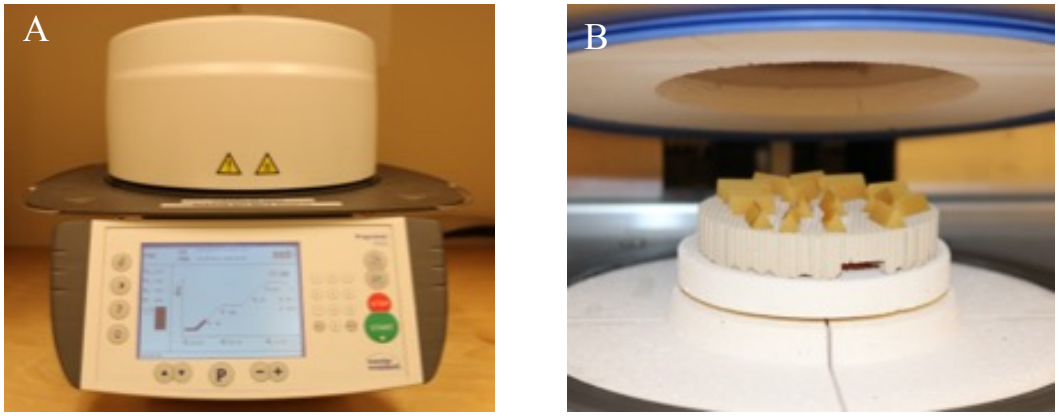

Figure 19: OBS specimen crystallization Ivoclar Programat P500 furnace

TABLE 4 — Crystallization Heating Cycle for Obsidian® Milling Blocks		
Ivoclar Programat® CS2, EP 5010, EP 5000, P300 or similar		
Vacuum Quality	72 mbar	N/A
Standby Temperature / Closing Time S	400ºC	3 minutes
Heating Rate t_1↗	90ºC/min	N/A
Holding Temperature T_1 / Holding Time H_1	780ºC	10 seconds
Heating Rate t_2↗	40°C/min	N/A
Holding Temperature T_2 / Holding Time H_2	820ºC	10 minutes
Cooling Rate ↘ t_L	50ºC/min	N/A
Long-term Cooling L	680ºC	N/A
Vacuum 1 Level $V1_1$ (on) / $V2_1$ (off)	400ºC	780ºC
Vacuum 2 Level $V1_2$ (on) / $V2_2$ (off)	780ºC	819ºC

Figure 20: OBS crystallization instruction[168]

3.4.4 Ageing

An Isotemp Incubator Model 630D (Fisher Scientific, Ottawa, Canada) was used to store half of the RC specimens in distilled water at 37 °C for 30 d before being tested (Figure 21). OBS specimens were not aged because the water absorption/desorption of glass-ceramic/ceramic material in the above-mentioned conditions would be negligible[130, 173, 174]. All testing was executed under dry conditions, except from the vapor form of water naturally present in the ambient air of the laboratory.

Figure 21: Specimens being water-aged in an Isotemp Incubator Model 630 at 37°C

3.5 Mechanical Properties Testing

σ_f and E_f were obtained from a 3pb test and K_{IC} from the NTP specimen K_{IC} test.

3.5.1 3-Point Bending (3pb) Flexural Strength and Modulus Test

Prior to testing, each specimen was rigorously inspected under a stereo light microscope (Olympus, Tokyo, Japan) for any defects or wax residue (Figure 22-A). Specimens that had visible edge defects were excluded to avoid any premature failure due to uncharacteristic processing flaws. Each specimen was marked on the side that would undergo compressive forces during testing, i.e. the upper side (Figure 22-B).

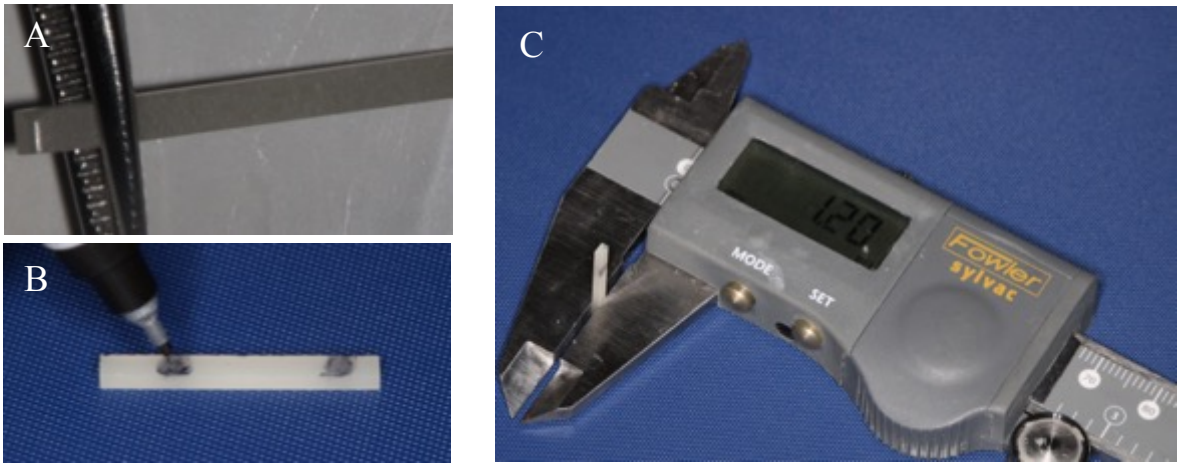

Figure 22: Specimen observation (A), marking (B) and measurement (C)

All bars were individually measured for width and thickness with a digital caliper (Fowler, Sylvac, Switzerland) (Figure 22-C) before they were placed on a custom holding device (UBC Faculty of Dentistry, Vancouver, Canada) that allowed a precise alignment on two free-to-roll rollers centrally separated by 12 mm. Measurements were then manually entered into the testing software. An Instron 4301 universal testing machine controlled by Bluehill 2 software (Instron, Norwood, USA) (Figure 23-A) was used to centrally load the samples at a crosshead speed of 1 mm/min until failure occurred (Figure 23-B). All specimen fragments were collected and classified per group in a binder.

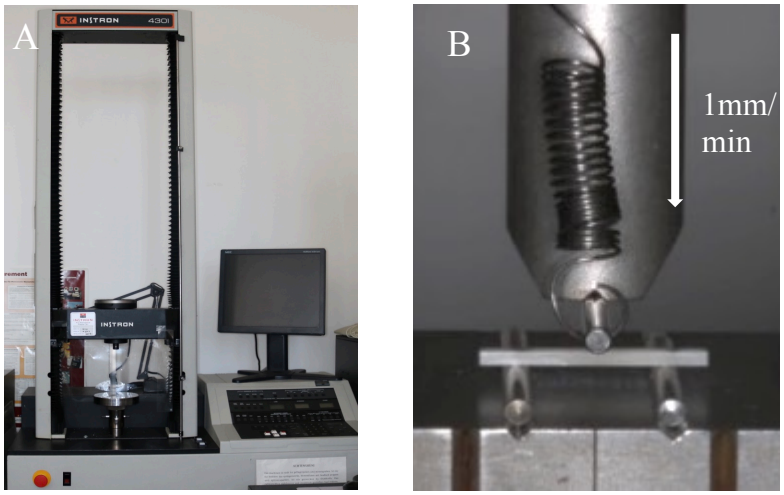

Figure 23: Instron universal testing machine (A) and 3pb test (B)

As the extension of the moving portion constantly increases during testing, a static load cell of 1 kN (Instron, Norwood, USA) allowed progressive monitoring and recording of the applied force until fracture occurred. This function led to the progressive formation of a graphically visible slope. With the maximum load being recorded, σ_f (MPa) could be calculated from the formula:

$$\sigma_f = \frac{3PL}{2bt^2}$$

Equation 5: Flexural strength formula

where P = maximum load; L = span (12 mm); b = specimen width; and t = specimen thickness.

E_f (GPa) was determined from the straight portion of the δP/δd slope obtained during testing and according to Equation 6:

$$E_f = \frac{L^3}{4bt^3}\frac{\delta P}{\delta d}$$

Equation 6: Flexural modulus formula

where P = maximum load; L = span (12mm); b = specimen width; t = specimen thickness; and d = the displacement.

3.5.2 Notchless Triangular Prism (NTP) Specimen Fracture Toughness Test

Prisms were carefully observed under a stereo light microscope (Olympus, Tokyo, Japan) to withdraw irregular samples and to select a flawless edge from which the crack will initiate (Figure 24-A). Once selected, the opposing surface was labelled with a Sharpie marker to ensure that the direction of crack propagation was known, which was eventually useful during fractography (Figure 24-B). Next, prisms were secured in one half of the specimen holder (Figure 24-C) and a ~0.1 mm deep defect was introduced, under the same microscope, with a sharp GEM stainless steel blade (Ted Pella Inc., Redding, USA) to help crack initiation (Figure 24-D and Figure 25-A). Due to OBS specimen's hardness, the defect was produced with a diamond-wafering blade (UKAM, Valencia, USA) and subsequently validated under a microscope to confirm a truly sharp shaped defect, not a blunted one. The second half of the holder was then used to secure the NTP specimen, using a custom-fabricated mounting block, containing a spacer blade to reproduce the CNSR specimen configuration (Figure 25-B, C).

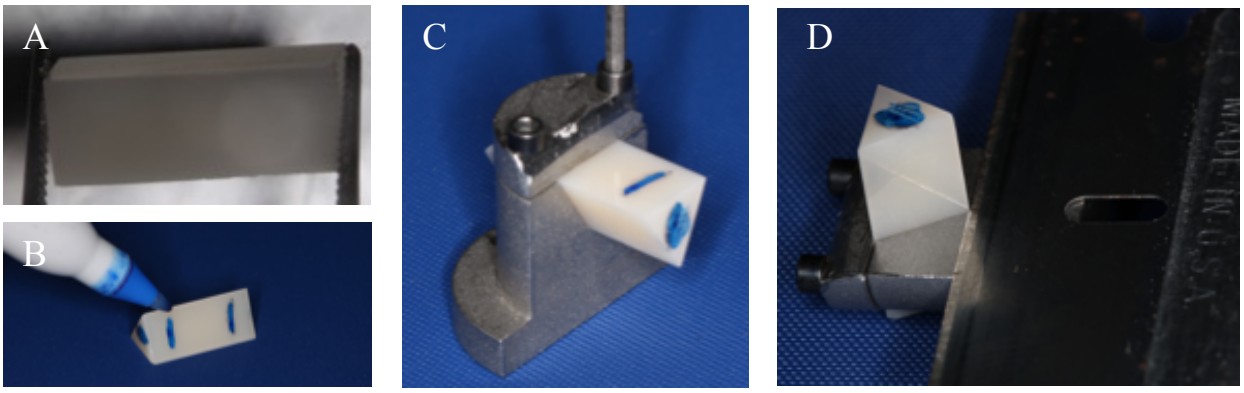

Figure 24: Prism observation (A), marking (B), half-fixation (C) and defect incorporation (D)

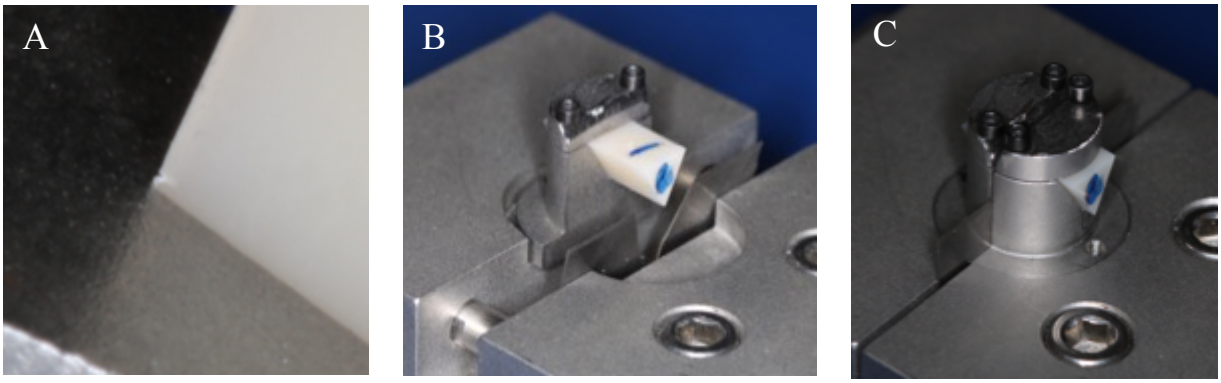

Figure 25: Defect (A), mounting jig and spacer (B) and second half-fixation (C)

The Instron 4301 machine was used to test the specimens in tension at a crosshead speed of 0.1 mm/min until crack arrest or sample fracture (Figure 26-A, B)[175]. Again, all fractured samples were collected and compiled in a binder.

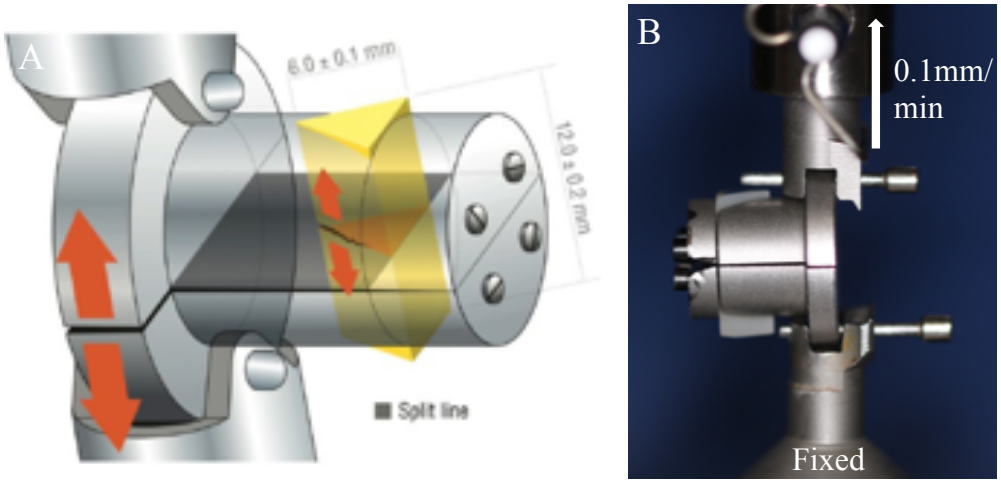

Figure 26: NTP testing motion (A)[172] and specimen testing (B)

Fracture toughness (MPa·m$^{1/2}$) values were obtained according to the following equation:

$$K_{1C}=Y^{*}_{min}\frac{P_{max}}{DW^{1/2}}$$

Equation 7: Fracture toughness formula

where Y^*_{min} = dimensionless stress intensity coefficient factor minimum (28); D = specimen diameter (12 mm); W = specimen length (10.5 mm).

3.6 Scanning Electron Microscopy (SEM) Characterization

The scanning electron microscope is a powerful tool that produces high resolution images at the nanoscale level by scanning the surface of a sample of interest with a focused electron beam. It is often used in fractography to characterize fractured surfaces, identify intrinsic flaws, defects, zones of slow and rapid crack growth and ultimately to determine the mode of failure.

To enable visualization or improve image quality of non-conductive materials, such as polymers and ceramics, sputter coating with a conductive element is required. This procedure also helps to prevent charging on the surface of the specimens, to reduce thermal damages and to increase the amount of detectable surface secondary electrons.

In this study, only two samples per group following K_{IC} testing were analyzed through SEM: one that fractured close to the average value and one that failed prematurely (value lower than the mean). Following a specific sequence, fractured halves (2 sides per sample) were mounted on a SEM stud (Figure 27-A) and subsequently gold coated (Figure 27-C) with an Edwards S150A sputter coater (Edwards Vacuum, Crawley, UK) (Figure 27-B). Then, they were transferred to a revolving holder (Figure 27-D) and observed under a SEM Hitachi, S-3000N (Hitachi, Japan) (Figure 27-E) at different magnifications (50x, 500x, 1500x and 3000x) in order to characterize the fractured surfaces (Figure 27-F). A minimum of four photomicrographs were captured per each half and saved in JPG format. All high-magnification images were taken in the area of slow crack propagation with their specific location being recorded in a laboratory handbook.

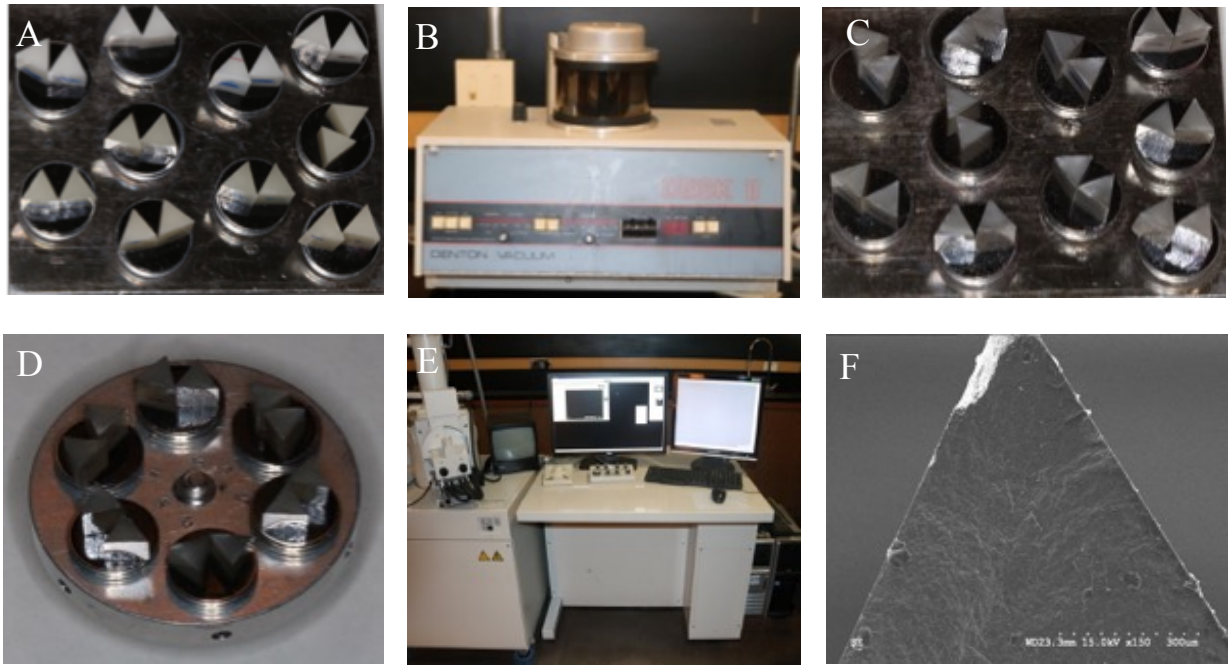

Figure 27: Prism halves mounting (A), sputter coater (B), gold-coated halves (C), revolving holder (D), SEM(E) and obtained image at 50x (F)

3.7 Statistical Analysis

Collected data was first verified for normality and then analyzed by two-way ANOVA followed by Scheffé multiple mean comparison ($\alpha = 0.05$), using SPSS software (IBM, Armonk, NY, USA). Scheffé is a parametric post-hoc test that provides precision following significant results obtained with ANOVA. More specifically, it allows comparison of all possible mean pairs to precisely identify the ones that are significantly different. The Scheffé test is also valid in case of unequal sample size but requires equality of variance. In this project, the above-mentioned statistical methodology was repeated to compare all materials among themselves and according to the tested mechanical properties and conditions.

In a simpler manner, a student t-test was employed to compare mean values obtained from dry and aged conditions for each material, taken individually. This procedure was useful to determine if water storage had a significant impact on a given material and for a given property.

Weibull statistics were also employed to analyze σ_f and K_{IC} results. This method provided a graphical visualization of clinically relevant parameters, the Weibull modulus (m) and the characteristic Weibull σ_f/K_{IC} attributed to the different tested materials. Weibull modulus is an indicator of the reliability of a material and is determined by the slope of a linear trend line fitted to the results in a Weibull graph. For instance, a high Weibull modulus material, characterized by a steep slope and a narrow distribution of defects, will fracture more predictably around the Weibull characteristic value. Weibull characteristic value is the value corresponding to a probability of failure P_f = 63.2%. The following equation was used to allow a graphical representation of the results:

$$\ln\left[\ln\left(\frac{1}{1-P_f}\right)\right] = m\ln\sigma - m\ln\sigma_\theta$$

Equation 8: Weibull formula producing graphic and Weibull modulus

where P_f = probability of failure; m = Weibull modulus; σ = fracture stress; and σ_θ = characteristic strength.

Chapter 4: Results

Table 5 summarizes all means and standard deviations (SD) obtained in this study along with the statistical analysis. With regards to σ_f, OBS exhibited the highest mean at 242.26 ± 30.96 MPa and dry tested RC materials ranged between 148.16 ± 10.04 MPa and 205.50 ± 22.53 MPa following the sequence OBS > CER = KZR > CAM > VE. Taken separately, ageing significantly reduced values of all RC materials but also altered the ranking when compared to each other: CER > KZR > CAM = VE. Weibull statistics revealed an increase in reliability for aged CER and KZR compared to their dry homologue. With regards to E_f, again, OBS had a superior mean at 76.46 ± 6.00 GPa. VE stood out from the RC materials with a dry mean value of 33.02 ± 2.96 GPa, whereas others varied from 9.25 ± 0.56 GPa to 12.92 ± 1.36 GPa as sequenced: OBS > VE > CAM = KZR > CER. Interestingly, all aged RC materials were found to be statistically different when compared; VE > CAM > KZR > CER, while when taken individually, only VE was not significantly affected by water storage.

Among all materials, OBS demonstrated a superior resistance to crack propagation with a K_{IC} of 1.47 ± 0.19 MPa·m$^{1/2}$. Dry testing of RC materials revealed a significantly higher value for KZR at 1.37 ± 0.33 MPa·m$^{1/2}$ compared to the three others that were not significantly different: OBS = KZR > VE = CAM = CER. When materials were compared individually, ageing significantly increased VE's mean value, but decreased KZR. The ranking VE = KZR > CAM = CER was obtained when materials were compared with each other. Weibull moduli decreased for VE, CER and CAM as a consequence of ageing, while it augmented for KZR.

Table 5: Results (mean + SD) and statistical analysis

		Vita Enamic (VE)		Cerasmart (CER)		KZR-CAD-HR2 (KZR)		Camouflage (CAM)		Obsidian (OBS)
		Dry	Aged	Dry	Aged	Dry	Aged	Dry	Aged	Dry
Test	σ_f	$148.16 \pm 10.04^{a*}$ $m = 17.71$ $W_c = 152.62$	$135.71 \pm 9.21^{A*}$ $m = 17.84$ $W_c = 139.77$	$205.50 \pm 22.53^{b*}$ $m = 10.78$ $W_c = 215.23$	$172.07 \pm 11.84^{B*}$ $m = 17.27$ $W_c = 177.39$	$196.62 \pm 23.20^{b*}$ $m = 10.05$ $W_c = 206.61$	$160.26 \pm 8.67^{C*}$ $m = 22.25$ $W_c = 164.13$	$173.75 \pm 18.35^{c*}$ $m = 11.35$ $W_c = 181.63$	$144.01 \pm 17.60^{A*}$ $m = 9.72$ $W_c = 151.55$	242.26 ± 30.96^{d} $m = 9.43$ $W_c = 255.21$
	E_f	33.02 ± 2.96^{a}	33.05 ± 2.67^{A}	$9.25 \pm 0.56^{b*}$	$8.59 \pm 0.62^{B*}$	$11.31 \pm 1.34^{bc*}$	$10.02 \pm 0.65^{C*}$	$12.92 \pm 1.36^{c*}$	$12.15 \pm 0.93^{D*}$	76.46 ± 6.00^{d}
	K_{IC}	$0.83 \pm 0.16^{a*}$ $m = 6.20$ $W_c = 0.89$	$1.00 \pm 0.32^{A*}$ $m = 3.74$ $W_c = 1.11$	0.64 ± 0.11^{a} $m = 7.15$ $W_c = 0.68$	0.60 ± 0.12^{B} $m = 5.78$ $W_c = 0.64$	$1.37 \pm 0.33^{b*}$ $m = 4.80$ $W_c = 1.50$	$0.85 \pm 0.10^{A*}$ $m = 10.40$ $W_c = 0.89$	0.68 ± 0.11^{a} $m = 7.20$ $W_c = 0.72$	0.60 ± 0.15^{B} $m = 4.93$ $W_c = 0.65$	1.47 ± 0.19^{b} $m = 8.80$ $W_c = 1.55$

#: Identical superscript letters indicate statistical difference within a test; lowercase for dry, uppercase for aged (Two-way Anova followed by Scheffé [$\alpha = 0.05$] test).

∗: Identifies significant difference based on pairwise t-test ($\alpha = 0.05$) comparisons of a same material under different conditions within a test.

W_c: Weibull characteristic value; m: Weibull modulus.

4.1 Flexural Strength (σ_f)

For each material and condition, Table 6 summarizes final group size, means and standard deviation (SD), student t-test results, Weibull characteristic strength (σ) and modulus (m). Due to sample preparation imperfections, misalignment or possibly big size intrinsic flaws, a few outliers were excluded from the calculation.

Table 6: Flexural strength mean results and statistical analysis

Material	Group size [n]	σ_f(MPa) [Mean ± SD]	Dry vs Aged Student t-test Sig. ≤ 0.05	Weibull Characteristic Strength (MPa) [σ]	Weibull Modulus [m]
VE dry	21	148.16 ± 10.04	0.00	152.62	17.71
VE aged	25	135.71 ± 9.21		139.77	17.84
CER dry	25	205.50 ± 22.53	0.00	215.23	10.78
CER aged	24	172.07 ± 11.84		177.39	17.27
KZR dry	25	196.62 ± 23.20	0.00	206.61	10.05
KZR aged	20	160.26 ± 8.67		164.13	22.25
CAM dry	25	173.75 ± 18.35	0.00	181.63	11.35
CAM aged	25	144.01 ± 17.60		151.55	9.72
OBS	25	242.26 ± 30.96	N/A	255.21	9.43

Results are illustrated in Figure 28 with box and whisker plots representing the median, minimum and maximum of all materials for dry and aged conditions. The graph analysis shows that OBS specimens, overall, fractured at higher values but followed a wider distribution. All dry tested RC material obtained superior mean values compared to their aged homologue.

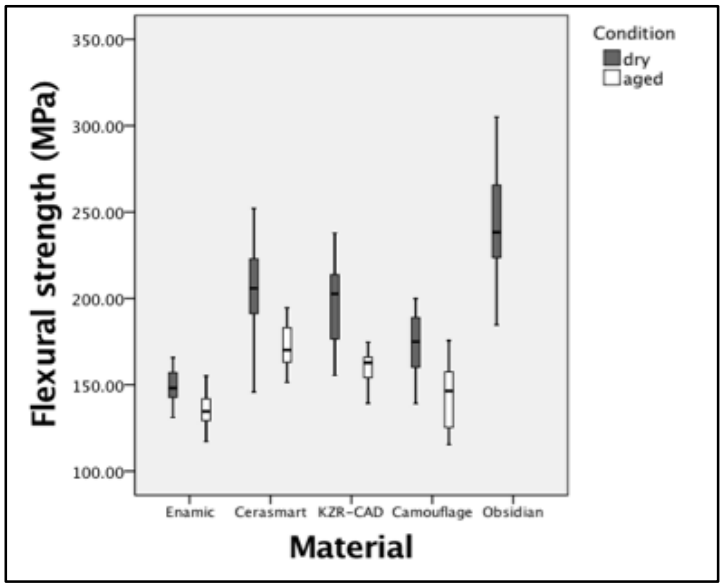

Figure 28: Flexural strength boxplot

Scheffé post hoc results (Figure 29) demonstrated areas of significant difference between tested materials, discernable by the subsets for non-aged and aged condition, respectively.

Scheffe[a,b,c]

Material	N	Subset 1	2	3	4
Enamic	21	148.164			
Camouflage	25		173.746		
KZR-CAD	25			196.617	
Cerasmart	25			205.501	
Obsidian	25				242.257
Sig.		1.000	1.000	.755	1.000

Means for groups in homogeneous subsets are displayed.
Based on observed means.
The error term is Mean Square(Error) = 501.765.

a. Uses Harmonic Mean Sample Size = 24.083.

b. The group sizes are unequal. The harmonic mean of the group sizes is used. Type I error levels are not guaranteed.

c. Alpha = 0.05.

Scheffe[a,b,c]

Material	N	Subset 1	2	3
Enamic	25	135.710		
Camouflage	25	144.005		
KZR-CAD	20		160.263	
Cerasmart	24			172.069
Sig.		.172	1.000	1.000

Means for groups in homogeneous subsets are displayed.
Based on observed means.
The error term is Mean Square(Error) = 156.902.

a. Uses Harmonic Mean Sample Size = 23.301.

b. The group sizes are unequal. The harmonic mean of the group sizes is used. Type I error levels are not guaranteed.

c. Alpha = 0.05.

Figure 29: Scheffé post-hoc σ_f analysis (non-aged and aged respectively)

In light of the compiled data and statistical analysis for the σ_f property, a few observations were made:

- Among all materials, OBS had the highest σ_f mean value, but the widest SD.
- When dry materials were compared together, they were all significantly different except for KZR and CER, as shown in subset 3 of the non-aged Scheffé σ_f analysis (Figure 29).
- Observed σ_f dry tested materials ranking: OBS > CER = KZR > CAM > VE
- When aged materials were compared together, they were all significantly different except for VE and CAM, as shown in subset 1 of the aged Scheffé σ_f analysis (Figure 29).
- Observed σ_f aged tested materials ranking: CER > KZR > CAM = VE
- Ageing had a statistically significant decreasing effect on mean values of all RC materials, thus rejecting the second null hypothesis for the σ_f property.

Figure 30 displays Weibull plots of the σ_f results for the different tested groups. Weibull characteristic (MPa) values are represented by dotted arrows on the superior horizontal axis and the reliability, *m*, by the slope, i.e. the tangent of the angle formed by the trend line and the horizontal axis. As visible on the graph and confirmed by the values in Table 6, all RC materials found their Weibull characteristic strength diminished after ageing. CER and KZR had their *m* increased drastically after ageing going, respectively, from 10.78 to 17.27 and 10.05 to 22.25. Interestingly, VE was the most predictable material with dry and aged *m* values of 17.71 and 17.84 respectively. CAM was the only RC material found to be negatively affected by water storage in terms of reliability. With values further located to the right, the OBS control material showed stronger characteristic strength but its softer slope at 9.43 makes it less reliable.

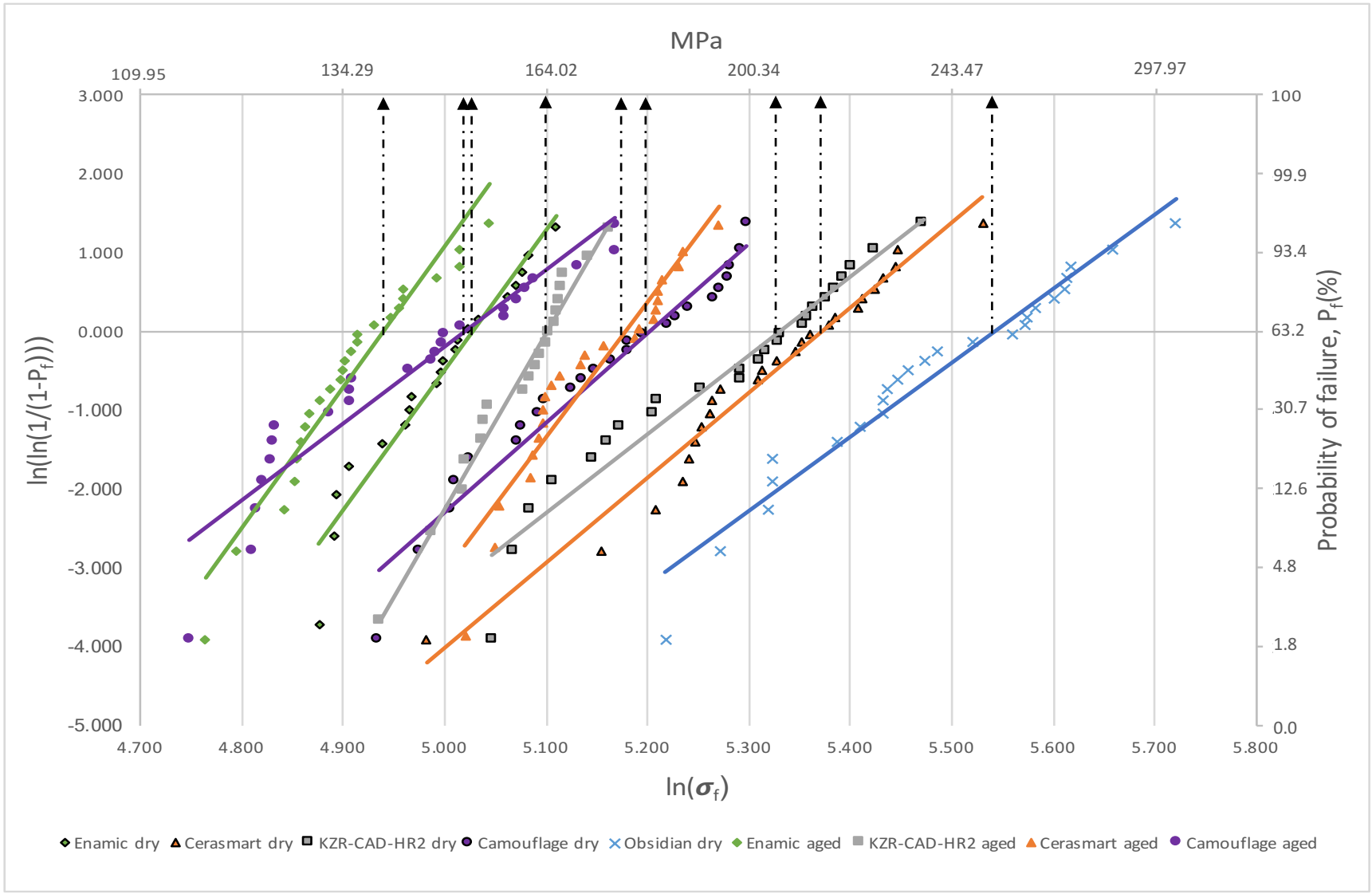

Figure 30. Weibull statistic graphical representation

4.2 Flexural Modulus (E_f)

For each material and condition, Table 7 summarizes final group size, mean and SD and the results of the student t-test. Again, due to sample preparation imperfections, misalignment or possibly big size intrinsic flaws, a few outliers were excluded from the calculation.

Table 7: Flexural modulus mean results and statistical analysis

Material	Group size [n]	E_f (GPa) [Mean ± SD]	Dry vs aged Student t-test [Sig. ≤ 0.05]
VE dry	21	33.02 ± 2.96	0.974
VE aged	25	33.05 ± 2.67	
CER dry	25	9.25 ± 0.56	0.00
CER aged	24	8.59 ± 0.62	
KZR dry	25	11.31 ± 1.34	0.00
KZR aged	20	10.02 ± 0.65	
CAM dry	25	12.92 ± 1.36	0.024
CAM aged	25	12.15 ± 0.93	
OBS	24	76.46 ± 6.00	N/A

Results are illustrated in Figure 31 with box and whisker plots representing the median, minimum and maximum of all materials for both conditions. The graphical representation revealed that OBS obtained the highest E_f values accompanied with the largest SD. Among RC materials, VE stood out with considerably superior results while the DF RC materials tested at lower values.

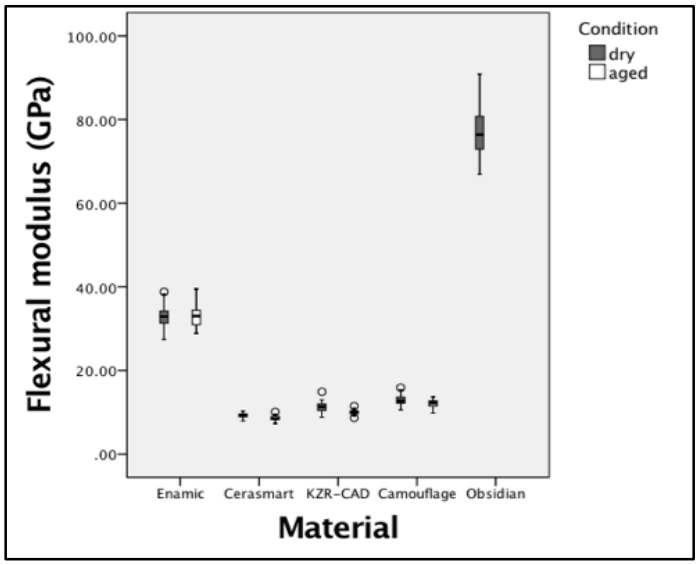

Figure 31: Flexural modulus boxplot

Scheffé post hoc results (Figure 32) demonstrated areas of significant difference between tested materials, discernable by the respective subsets for non-aged and aged conditions.

Scheffe[a,b,c]

Material	N	Subset 1	2	3	4
Cerasmart	25	9.2484			
KZR-CAD	25	11.3068	11.3068		
Camouflage	25		12.9164		
Enamic	21			33.0195	
Obsidian	24				76.4629
Sig.		.265	.521	1.000	1.000

Means for groups in homogeneous subsets are displayed.
Based on observed means.
The error term is Mean Square(Error) = 9.551.

a. Uses Harmonic Mean Sample Size = 23.891.

b. The group sizes are unequal. The harmonic mean of the group sizes is used. Type I error levels are not guaranteed.

c. Alpha = 0.05.

Scheffe[a,b,c]

Material	N	Subset 1	2	3	4
Cerasmart	24	8.5921			
KZR-CAD	20		10.0160		
Camouflage	25			12.1516	
Enamic	25				33.0464
Sig.		1.000	1.000	1.000	1.000

Means for groups in homogeneous subsets are displayed.
Based on observed means.
The error term is Mean Square(Error) = 2.320.

a. Uses Harmonic Mean Sample Size = 23.301.

b. The group sizes are unequal. The harmonic mean of the group sizes is used. Type I error levels are not guaranteed.

c. Alpha = 0.05.

Figure 32: Scheffé post-hoc E_f analysis (non-aged and aged respectively)

Compiled data and statistical analysis for the E_f property revealed the following observations:

- Among all materials, OBS had the highest E_f mean value, but the widest SD.

- When dry materials were compared together, they were all significantly different except for CAM, KZR and CER, as shown in the subsets 1 and 2 of the non-aged Scheffé E_f analysis (Figure 32).
- Observed E_f dry tested materials ranking: OBS > VE > CAM = KZR > CER
- When aged materials were compared together, they were all significantly different as shown in the aged Scheffé E_f analysis (Figure 32).
- Observed E_f aged tested materials ranking: VE > CAM > KZR > CER
- Except for VE, ageing had a statistically significant decreasing effect on mean values of RC materials.

4.3 Fracture Toughness (K_{IC})

Table 8 summarizes final group size, mean and SD, student t-test results, Weibull characteristic and modulus (m) for each material and condition. Compared to other groups, CER dry and OBS had their group size appreciably reduced after the exclusion of outliers. Characterized by a premature or delayed failure, a few samples were found with more than one propagating crack while some had minor preparation imperfections and dimensional variations that caused sliding of the specimen in the holder during testing or hypothetical stress transmission from the holder. Compared to the bars, fabrication of prisms required more manipulation and therefore, may have influenced the amount of surface flaws. Also, blunted defects for crack initiation that were not detectable by microscope observation could have led to higher results.

Table 8: Fracture toughness mean results and statistical analysis

Material	Group Size [n]	K_{IC} (MPa·m$^{1/2}$) [Mean ± SD]	Dry vs Aged Student t-test Sig. ≤ 0.05	Weibull Characteristic (MPa·m$^{1/2}$) [K_{IC}]	Weibull Modulus [m]
VE dry	21	0.83 ± 0.16	0.025	0.89	6.20
VE aged	25	1.00 ± 0.32		1.11	3.74
CER dry	16	0.64 ± 0.11	0.293	0.68	7.15
CER aged	24	0.60 ± 0.12		0.64	5.78
KZR dry	21	1.37 ± 0.33	0.00	1.50	4.80
KZR aged	21	0.85 ± 0.10		0.89	10.40
CAM dry	20	0.68 ± 0.11	0.057	0.72	7.20
CAM aged	21	0.60 ± 0.15		0.65	4.93
OBS	17	1.47 ± 0.19	N/A	1.55	8.80

Results are illustrated in Figure 33 with box and whisker plots representing the median, minimum and maximum K_{IC} of all materials for both conditions. The graphical representation demonstrated that OBS and KZR dry fractured the highest but KZR mean values drastically dropped after water storage. VE was the only material that had superior aged values compared to dry while CER and CAM had the lowest mean values for both conditions.

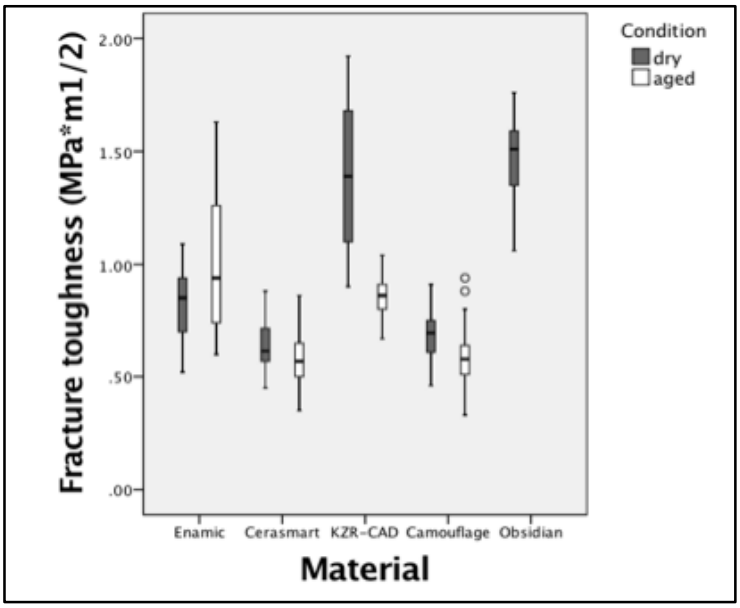

Figure 33: Fracture toughness boxplot

Scheffé post hoc results (Figure 34) demonstrated areas of significant difference between tested materials, discernable by the respective subsets for non-aged and aged conditions.

Scheffe[a,b,c]

Material	N	Subset 1	Subset 2
Cerasmart	16	.6356	
Camouflage	20	.6765	
Enamic	21	.8286	
KZR-CAD	21		1.3686
Obsidian	17		1.4700
Sig.		.082	.669

Means for groups in homogeneous subsets are displayed.
Based on observed means.
The error term is Mean Square(Error) = .041.

a. Uses Harmonic Mean Sample Size = 18.757.

b. The group sizes are unequal. The harmonic mean of the group sizes is used. Type I error levels are not guaranteed.

c. Alpha = 0.05.

Scheffe[a,b,c]

Material	N	Subset 1	Subset 2
Cerasmart	24	.5954	
Camouflage	21	.5967	
KZR-CAD	21		.8529
Enamic	25		.9976
Sig.		1.000	.119

Means for groups in homogeneous subsets are displayed.
Based on observed means.
The error term is Mean Square(Error) = .039.

a. Uses Harmonic Mean Sample Size = 22.611.

b. The group sizes are unequal. The harmonic mean of the group sizes is used. Type I error levels are not guaranteed.

c. Alpha = 0.05.

Figure 34: Scheffé post-hoc K_{IC} analysis (non-aged and aged respectively)

Statistical analysis of the results for the K_{IC} property allowed multiple observations:

- Among all materials, OBS had the highest mean value.
- When dry materials were compared together, only VE, CAM and CER were statistically different from OBS and KZR as only two subsets were generated (Figure 34).
- Observed K_{IC} dry tested materials ranking: OBS = KZR > VE = CAM = CER
- When aged materials were compared together, VE and KZR were significantly different from CAM as again marked by only 2 subsets (Figure 34).
- Observed K_{IC} aged tested materials ranking: VE = KZR > CAM = CER
- Ageing had a statistically significant decreasing effect on mean values of VE and KZR (Table 8).

Figure 35 displays Weibull plots of the K_{IC} results for the different tested groups. As previously explained in the σ_f results, Weibull modulus and Weibull characteristic K_{IC} values (expressed in $MPa \cdot m^{1/2}$) are represented by dotted arrows on the superior horizontal axis and the predictability coefficient, *m*, by the slope. The graphical representation and summarized results in Table 8 indicated a decrease in Weibull characteristic value after ageing for CER, CAM and KZR while an augmentation was noted for VE. VE, CER and CAM had their *m* decreased after ageing going from 6.20 to 3.74, 7.15 to 5.78 and 7.20 to 4.95, respectively. KZR was the only RC material that saw its reliability increased considerably after ageing from 4.80 to 10.40. OBS tested the highest with a Weibull characteristic of 1.55 $MPa \cdot m^{1/2}$ but ranked second behind KZR aged with a slope of 8.80.

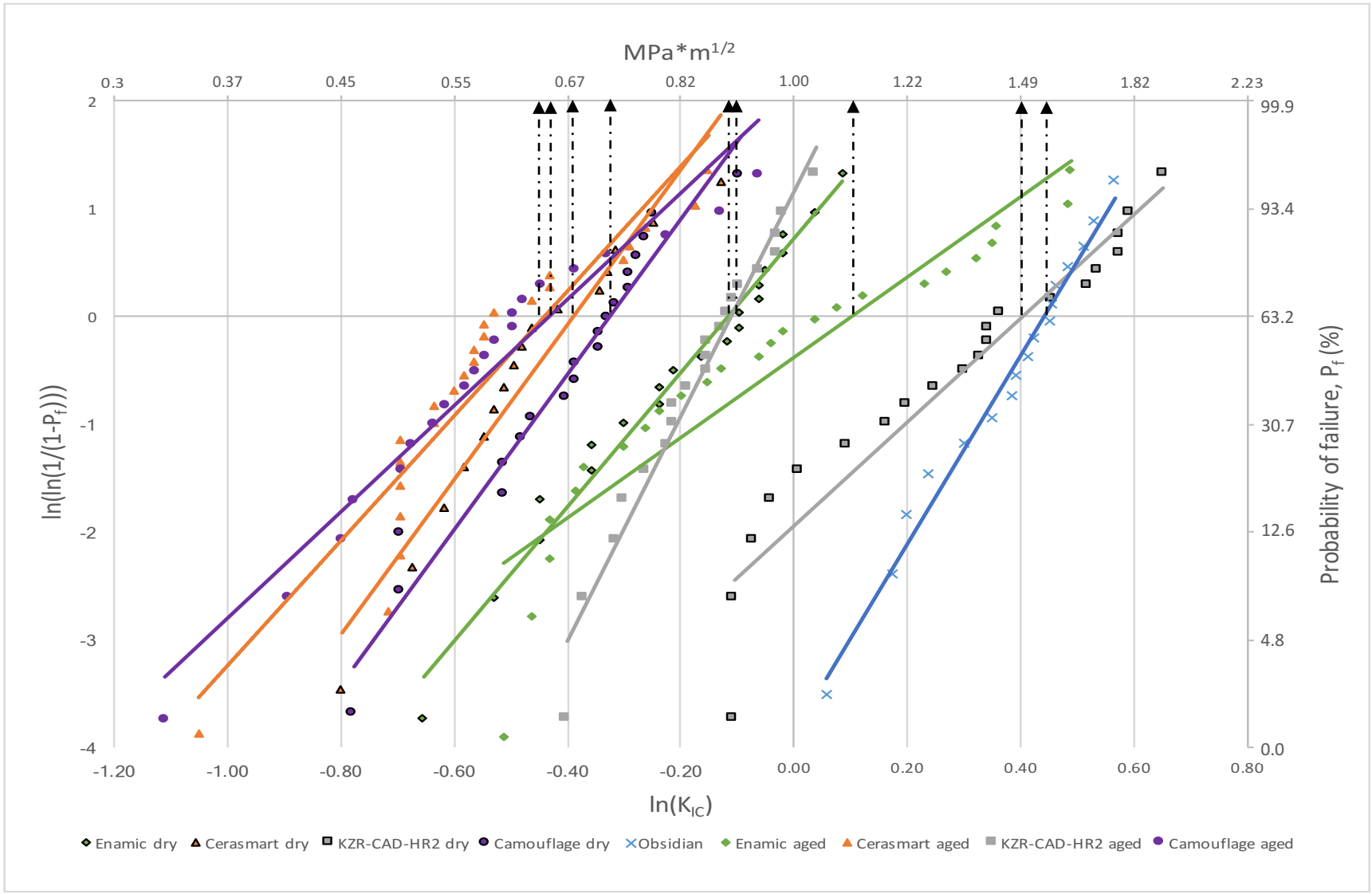

Figure 35. Weibull statistics graphical representation

Interestingly, all K_{IC} groups had a few specimens with crack arrest without separation after testing, as illustrated in Figure 36. These samples were representative of the mean values of their associated group.

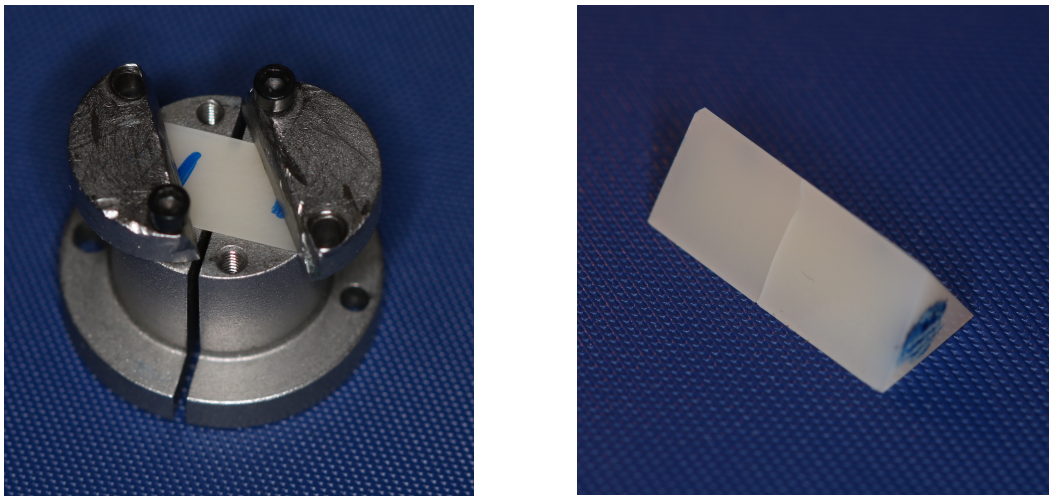

Figure 36: Tested prism exhibiting controlled crack arrest

4.4 SEM Analysis

Images obtained by SEM allowed for characterization of the fractured surfaces of different materials and therefore, identification of features related to the internal structure that could have influenced the results. Figure 37 shows the area of crack initiation from the manually introduced defect with zones of slow and rapid crack propagation. Figures 38-41 are representative of the obtained non-aged and aged images. For comparison purposes, only 3000x magnification images were included because they were more revealing of the internal structure. In the present project, three types of structures were observed: a ceramic network structure with resin matrix (VE), a resin matrix structure with embedded filler (CER, KZR, CAM) and a glass-ceramic/ceramic structure (OBS). Moreover, some material and condition specific observations related to the presence of voids, stress lines, amounts of glassy matrix and roughness of the fractured surface were elaborated:

- Rougher fracture pattern was observed in VE aged compared to dry;
- Stress lines and voids were present in VE specimens;
- Voids were present in CER and CAM specimens;
- No difference was noted between dry and aged CER or CAM specimens regarding the roughness fracture pattern;
- KZR dry specimens presented a rougher pattern compared to aged;
- OBS showed voids, a large glassy matrix and a small dispersed crystalline phase.

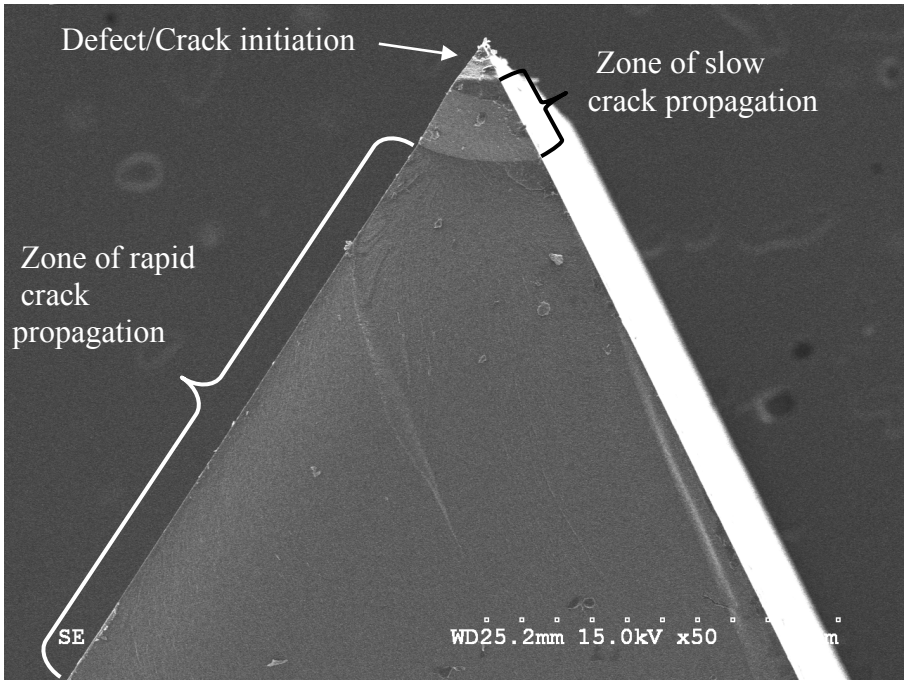

Figure 37: SEM image – CER dry

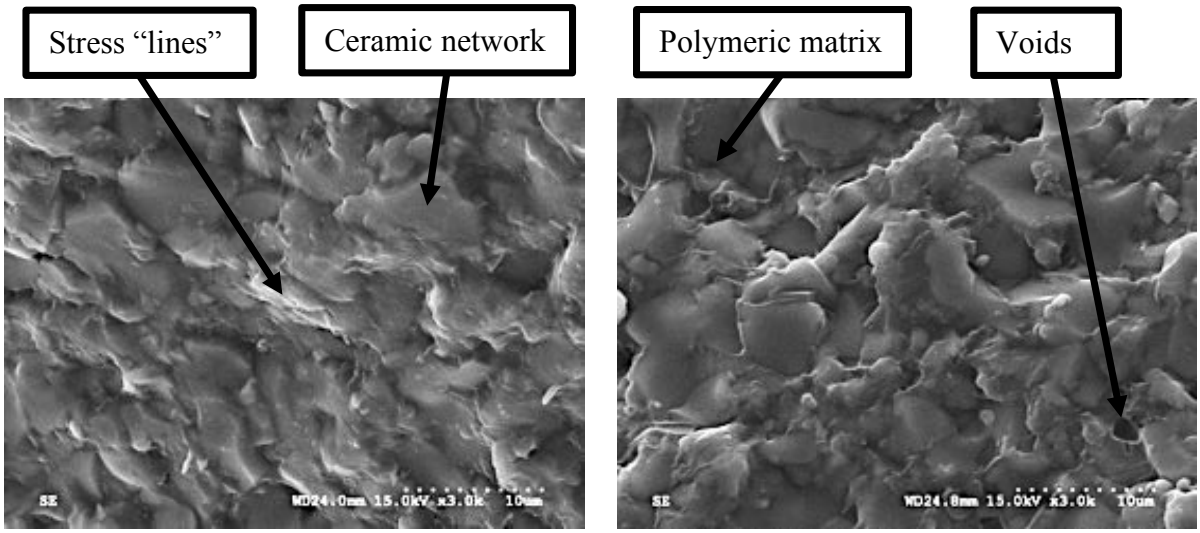

Figure 38: SEM images – VE dry sample; VE aged sample

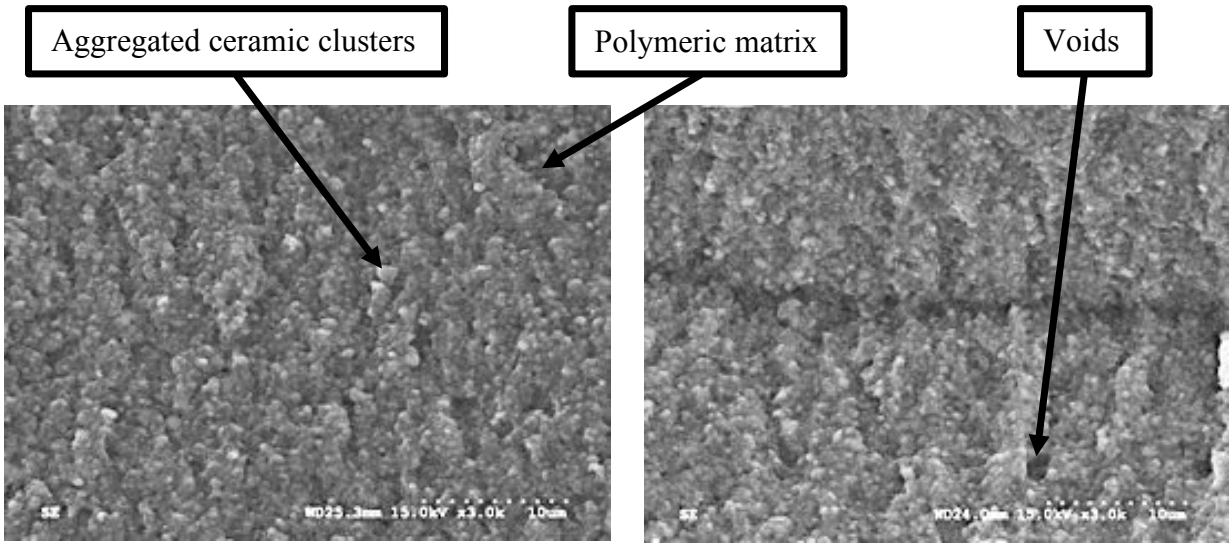

Figure 39: SEM images – CER dry sample; CER aged sample.

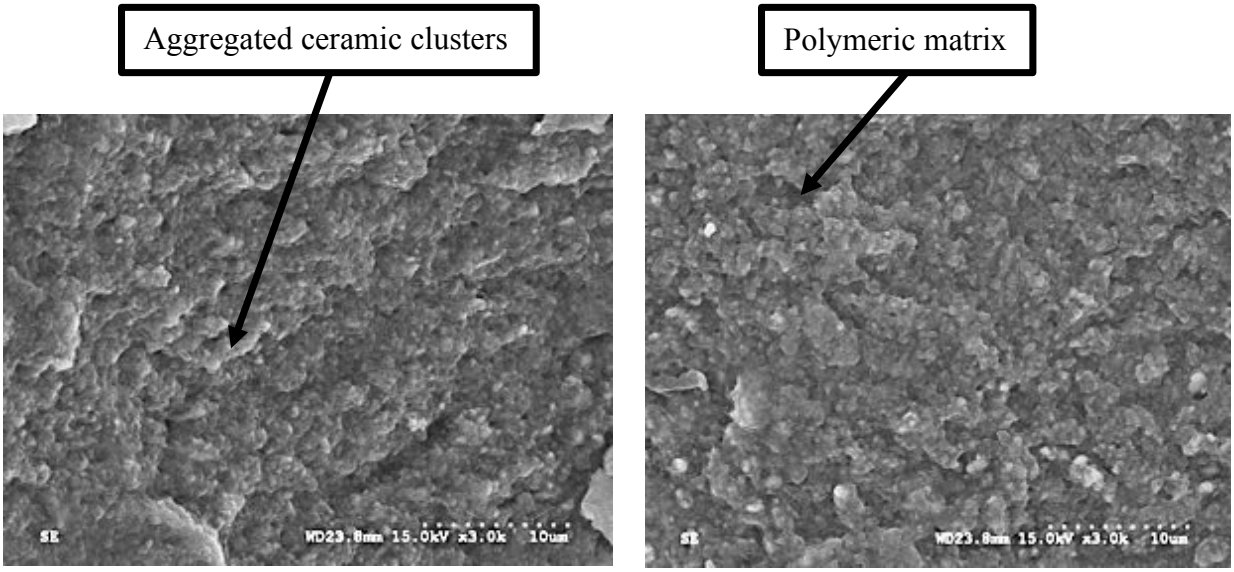

Figure 40. SEM images – KZR dry sample; KZR aged sample

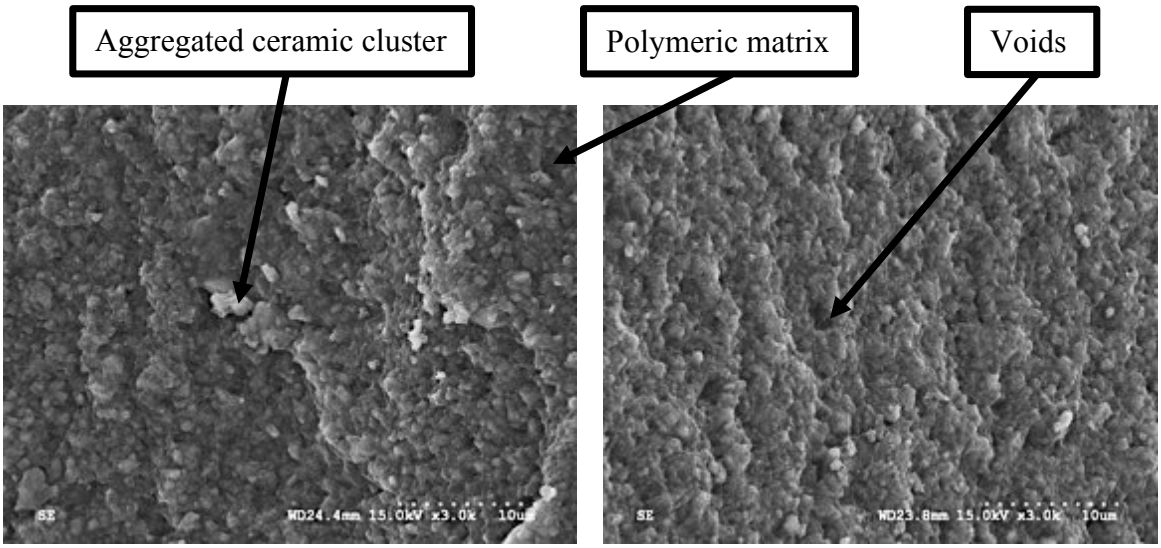

Figure 41. SEM images – CAM dry sample; CAM aged sample

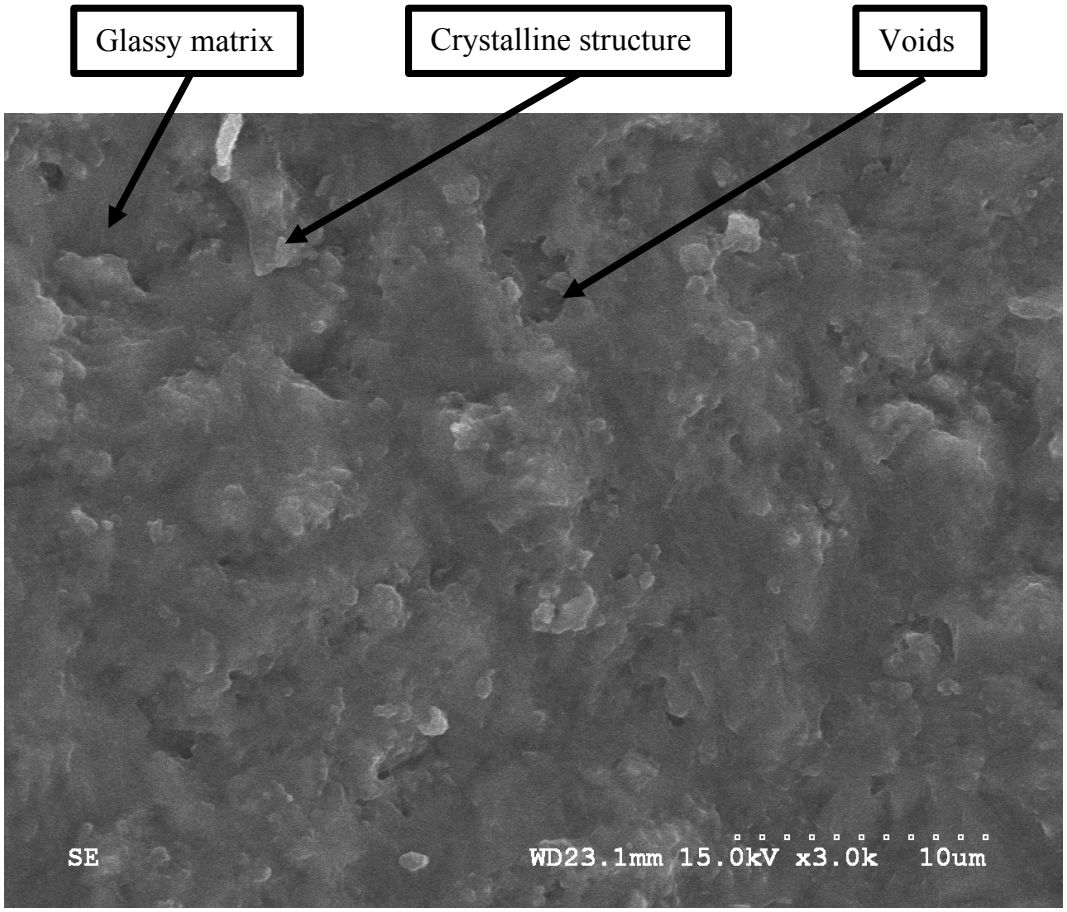

Figure 42: SEM image – OBS sample

Chapter 5: Discussion

Results obtained in this project were in concordance with previous studies that have evaluated some of the same products. More precisely, the σ_f values of VE[2, 4, 104, 176-179] and CER[2, 77, 104, 176] as well as the E_f of VE[2, 4, 177, 180, 181] and CER[2, 77] were within the same range when considering the SD and were similarly obtained with a 3pb test. Such direct comparisons, even within a same test, should be carefully made because of the influence of the tested samples' geometry on strength measurements[158]. Only one study using a biaxial σ_f test revealed similar values for KZR[182]. Results from a biaxial flexure and 3pb test have been found to correlate, although values obtained with the former are usually higher[183]. K_{IC} values of VE[4, 177, 184, 185] were also within the same range although different methods were employed. This brought validity to our results because K_{IC} is a geometrically independent property and therefore direct comparisons can be made. However, for certain properties, some authors reached different results[76, 176, 179], prompting further analysis of possible causes for the data diversity. Table 9 summarizes these observations. Unfortunately, no other research characterizing the mechanical properties of CAM and OBS could be found, thus preventing any direct comparison. Nevertheless, to add validity to the choice of the experimental control material, OBS results were compared to another commercially available lithium disilicate material. Across previous studies, IPS e.max CAD (Vita Zahnfabrik, Germany) material exhibited higher σ_f and K_{IC} and similar E_f values over OBS[4, 76, 186].

Table 9: Compilation of mechanical testing of CAD/CAM blocks

Material	Authors	Condition	σ_f (MPa) [3pb]	E_f (GPa) [3pb]	K_{IC} (MPa·m$^{1/2}$) [method]
VE	Lauvanutanon et al., 2014[2]	Dry	140.7 ± 8.5	28.5 ± 1.1	
		H_20, 7 d	133.0 ± 10.3	28.3 ± 0.8	
	Albero et al., 2015[78]	Dry	180.9 ± 42.2		
	Awada and Nathanson, 2015[77]	Dry	137	21.1	
	Goujat et al., 2017[176]	Dry	148.7 ± 9.5	23.3 ± 6.4	1.4 [SEVNB]
	Lawson et al., 2016[76]	H_20, 1 d	202.1 ± 17.9	21.5 ± 1.6	
	Lim et al., 2016[180]	Dry	126.5 ± 2.7 [B3B]	29.03 ± 2.98	
	Ruse and Sadoun, 2014[4]	Dry	139.68 ± 8.61	27.11 ± 2.23	0.88 ± 0.30 [NTP]
		H_20, 30 d	123.25 ± 8.16		0.96 ± 0.15 [NTP]
	Swain et al., 2016[177]	H_20, 1 d	144.4 ± 9.61	31.7 ± 1.4	1 ± 0.04 [SENVB]
					1.41 ± 0.17 [IS]
	Tsujimoto et al., 2017[104]	H_20, 1 d	143.6 ± 9.7	23.2 ± 1.4	
	Della Bona et al., 2014[184]	Dry			1.09 ± 0.05 [SEVNB]
	Coldea et al., 2015[178]	Dry	152.27 ± 8.91	37.95 ± 0.34	
	Ramos et al., 2018[185]	Mineral oil	159.0 ± 20.6 [B3B]	35.48 ± 0.02	0.86 ± 0.27 [B3B]
	Sonmez et al., 2018[179]	Dry	152.1 ± 2.9	34.7 ± 2.2 [PE]	1.23 ± 0.02 [IF]
CER	Lauvanutanon et al., 2014[2]	Dry	242.0 ± 11.6	10.0 ± 0.2	
		H_20, 7 d	197.3 ± 10.8	9.0 ± 0.2	
	Awada and Nathanson, 2015[77]	Dry	219 ± 20	7.9 ± 0.25	
	Goujat et al., 2017[176]	Dry	216.5 ± 28.3	25.0	1.2 ± 0.17 [SEVNB]
	Lawson et al., 2016[76]	H_20, 1 d	234.5 ± 24.8	12.1 ± 0.8	
	Tsujimoto et al., 2017[104]	H_20, 1 d	197.3 ± 14.2	12.2 ± 1.1	
KZR	Okada et al., 2018[182]	Dry	~230 [B3B]		
		PS, 90°C, 28 d	~170 [B3B]		
CAM	No available data characterizing the mechanical properties				
OBS					
IPS e.max CAD	Ruse and Sadoun, 2014[4, 187]	Dry	353.05 ± 37.52	69.36 ± 6.22	1.79 ± 0.29
	Lawson et al., 2016[76]	Dry	376.9 ± 76.2	67.2 ± 1.3	
	Elsaka and Elnaghy, 2016[186]	Dry	348.33 ± 28.69	60.61 ± 1.64	2.01 ± 0.13 [SEVNB]

B3B: ball-on-three-balls; NTP: notchless triangular prism test; SEVNB: single edge "V" notched beam; IS: indentation strength; IF: indentation fracture; PE: pulse echo method; PS: physiologic saline solution

5.1 Effect of Testing Methodology

Factors such as the method of testing and specimen preparation have already been documented as sources of variation in the σ_f results. In 2010, Quinn and Quinn compared the 3pb and 4pb testing methodologies with a Weibull statistical analysis and found a 21% difference between both tests in favour of the 3pb. In other words, the 3pb test was expected to provide higher results compared to the 4pb for the same material because of the lower probability of encountering critical flaw size in a tested surface area (3pb) versus a volume area (4pb). The friction caused by the support and load points can also have a significant impact on the results as it would superimpose compressive force to the tensile face of the specimen. The use of rigid knife edge supports instead of rollers that are free to roll could lead to an increase of 11% in recorded values. Slight differences in specimen geometry, such as not being perfectly flat or parallel, could lead to misalignment and affect the results in a non-systematic manner[188]. Moreover, the magnitude of the specimen deflection in flexure tests can lead to a span reduction and therefore a systematic overestimation of strength[158]. The higher the σ_f/E ratio is, the higher the deflection at fracture will be. The crosshead testing speed may also have an impact as the inertial response of the testing machine increases with the test speed. Hence, crosshead speed recommendation were set at 0.75 ± 0.25 mm/min[189] and were taken into consideration in the present project. The difficulties of producing miniature size specimens without edge chipping or defect renders the bending test highly technique sensitive. It is sensitive enough that some authors proposed the B3B as an alternative testing method for CAD/CAM RCB strength characterization in order to overcome some of the limitations encountered with the bending strength test[157, 158]. In this study, special attention was given during the sample fabrication to limit any edge imperfections and samples with an observable defect under the microscope were excluded.

The determination of the E_f from a bending test can also be prone to some errors given the fact that some portion of the stress-strain curve may slightly differ from a straight line (as in the case of plastic deformation), thus relying on the judgment of the investigator to determine what line should be drawn from the data[157, 190]. Some authors advocate the combination of static (bending, tension or compression) and dynamic methods (resonant ultrasound spectroscopy and resonant beam technique) to accurately determine the elastic properties of a RC material[191]. In this study, only a static bending method was employed which is a limitation, although our results were concordant with previous studies. The E_f values were manually (segment-cursor) and automatically calculated from the stress-strain curve of a 3pb test and compared.

σ_f and E_f are popular mechanical properties often put forward by the manufacturer to promote new products. However, their testing methodologies are rarely described. Considering the above-mentioned variations, practitioners should exhibit rigor in evaluating the testing parameters in order to make evidenced based decisions. Certainly, these two properties should not be the only criteria used to base the selection of a material for a clinical situation, however this assertion is amplified by the actual lack of consensus for different testing methods[157, 189].

Dental-related articles about fracture mechanics have considerably increased over the last two decades[160] and more manufacturer seem to include the K_{IC} property in promoting their material[158]. Being an inherent material characteristic, K_{IC} is theoretically independent of the specimen geometry and testing modality. As quoted by Cesar et al. (2017), K_{IC} is not sensitive to variables such as the size and density of superficial and internal defects which are controlled by the processing method of the specimens. This clearly contrasts with the fracture strength and contributes towards providing a more detailed analysis of the fracture event as the size and shape of the initiating crack is defined[192].

Nevertheless, K_{IC} characterization is not without challenges and Belli et al. (2018) underscored the dichotomy of the wide range of existing K_{IC} values exceeding experimental error characterizing a material-specific property. The authors mentioned that although some uncontrollable variations may be attributed to the material (batch-to-batch differences, stochastic distribution of structural inhomogeneity), those that result from accumulation of errors in testing should be minimized to improve the accuracy and reproducibility of a method[161]. Further, according to the same authors, errors that occur during testing can be inherent to the method itself or be extrinsic to it. The first category involves sources of error that are individual to each method such as the size of the notch tip root radius (which should be smaller than the microstructural feature acting like a crack), inappropriate bending fixtures, equipment compliance, imprecise alignment of the specimen on the fixture, inaccuracies in numerical solution, etc. The second category concerns aspects that occur independently of the testing method. For instance, the measuring error of the loading cell or microscope resolution for crack length measurement. Some uncertainty is also related to Y_{min} which was estimated to be below 10% for the NTP test. Another potential source of error can occur with the presence of water molecules in contact with the crack tip during testing, resulting in a stress-induced subcritical crack growth (SCCG) and its result lowering effect mostly impacts glassy ceramic and polycrystalline oxide materials. In the present study, OBS material may have been affected by this phenomena since the specimens were tested in ambient air which inevitably contained a certain percentage of humidity. However, whether this lowering effect had a significant impact is unknown. The effect of geometry and resistance curve (R-curve) behaviour on K_{IC} values using quasi-static tests is an important consideration that can influence the performance of a material. The R-curve concept is complex but mainly describes the fracture behaviour which is influenced by the interaction of the growing crack with the

microstructure in brittle material. The R-curve is not an inherent property of a material and therefore its measurement is influenced by the specimen geometry, type of loading and initial crack size[161]. As a consequence, the selection of a K_{IC} method should take into consideration the type and microstructure of material being tested[157].

Mastering a K_{IC} testing technique is instrumental in reducing errors and the convenience of a method can improve the result accuracy and reproducibility. Therefore, a method that simplifies specimen fabrication, does not require any notches and reduces testing compliance such as the NTP test should be promoted[162, 166]. In this project, each group contained a few specimens with crack arrest, without separation, which is an indication of good control of the testing parameters (Figure 36 p.87)[166].

5.2 Effect of Material Composition

The variability of results among selected products found in this study can also be attributed to the material composition, microstructure and manufacturing process[5]. Mechanical properties are inherent characteristics of matrix and filler/network arrangement within a material[4], which can be optimized by the development of new fabrication techniques. This is especially true with the recent high-pressure high temperature (HP/HT) PICN materials, where diverse combinations of matrices/ceramic networks revealed positive impacts on multiple mechanical properties[139] or with the DF materials for which the HT polymerization process enhanced the degree of conversion compared to a light curing process[5, 80].

A polymerization process that combines specific HT and HP parameters has been hypothesized to reduce the size and number of voids and internal stress present in the microstructure of a PICN material which would have a positive impact on crack formation

resistance[137]. This process could contribute towards obtaining a high-density material with a high *Tg* indicating a higher matrix crosslink density[193]. In addition, the HT/HP polymerization process may positively affect the resin-filler interaction in PICN material, a phenomenon thought to have led to the favourable mechanical and physical properties seen in the work of Phan et al. (2014)[138]. Besides the high filler content per volume, the spatial distribution and continuity of the two constituent phases in IPN materials could also contribute towards improving stress distribution and resistance to breakdown[194].

As anticipated, VE testing results obtained in the present research project showed superior mechanical properties compared to classical light cured RC materials[137] and lower σ_f values compared to materials with a higher polymeric content such as CER, CAM and KZR. This is in accordance with Cui et al. (2017) who characterized the mechanical properties of a mixture of pure cured BisGMA/TEGDMA resin with values reflecting high σ_f (179 MPa), low E_f (3.63 GPa) and relatively high K_{IC} (2.27 MPa·m$^{1/2}$). This enabled the analysis of the effect of an enhanced polymerization process solely on the resin matrix properties in a dissociative perspective of the constituents forming an optimized experimental PICN material. The authors affirmed that the contribution of the network impacted the E_f rather than the σ_f and that the ductility of the matrix could explain the toughness values[80]. The majority of the selected materials in the present project contained a mixture of UDMA/TEGDMA. This may have been justified given the advantages of using UDMA over the controversial Bis-GMA such as its lower molecular weight which may result in a higher concentration of double bonds and lower viscosity thought to improve toughness properties and filler incorporation[138]. Nevertheless, differences in matrix composition and manufacturing process are expected to influence the mechanical and physical properties of RCBs.

The variation in V_f of the tested materials may also have influenced their mechanical properties. The K_{IC} values obtained for CER and CAM were lower than expected for materials containing a mixture of UDMA/TEGDMA cured through an industrial polymerization process and with a reasonable amount of filler. Although the V_f of CER was estimated at around 55%, it was unknown for KZR and CAM. Unfortunately, only limited information regarding the composition, microstructure and manufacturing process of these three materials was published by the manufacturer, thus limiting interpretation of the results. Nevertheless, the fact that CER has a filler content per volume at (55%) or not far below (57-65%) the optimal amount respectively identified by Kim et al. (2002)[48] and Ilie et al. (2012)[50] to obtain favourable K_{IC} values for RC materials suggests other explanations, such as a weak or non-optimal filler-resin coupling interface. Hence, crack propagation could have occurred at the matrix/filler interface instead of inside the matrix, thus lowering the necessary energy to produce two new surfaces. This may also explain why these materials were not significantly affected by water ageing since not much of the interface surface was hydrolyzed. Moreover, as Lim et al. (2016) mentioned, increased σ_f properties may result in a wider granulometric distribution of filler which may amplify crack deflection[180].

Considering the difficulties associated with a higher filler incorporation, i.e. past 60% noted by Ilie and Hickel, it is possible that the manufacturing process and curing mode have helped to attain a higher V_f without too significantly compromising the internal structural integrity with voids and defects as seen with VE K_{IC} results and SEM images[8].

VE, which had the highest known filler content, obtained the highest E_f (~33 GPa) values among the RCBs and the closest to natural dentin. This was not surprising considering that the E_f increases exponentially with the inorganic filler content properly silanized or chemically linked to the polymeric matrix. Conversely, a lower filler content and/or higher matrix content would justify

a lower range (~8-12 GPa) value for DF RCB. Such results are well below that of natural dentin and hypothesized to incur restorative deformation under load, accelerated wear and hoop stress causing crown debonding[8, 76]. Similarly to Lim et al. (2016), it was noticed that the VE 3pb samples fractured with lesser fragments compared to other RCBs, which may be suggestive of the materials' ability to endure more mechanical stress and elastic deformation before fracture[180].

Similarly, lower than anticipated results were observed for OBS, a material that is allegedly classified by the manufacturer as lithium silicate material with a biaxial σ_f of 385 ± 45 MPa. Although very limited information is available regarding OBS material, the SEM images of the fractured surfaces showed a large glassy matrix embedding a reduced crystal phase with the presence of visible voids and defects. Moreover, the surface roughness in the zone of slow crack propagation was relatively smooth which suggests that the crack may have propagated in the glassy matrix instead of being impeded by the presence of crystals. This could explain the relatively low σ_f and K_{IC} values for this type of material, perhaps the result of an incomplete crystallization process[159].

As materials of different shades were compared with each other, the shade of the material may have had an impact on the results. Differences in light transmission of a RC is inherent in the refraction index between the filler particles and the matrix. The character, content, amount and size of the particles impact the refractive index, so CAD/CAM blocks of different shades but made of the same material may exhibit different mechanical properties[119]. Further research comparing the mechanical/physical properties of the same material but with different shades, as well as the possible anisotropic properties of a colour gradient material, is suggested.

5.3 Effect of Water Ageing

Water sorption of RC materials is known to have the potential to degrade its constituents (matrix, filler and especially the coupling interface) and negatively affect its mechanical properties[59, 65, 103]. In this regard, a brief review of the influencing factors was presented in the introduction (p. 23). In this project, water ageing had the anticipated effect and all σ_f and E_f means significantly decreased with the exception of VE material for which no significant difference was noted in E_f. These results could be explained by the hydrolysis of the matrix/filler coupling interface combined with water penetration in the matrix causing the network to soften and swell as well as a reduction of frictional forces between the polymer chains[2, 58]. These findings support similar studies that tested the same products under water ageing conditions[2, 4, 195].

Paradoxically, ageing significantly increased K_{IC} results for VE and the SEM images revealed a fracture pattern that appeared rougher for aged samples compared to dry. This observation corroborates results for which extra energy was needed to create coarser surfaces. However, to objectively assess the topography of the fractured surfaces, a profilometer would have been a useful tool. Nevertheless, according to Drummond (2008), an increase in K_{IC} for aged RC may be attributed to the effect of internal stress release and the increase of the plastic zone ahead of a propagating crack[59]. Whether this assertion is applicable for all types of RCBs remains to be verified because only the PICN material (VE) demonstrated an increase in K_{IC} in this research project. The answer may partly reside in the degradation of the filler/matrix interface and/or matrix degradation which inevitably represents a higher surface and volume, respectively, with the DF material compared to a PICN material. The effect of spatial distribution and continuity of the two constituent phases as well as the matrix/filler interaction discussed earlier, typical of PICN materials, may also contribute to reversing the deleterious effect of a relatively prolonged water

ageing period on K_{IC}. KZR is the only DF material that had its K_{IC} significantly lowered after ageing. Interestingly, it is the only material containing fluoride ions engineered for the purpose of sustained release. Such release logically suggests that the material loses integrity with time, which can lead to internal changes and accelerated degradation in a wet environment, although such impact should be precisely investigated. Moreover, it is possible that the coupling interface in KZR, which was initially good, degraded rapidly under the influence of water. In line with the presented results, the SEM images of KZR presented a rougher pattern of the fractured dry sample compared to aged.

5.3.1 Weibull Analysis

Weibull analysis of the σ_f and K_{IC} results yielded interesting findings. Despite some fluctuation, the data distribution showed a linear trend which suggested the presence of different family types of flaws in the tested materials. The homogeneity of flaw distribution in the entire volume of a material can be characterized by a higher modulus which, in turn, resulted in higher structural reliability and lower failure probability[172]. In other words, a difference in the Weibull coefficient indicated a difference in flaw population and a lower Weibull characteristic suggested the presence of bigger flaw size for a similar specimen size and for a given test.

The effect of water ageing seemed to have considerably improved the σ_f reliability of two DF materials (CER and KZR) despite a significant Weibull characteristic drop. This again suggested the presence of a stress relaxation mechanism from the polymeric matrix caused by water absorption and the degradation that it caused. Moreover, even after ageing, VE was the most reliable material. As mentioned above, this may have been due to the polymer phase that distributed plastic deformation during loading with the effect of increasing crack resistance[180].

Weibull analysis of K_{IC} results showed a decrease in reliability for all RCBs except KZR that showed improvement despite a dramatic decrease in characteristic value. Conversely, the characteristic value of VE increased but the material was less reliable after ageing. These observations might be explained by the difference in microstructure as discussed earlier.

When using materials that saw their reliability increased and characteristic strength decreased after ageing, one could consider oversizing the design of a restoration, i.e. by slightly increasing the thickness, to accommodate for the drop in strength while still benefiting from an increase in reliability.

5.4 Future Predictions and Recommendations

One of the goals of a restorative material is to mimic the properties of tooth structure (dentin and enamel) to ultimately provide a durable, functional and esthetic alternative for that which has been lost. However, no known material has successfully fulfilled this task to the level achieved by nature. Nevertheless, PICN material such as VE has revealed itself to be truly innovative and stood out from the DF RCBs in several ways. Promising work has been conducted trying to improve/refine the constituents' balance and optimize the polymerization parameters of this new class of material[4, 80, 99, 137-139, 193, 196]. Material with anisotropic properties may also represent a new niche of research, again propelled by CAD/CAM technology's popularity and PICN innovation[126].

Very few short term clinical trials have been conducted with the aim to study the in-vivo behaviour of RCB restorations. Despite some arguable initial success for certain types of restorations (inlays/onlays), attempting any generalization with regards to the use of these materials as a prescribed standard of care would be very much premature[35]. At this point,

CAD/CAM RCBs are, in my personal opinion, a viable option for long-term provisional crowns and onlays. This is considering their similarities with the direct and indirect light cured RC materials but also the availability of material with superior mechanical properties such as glass-ceramic/ceramics and polycrystalline ceramics. Interestingly, Hussain et al. (2017) did not find the use of RCBs to be favorable over conventional resin[118]. Clearly, the high debonding rate observed for crowns made of Lava Ultimate (3M ESPE, USA), as mentionned in the introduction, should inspire caution among not only practitioners but also manufacturers.

In light of the results obtained in this research project and the literature consulted to the elaboration of this thesis, a few personal observations/recommendations that could have enhanced the level of evidence include:

1. Many new products lack independent research characterizing their mechanical properties. Often, the only available data is from the manufacturer which poses a risk of bias. Also, the publication of meaningful mechanical properties such as K_{IC} and cyclic fatigue is still lacking;
2. The majority of the RCBs are marketed with very restricted information regarding their exact constituents, manufacturing process and testing parameters which limit further analysis;
3. More evidence-based uniformity regarding in-vitro mechanical properties testing is required to permit large scale comparisons. This also includes ageing parameters for which thermocycling and long-term storage have been found to impact the results;
4. More clinical research, ideally RCTs, should be performed before and after the commercialization of new CAD/CAM RCBs.

Chapter 6: Conclusion

The statistical analysis of the evaluated mechanical properties revealed a significant difference among the tested CAD/CAM blocks for σ_f but not unanimously for E_f and K_{IC}. More precisely, PICN exhibited significantly lower σ_f and higher E_f values compared to DF materials, while for K_{IC} only one DF (KZR) was found to be superior. The ceramic CAD/CAM block exhibited superior σ_f, E_f and K_{IC} compared to the RCBs, with the exception of KZR which had similar K_{IC} values. Therefore, the first null hypothesis, that there is no significant difference between the different materials regarding their σ_f, E_f and K_{IC}, could not be fully rejected. Similarly, ageing in 37 °C water for 30 d had a significant negative effect on σ_f, but not on E_f and K_{IC} of the different RCBs and therefore cannot justify the total rejection of the second null hypothesis. Contrary to DF materials, ageing did not significantly affect E_f of PICN, although this may not be of clinical significance. With regards to K_{IC}, ageing significantly lowered KZR values while it improved those of the PICN material. In light of the characterization of mechanical properties, PICN material distinguished itself over DF materials but without surpassing glass-ceramic blocks. The selection of any restorative material requires a thorough analysis of its advantages and limitations to inform the clinical decision in a case-by-case approach.

Bibliography

[1] van Noort R. The future of dental devices is digital. Dental materials. 2012;28:3-12.

[2] Lauvanutanon S, Takahashi H, Shiozawa M, Iwasaki N, Asakawal Y, Oki M, et al. Mechanical properties of composite resin blocks for CAD/CAM. Dental materials journal. 2014;33:705-10.

[3] Spitznagel FA, Horvath SD, Guess PC, Blatz MB. Resin bond to indirect composite and new ceramic/polymer materials: a review of the literature. Journal of esthetic and restorative dentistry. 2014;26:382-93.

[4] Ruse ND, Sadoun MJ. Resin-composite Blocks for Dental CAD/CAM Applications. Journal of dental research. 2014;93:1232-4.

[5] Mainjot AK, Dupont NM, Oudkerk JC, Dewael TY, Sadoun MJ. From Artisanal to CAD-CAM Blocks: State of the Art of Indirect Composites. Journal of dental research. 2016;95:487-95.

[6] Ferracane JL. Resin-based composite performance: are there some things we can't predict? Dental materials. 2013;29:51-8.

[7] Bayne SC. Correlation of clinical performance with 'in vitro tests' of restorative dental materials that use polymer-based matrices. Dental materials. 2012;28:52-71.

[8] Ilie N, Hickel R. Investigations on mechanical behaviour of dental composites. Clinical oral investigations. 2009;13:427-38.

[9] 3M ESPE. Lava™ Ultimate CAD/CAM Restorative; 2012 [Cited Sept 16th, 2018]. Available from: https://www.3m.com/3M/en_US/dental-us/products/lava-ultimate/.

[10] Zimmermann M, Koller C, Reymus M, Mehl A, Hickel R. Clinical Evaluation of Indirect Particle-Filled Composite Resin CAD/CAM Partial Crowns after 24 Months. Journal of prosthodontics. 2017;00:1-6.

[11] Schepke U, Meijer HJ, Vermeulen KM, Raghoebar GM, Cune MS. Clinical Bonding of Resin Nano Ceramic Restorations to Zirconia Abutments: A Case Series within a Randomized Clinical Trial. Clinical implant dentistry and related research. 2016;18:984-92.

[12] Vanoorbeek S, Vandamme K, Lijnen I, Naert I. Computer-aided designed/computer-assisted manufactured composite resin versus ceramic single-tooth restorations: a 3-year clinical study. The International journal of prosthodontics. 2010;23:223-30.

[13] Beck F, Lettner S, Graf A, Bitriol B, Dumitrescu N, Bauer P, et al. Survival of direct resin restorations in posterior teeth within a 19-year period (1996-2015): A meta-analysis of prospective studies. Dental materials. 2015;31:958-85.

[14] Demarco FF, Correa MB, Cenci MS, Moraes RR, Opdam NJ. Longevity of posterior composite restorations: not only a matter of materials. Dental materials. 2012;28:87-101.

[15] Heintze SD, Rousson V. Clinical effectiveness of direct class II restorations - a meta-analysis. The journal of adhesive dentistry. 2012;14:407-31.

[16] Heintze SD, Ilie N, Hickel R, Reis A, Loguercio A, Rousson V. Laboratory mechanical parameters of composite resins and their relation to fractures and wear in clinical trials-A systematic review. Dental materials. 2017;33:e101-e14.

[17] Peutzfeldt A, Asmussen E. Modulus of resilience as predictor for clinical wear of restorative resins. Dental materials. 1992;8:146-8.

[18] De Groot R, Van Elst HC, Peters MC. Fracture mechanics parameters for failure prediction of composite resins. Journal of dental research. 1988;67:919-24.

[19] Truong VT, Tyas MJ. Prediction of in vivo wear in posterior composite resins: a fracture mechanics approach. Dental materials. 1988;4:318-27.

[20] Miyazaki T, Hotta Y. CAD/CAM systems available for the fabrication of crown and bridge restorations. Australian dental journal. 2011;56 Suppl 1:97-106.

[21] Fasbinder DJ. Restorative material options for CAD/CAM restorations. Compendium of continuing education in dentistry (Jamesburg, NJ : 1995). 2002;23:911-6, 8, 20 passim; quiz 24.

[22] Tapie L, Lebon N, Mawussi B, Fron Chabouis H, Duret F, Attal JP. Understanding dental CAD/CAM for restorations--the digital workflow from a mechanical engineering viewpoint. International journal of computerized dentistry. 2015;18:21-44.

[23] Lebon N, Tapie L, Duret F, Attal JP. Understanding dental CAD/CAM for restorations - dental milling machines from a mechanical engineering viewpoint. Part A: chairside milling machines. International journal of computerized dentistry. 2016;19:45-62.

[24] Lebon N, Tapie L, Duret F, Attal JP. Understanding dental CAD/CAM for restorations--dental milling machines from a mechanical engineering viewpoint. Part B: labside milling machines. International journal of computerized dentistry. 2016;19:115-34.

[25] Miyazaki T, Hotta Y, Kunii J, Kuriyama S, Tamaki Y. A review of dental CAD/CAM: current status and future perspectives from 20 years of experience. Dental materials journal. 2009;28:44-56.

[26] Albuha Al-Mussawi RM, Farid F. Computer-Based Technologies in Dentistry: Types and Applications. Journal of dentistry. 2016;13:215-22.

[27] Blackwell E, Nesbit M, Petridis H. Survey on the use of CAD-CAM technology by UK and Irish dental technicians. British dental journal. 2017;222:689-93.

[28] Zaruba M, Mehl A. Chairside systems: a current review. International journal of computerized dentistry. 2017;20:123-49.

[29] Solaberrieta E, Arias A, Brizuela A, Garikano X, Pradies G. Determining the requirements, section quantity, and dimension of the virtual occlusal record. The Journal of prosthetic dentistry. 2016;115:52-6.

[30] Solaberrieta E, Garmendia A, Brizuela A, Otegi JR, Pradies G, Szentpetery A. Intraoral Digital Impressions for Virtual Occlusal Records: Section Quantity and Dimensions. BioMed research international. 2016;2016:7173824.

[31] Khraishi H, Duane B. Evidence for use of intraoral scanners under clinical conditions for obtaining full-arch digital impressions is insufficient. Evidence-based dentistry. 2017;18:24-5.

[32] Fasbinder DJ. Materials for chairside CAD/CAM restorations. Compendium of continuing education in dentistry (Jamesburg, NJ : 1995). 2010;31:702-4, 6, 8-9.

[33] Anusavice KJ, Shen C, Rawls HR. Phillips' science of dental materials: Elsevier Health Sciences; 2013.

[34] Ilie N, Hickel R. Resin composite restorative materials. Australian dental journal. 2011;56 Suppl 1:59-66.

[35] Ferracane JL. Resin composite--state of the art. Dental materials. 2011;27:29-38.

[36] Darvell BW. Materials Science for Dentistry. 9th ed: Woodhead Publishing Limited. 2009.

[37] Klapdohr S, Moszner N. New inorganic component for dental filling composites. Monatshefte für Chemie / Chemical Monthly. 2005;136:21–45.

[38] Randolph LD, Palin WM, Leloup G, Leprince JG. Filler characteristics of modern dental resin composites and their influence on physico-mechanical properties. Dental materials. 2016;32:1586-99.

[39] Cramer NB, Stansbury JW, Bowman CN. Recent advances and developments in composite dental restorative materials. Journal of dental research. 2011;90:402-16.

[40] Ruse ND. What is a "compomer"? Journal of the Canadian Dental Association. 1999;65:500-4.

[41] Willems G, Lambrechts P, Braem M, Celis JP, Vanherle G. A classification of dental composites according to their morphological and mechanical characteristics. Dental materials. 1992;8:310-9.

[42] Gajewski VE, Pfeifer CS, Froes-Salgado NR, Boaro LC, Braga RR. Monomers used in resin composites: degree of conversion, mechanical properties and water sorption/solubility. Brazilian dental journal. 2012;23:508-14.

[43] Ilie N, Hickel R. Macro-, micro- and nano-mechanical investigations on silorane and methacrylate-based composites. Dental materials. 2009;25:810-9.

[44] Masouras K, Silikas N, Watts DC. Correlation of filler content and elastic properties of resin-composites. Dental materials. 2008;24:932-9.

[45] Balos S, Pilic B, Petronijevic B, Markovic D, Mirkovic S, Sarcev I. Improving mechanical properties of flowable dental composite resin by adding silica nanoparticles. Vojnosanitetski pregled. 2013;70:477-83.

[46] Kahler B, Kotousov A, Swain MV. On the design of dental resin-based composites: a micromechanical approach. Acta biomaterialia. 2008;4:165-72.

[47] Sabbagh J, Ryelandt L, Bacherius L, Biebuyck JJ, Vreven J, Lambrechts P, et al. Characterization of the inorganic fraction of resin composites. Journal of oral rehabilitation. 2004;31:1090-101.

[48] Kim KH, Ong JL, Okuno O. The effect of filler loading and morphology on the mechanical properties of contemporary composites. The Journal of prosthetic dentistry. 2002;87:642-9.

[49] Sakaguchi RL, Wiltbank BD, Murchison CF. Prediction of composite elastic modulus and polymerization shrinkage by computational micromechanics. Dental materials. 2004;20:397-401.

[50] Ilie N, Hickel R, Valceanu AS, Huth KC. Fracture toughness of dental restorative materials. Clinical oral investigations. 2012;16:489-98.

[51] Sideridou ID, Karabela MM. Effect of the amount of 3-methacyloxypropyltrimethoxysilane coupling agent on physical properties of dental resin nanocomposites. Dental materials. 2009;25:1315-24.

[52] Elshereksi NW, Ghazali M, Muchtar A, Azhari CH. Review of titanate coupling agents and their application for dental composite fabrication. Dental materials journal. 2017;36:539-52.

[53] Mohsen NM, Craig RG. Effect of silanation of fillers on their dispersability by monomer systems. Journal of oral rehabilitation. 1995;22:183-9.

[54] Aydinoglu A, Yoruc ABH. Effects of silane-modified fillers on properties of dental composite resin. Materials science & engineering C, Materials for biological applications. 2017;79:382-9.

[55] Ferracane JL, Antonio RC, Matsumoto H. Variables affecting the fracture toughness of dental composites. Journal of dental research. 1987;66:1140-5.

[56] Peutzfeldt A. Resin composites in dentistry: the monomer systems. European journal of oral sciences. 1997;105:97-116.

[57] Lovell LG, Lu H, Elliott JE, Stansbury JW, Bowman CN. The effect of cure rate on the mechanical properties of dental resins. Dental materials. 2001;17:504-11.

[58] Ferracane JL, Berge HX, Condon JR. In vitro aging of dental composites in water--effect of degree of conversion, filler volume, and filler/matrix coupling. Journal of biomedical materials research. 1998;42:465-72.

[59] Drummond JL. Degradation, fatigue, and failure of resin dental composite materials. Journal of dental research. 2008;87:710-9.

[60] Drummond JL, Miescke KJ. Weibull models for the statistical analysis of dental composite data: aged in physiologic media and cyclic-fatigued. Dental materials. 1991;7:25-9.

[61] Arikawa H, Kuwahata H, Seki H, Kanie T, Fujii K, Inoue K. Deterioration of mechanical properties of composite resins. Dental materials journal. 1995;14:78-83.

[62] Hahnel S, Henrich A, Burgers R, Handel G, Rosentritt M. Investigation of mechanical properties of modern dental composites after artificial aging for one year. Operative dentistry. 2010;35:412-9.

[63] Soderholm KJ, Roberts MJ. Influence of water exposure on the tensile strength of composites. Journal of dental research. 1990;69:1812-6.

[64] Oysaed H, Ruyter IE. Composites for use in posterior teeth: mechanical properties tested under dry and wet conditions. Journal of biomedical materials research. 1986;20:261-71.

[65] Ferracane JL, Hopkin JK, Condon JR. Properties of heat-treated composites after aging in water. Dental materials. 1995;11:354-8.

[66] Sarrett DC, Soderholm KJ, Batich CD. Water and abrasive effects on three-body wear of composites. Journal of dental research. 1991;70:1074-81.

[67] Lloyd CH. The fracture toughness of dental composites. III. The effect of environment upon the stress intensification factor (KIC) after extended storage. Journal of oral rehabilitation. 1984;11:393-8.

[68] Pilliar RM, Vowles R, Williams DF. The effect of environmental aging on the fracture toughness of dental composites. Journal of dental research. 1987;66:722-6.

[69] Soderholm KJ, Mukherjee R, Longmate J. Filler leachability of composites stored in distilled water or artificial saliva. Journal of dental research. 1996;75:1692-9.

[70] Calais JG, Soderholm KJ. Influence of filler type and water exposure on flexural strength of experimental composite resins. Journal of dental research. 1988;67:836-40.

[71] Darvell BW. Material Science for Dentistry. 9th ed: Woodhead Publishing Limited. 2009.

[72] Asaoka K, Hirano S. Diffusion coefficient of water through dental composite resin. Biomaterials. 2003;24:975-9.

[73] Poticny DJ, Klim J. CAD/CAM in-office technology: innovations after 25 years for predictable, esthetic outcomes. Journal of the American Dental Association. 2010;141 Suppl 2:5s-9s.

[74] 3M ESPE. 3M Paradigm MZ100 block – Technical Product Profile; 2000 [cited Aug 28th, 2017]. Available from: http://multimedia.3m.com/mws/media/77596O/paradigmtm-mz100-block-for-cerecr-technical-product-profile.pdf.

[75] Creamed. AMBARINO High Class hybrid ceramics - Technical data sheet; 2008 [Cited Sept 16th, 2018]. Available from: https://creamed.jimdo.com/.

[76] Lawson NC, Bansal R, Burgess JO. Wear, strength, modulus and hardness of CAD/CAM restorative materials. Dental materials. 2016.

[77] Awada A, Nathanson D. Mechanical properties of resin-ceramic CAD/CAM restorative materials. The Journal of prosthetic dentistry. 2015;114:587-93.

[78] Albero A, Pascual A, Camps I, Grau-Benitez M. Comparative characterization of a novel cad-cam polymer-infiltrated-ceramic-network. Journal of clinical and experimental dentistry. 2015;7:e495-500.

[79] Vita Zahnfabrik. Vita Enamic® - Product Information; 2013 [Cited Sept 16th. 2018]. Available from: http://vitanorthamerica.com/products/cadcam/vita-enamic/.

[80] Cui B, Li J, Wang H, Lin Y, Shen Y, Li M, et al. Mechanical properties of polymer-infiltrated-ceramic (sodium aluminum silicate) composites for dental restoration. Journal of dentistry. 2017;62:91-7.

[81] Vericom. Polyglass Blank - Hybrid Ceramic for CAD/CAM; 2013 [Cited Sept 15th, 2018]. Available from: https://vericom.en.ec21.com/.

[82] Dental Laboratory Milling Supplies. Crystal Ultra - Dental CAD/CAM Material; 2013 [Cited Sept 16th, 2018]. Available from: http://crystalultra.com/.

[83] Knight Dental Group. NanoCera Advanced - Hybrid Ceramic; 2014 [Cited Sept 16th, 2018]. Available from: http://www.knightdentalgroup.com/subpage_product_Studio.php?ProductID=49.

[84] Yamakin Co. Hybrid Ceramics Block for CAD/CAM Use - Developed from Ceramics Cluster Filler, YAMAKIN's Unique Material - KZR-CAD HR; 2014 [Cited Sept 14th, 2018]. Available from: https://www.yamakin-global.com/kzr_cad_hr2/index.html.

[85] GC Corp. Cerasmart from GC - The new hybrid ceramic CAD/CAM solution; 2014 [Cited Sept 14th, 2018]. Available from: https://www.gceurope.com/fr/products/cerasmart/.

[86] Yamakin Co. Hybrid Ceramics Block for CAD/CAM Use - KZR-CAD HR2; 2015 [Cited Sept 14th, 2018]. Available from: https://www.yamakin-global.com/kzr_cad_hr2/index.html.

[87] Shofu Dental Corp. Shofu Block and Disk HC - CAD/CAM Ceramic Based Restorative; 2015 [Cited Sept 15th, 2018]. Available from: http://www.shofu.com/en/products/ceramics-dentures/new/shofu-block-disk-hc/.

[88] Coltène. Brillant Crios - Reinforced Composite Bloc for Permanent Restoration; 2016 [Cited Sept 15th, 2018]. Available from: https://www.coltene.com/pim/DOC/BRO/docbro60021815-06-16-en-brilliant-crios-product-guideline-viewsenaindv1.pdf.

[89] DMG Chemisch-Pharmazeutische Fabrik GmbH. LuxaCam Composite - Round / Block; 2016 [Cited Sept 16th, 2018]. Available from: https://www.dmg-dental.com/fileadmin/user_upload/International/Instructions_for_use/GI_LuxaCamRondeBlock_092010_int.pdf.

[90] Vita Zahnfabrik. VITA ENAMIC® multiColor - Product Information; 2017 [Cited Sept 16th, 2018]. Available from: https://www.vitanorthamerica.com/en-US/VITA-ENAMIC-multiColor-276.html.

[91] US FDA. Mazic Duro Premarket Notification; 2017 [Cited Sept 16th, 2018]. Available from: https://www.accessdata.fda.gov/scripts/cdrh/cfdocs/cfpmn/pmn.cfm?ID=K163346

[92] COCERAM Medical Ceramics GmbH. Nacera® Hybrid CAD/CAM system; 2017 [Cited Sept 16th, 2018]. Available from: http://nacera-hybrid.de/en/.

[93] Glidewell Dental Laboratories. CAMouflage® NOW Milling Blocks - Product information; 2017 [Cited Sept 16th, 2018]. Available from: https://glidewelldental.com/services/composites/camouflage-now

[94] Noritake K. Katana Avencia block - Product Information; 2017 [Cited Sept 16th, 2018] Available from: https://www.kuraraynoritake.jp/product/cad_material/katana_avensia_block_ce.html.

[95] Voco GmbH. Grandio Block - Nano-Hybrid composite CAD/CAM block - Product Information; 2017 [Cited Sept 16th, 2018]. Available from: https://www.voco.dental/en/digital/material/cad-cam-material.aspx.

[96] FGM Produtos Odontológicos. Brava Block - Product Information; 2018 [Cited Sept 16th, 2018]. Available from: http://www.fgm.ind.br/site/produtos/estetica-en/brava-block/?lang=en.

[97] Tokuyama Dental. Estelite Block - Product Information; 2017 [Cited Sept 16th, 2018]. Available from: https://www.tokuyama-dental.co.jp/products/product244.html.

[98] Ivoclar Vivadent AG. Tetric® CAD - Scientific Documentation; 2017 [Cited Sept 16th, 2018]. Available from: http://mena.ivoclarvivadent.com/en-me/p/laboratory-professionals/tetric-cad.

[99] Nguyen JF, Migonney V, Ruse ND, Sadoun M. Properties of experimental urethane dimethacrylate-based dental resin composite blocks obtained via thermo-polymerization under high pressure. Dental materials. 2013;29:535-41.

[100] Kamonkhantikul K, Arksornnukit M, Lauvahutanon S, Takahashi H. Toothbrushing alters the surface roughness and gloss of composite resin CAD/CAM blocks. Dental materials journal. 2016;35:225-32.

[101] Giordano RA. Modern Indirect Restorations: The Right Material for Every Situation. Compendium of continuing education in dentistry. 2016;37:656-8.

[102] Kim JE, Kim JH, Shim JS, Roh BD, Shin Y. Effect of air-particle pressures on the surface topography and bond strengths of resin cement to the hybrid ceramics. Dental materials journal. 2017;36:454-60.

[103] Lauvahutanon S, Shiozawa M, Takahashi H, Iwasaki N, Oki M, Finger WJ, et al. Discoloration of various CAD/CAM blocks after immersion in coffee. Restorative dentistry & endodontics. 2017;42:9-18.

[104] Tsujimoto A, Barkmeier WW, Takamizawa T, Latta MA, Miyazaki M. Influence of Thermal Cycling on Flexural Properties and Simulated Wear of Computer-aided Design/Computer-aided Manufacturing Resin Composites. Operative dentistry. 2017;42:101-10.

[105] Tsitrou EA, Northeast SE, van Noort R. Brittleness index of machinable dental materials and its relation to the marginal chipping factor. Journal of dentistry. 2007;35:897-902.

[106] He LH, Swain M. A novel polymer infiltrated ceramic dental material. Dental materials. 2011;27:527-34.

[107] Gordan VV, Garvan CW, Blaser PK, Mondragon E, Mjor IA. A long-term evaluation of alternative treatments to replacement of resin-based composite restorations: results of a seven-year study. Journal of the American Dental Association (1939). 2009;140:1476-84.

[108] Saygili G, Sahmali S, Demirel F. Colour stability of porcelain repair materials with accelerated ageing. Journal of oral rehabilitation. 2006;33:387-92.

[109] Elsaka SE. Repair bond strength of resin composite to a novel CAD/CAM hybrid ceramic using different repair systems. Dental materials journal. 2015;34:161-7.

[110] El Zohairy AA, De Gee AJ, Mohsen MM, Feilzer AJ. Microtensile bond strength testing of luting cements to prefabricated CAD/CAM ceramic and composite blocks. Dental materials. 2003;19:575-83.

[111] Van Noort R, Noroozi S, Howard IC, Cardew G. A critique of bond strength measurements. Journal of dentistry. 1989;17:61-7.

[112] Scherrer SS, Cesar PF, Swain MV. Direct comparison of the bond strength results of the different test methods: a critical literature review. Dental materials. 2010;26:e78-93.

[113] Bakopoulou A, Papadopoulos T, Garefis P. Molecular toxicology of substances released from resin-based dental restorative materials. International journal of molecular sciences. 2009;10:3861-99.

[114] Van Landuyt KL, Nawrot T, Geebelen B, De Munck J, Snauwaert J, Yoshihara K, et al. How much do resin-based dental materials release? A meta-analytical approach. Dental materials. 2011;27:723-47.

[115] Ruse N. Fracture mechanics characterization of dental biomaterials. Dental Biomaterials: Imaging, Testing and Modelling. 2014:261.

[116] Grenade C, De Pauw-Gillet MC, Pirard C, Bertrand V, Charlier C, Vanheusden A, et al. Biocompatibility of polymer-infiltrated-ceramic-network (PICN) materials with Human Gingival Keratinocytes (HGKs). Dental materials. 2017;33:333-43.

[117] Tassin M, Bonte E, Loison-Robert LS, Nassif A, Berbar T, Le Goff S, et al. Effects of High-Temperature-Pressure Polymerized Resin-Infiltrated Ceramic Networks on Oral Stem Cells. PloS one. 2016;11:e0155450.

[118] Hussain B, Thieu MKL, Johnsen GF, Reseland JE, Haugen HJ. Can CAD/CAM resin blocks be considered as substitute for conventional resins? Dental materials. 2017;33:1362-70.

[119] Stawarczyk B, Liebermann A, Eichberger M, Guth JF. Evaluation of mechanical and optical behavior of current esthetic dental restorative CAD/CAM composites. Journal of the mechanical behavior of biomedical materials. 2016;55:1-11.

[120] Guth JF, Zuch T, Zwinge S, Engels J, Stimmelmayr M, Edelhoff D. Optical properties of manually and CAD/CAM-fabricated polymers. Dental materials journal. 2013;32:865-71.

[121] Mormann WH, Stawarczyk B, Ender A, Sener B, Attin T, Mehl A. Wear characteristics of current aesthetic dental restorative CAD/CAM materials: two-body wear, gloss retention, roughness and Martens hardness. Journal of the mechanical behavior of biomedical materials. 2013;20:113-25.

[122] Gracis SE, Nicholls JI, Chalupnik JD, Yuodelis RA. Shock-absorbing behavior of five restorative materials used on implants. The International journal of prosthodontics. 1991;4:282-91.

[123] Soumeire J, Dejou J. Shock absorbability of various restorative materials used on implants. Journal of oral rehabilitation. 1999;26:394-401.

[124] Rohr N, Coldea A, Zitzmann NU, Fischer J. Loading capacity of zirconia implant supported hybrid ceramic crowns. Dental materials. 2015;31:e279-88.

[125] Coldea A, Swain MV, Thiel N. Mechanical properties of polymer-infiltrated-ceramic-network materials. Dental materials. 2013;29:419-26.

[126] Petrini M, Ferrante M, Su B. Fabrication and characterization of biomimetic ceramic/polymer composite materials for dental restoration. Dental materials. 2013;29:375-81.

[127] Ichim IP, Schmidlin PR, Li Q, Kieser JA, Swain MV. Restoration of non-carious cervical lesions Part II. Restorative material selection to minimise fracture. Dental materials. 2007;23:1562-9.

[128] Ausiello P, Rengo S, Davidson CL, Watts DC. Stress distributions in adhesively cemented ceramic and resin-composite Class II inlay restorations: a 3D-FEA study. Dental materials. 2004;20:862-72.

[129] Studart AR, Filser F, Kocher P, Gauckler LJ. Fatigue of zirconia under cyclic loading in water and its implications for the design of dental bridges. Dental materials. 2007;23:106-14.

[130] Studart AR, Filser F, Kocher P, Gauckler LJ. In vitro lifetime of dental ceramics under cyclic loading in water. Biomaterials. 2007;28:2695-705.

[131] Dejak B, Mlotkowski A. A comparison of stresses in molar teeth restored with inlays and direct restorations, including polymerization shrinkage of composite resin and tooth loading during mastication. Dental materials. 2015;31:e77-87.

[132] Boaro LC, Goncalves F, Guimaraes TC, Ferracane JL, Pfeifer CS, Braga RR. Sorption, solubility, shrinkage and mechanical properties of "low-shrinkage" commercial resin composites. Dental materials. 2013;29:398-404.

[133] da Veiga AM, Cunha AC, Ferreira DM, da Silva Fidalgo TK, Chianca TK, Reis KR, et al. Longevity of direct and indirect resin composite restorations in permanent posterior teeth: A systematic review and meta-analysis. Journal of dentistry. 2016;54:1-12.

[134] Ribeiro BC, Boaventura JM, Brito-Goncalves J, Rastelli AN, Bagnato VS, Saad JR. Degree of conversion of nanofilled and microhybrid composite resins photo-activated by different generations of LEDs. Journal of applied oral science. 2012;20:212-7.

[135] Soderholm KJ, Mariotti A. BIS-GMA--based resins in dentistry: are they safe? Journal of the American Dental Association. 1999;130:201-9.

[136] Goncalves F, Kawano Y, Pfeifer C, Stansbury JW, Braga RR. Influence of BisGMA, TEGDMA, and BisEMA contents on viscosity, conversion, and flexural strength of experimental resins and composites. European journal of oral sciences. 2009;117:442-6.

[137] Nguyen JF, Migonney V, Ruse ND, Sadoun M. Resin composite blocks via high-pressure high-temperature polymerization. Dental materials. 2012;28:529-34.

[138] Phan AC, Tang ML, Nguyen JF, Ruse ND, Sadoun M. High-temperature high-pressure polymerized urethane dimethacrylate-mechanical properties and monomer release. Dental materials. 2014;30:350-6.

[139] Nguyen JF, Ruse D, Phan AC, Sadoun MJ. High-temperature-pressure Polymerized Resin-infiltrated Ceramic Networks. Journal of dental research. 2014;93:62-7.

[140] Dirxen C, Blunck U, Preissner S. Clinical performance of a new biomimetic double network material. Open dentistry journal. 2013;7:118-22.

[141] Guth JF, Edelhoff D, Ihloff H, Mast G. Complete mouth rehabilitation after transposition osteotomy based on intraoral scanning: an experimental approach. The Journal of prosthetic dentistry. 2014;112:89-93.

[142] Bilgin MS, Erdem A, Tanriver M. CAD/CAM Endocrown Fabrication from a Polymer-Infiltrated Ceramic Network Block for Primary Molar: A Case Report. The Journal of clinical pediatric dentistry. 2016;40:264-8.

[143] Fasbinder DJ, Dennison JB, Heys DR, Lampe K. The clinical performance of CAD/CAM-generated composite inlays. Journal of the American Dental Association. 2005;136:1714-23.

[144] Bayne SC. Dental restorations for oral rehabilitation - testing of laboratory properties versus clinical performance for clinical decision making. Journal of oral rehabilitation. 2007;34:921-32.

[145] Lynch CD, Opdam NJ, Hickel R, Brunton PA, Gurgan S, Kakaboura A, et al. Guidance on posterior resin composites: Academy of Operative Dentistry - European Section. Journal of dentistry. 2014;42:377-83.

[146] Opdam NJ, van de Sande FH, Bronkhorst E, Cenci MS, Bottenberg P, Pallesen U, et al. Longevity of posterior composite restorations: a systematic review and meta-analysis. Journal of dental research. 2014;93:943-9.

[147] Morimoto S, Rebello de Sampaio FB, Braga MM, Sesma N, Ozcan M. Survival Rate of Resin and Ceramic Inlays, Onlays, and Overlays: A Systematic Review and Meta-analysis. Journal of dental research. 2016;95:985-94.

[148] Grivas E, Roudsari RV, Satterthwaite JD. Composite inlays: a systematic review. The European journal of prosthodontics and restorative dentistry. 2014;22:117-24.

[149] Fron Chabouis H, Smail Faugeron V, Attal JP. Clinical efficacy of composite versus ceramic inlays and onlays: a systematic review. Dental materials. 2013;29:1209-18.

[150] Alonso V, Caserio M. A clinical study of direct composite full-coverage crowns: long-term results. Operative dentistry. 2012;37:432-41.

[151] Guth JF, Almeida ESJS, Ramberger M, Beuer F, Edelhoff D. Treatment concept with CAD/CAM-fabricated high-density polymer temporary restorations. Journal of esthetic and restorative dentistry. 2012;24:310-8.

[152] Edelhoff D, Beuer F, Schweiger J, Brix O, Stimmelmayr M, Guth JF. CAD/CAM-generated high-density polymer restorations for the pretreatment of complex cases: a case report. Quintessence international. 2012;43:457-67.

[153] Schlichting LH, Maia HP, Baratieri LN, Magne P. Novel-design ultra-thin CAD/CAM composite resin and ceramic occlusal veneers for the treatment of severe dental erosion. The Journal of prosthetic dentistry. 2011;105:217-26.

[154] Beier US, Kapferer I, Burtscher D, Dumfahrt H. Clinical performance of porcelain laminate veneers for up to 20 years. The International journal of prosthodontics. 2012;25:79-85.

[155] Morimoto S, Albanesi RB, Sesma N, Agra CM, Braga MM. Main Clinical Outcomes of Feldspathic Porcelain and Glass-Ceramic Laminate Veneers: A Systematic Review and Meta-Analysis of Survival and Complication Rates. The International journal of prosthodontics. 2016;29:38-49.

[156] Quinn GD. On edge chipping testing and some personal perspectives on the state of the art of mechanical testing. Dental materials. 2015;31:26-36.

[157] Ilie N, Hilton TJ, Heintze SD, Hickel R, Watts DC, Silikas N, et al. Academy of Dental Materials guidance-Resin composites: Part I-Mechanical properties. Dental materials. 2017;33:880-94.

[158] Wendler M, Belli R, Petschelt A, Mevec D, Harrer W, Lube T, et al. Chairside CAD/CAM materials. Part 2: Flexural strength testing. Dental materials. 2017;33:99-109.

[159] Alkadi L, Ruse ND. Fracture toughness of two lithium disilicate dental glass ceramics. The Journal of prosthetic dentistry. 2016.

[160] Ruse N. Fracture mechanics characterization of dental biomaterials. Dental biomaterials: Imaging, testing and modelling: Woodhead Pub., Cambridge, UK; 2008. p. 261-93.

[161] Belli R, Wendler M, Zorzin JI, Lohbauer U. Practical and theoretical considerations on the fracture toughness testing of dental restorative materials. Dental materials. 2018;34:97-119.

[162] Soderholm KJ. Review of the fracture toughness approach. Dental materials. 2010;26:e63-77.

[163] Tyas MJ. Correlation between fracture properties and clinical performance of composite resins in Class IV cavities. Australian dental journal. 1990;35:46-9.

[164] Bubsey R, Munz D, Pierce W, Shannon Jr J. Compliance calibration of the short rod chevron-notch specimen for fracture toughness testing of brittle materials. International Journal of Fracture. 1982;18:125-33.

[165] Akiike S, Nose H, Hirota Y, Tawada Y, Komatsu S. [Comparison of three testing methods of fracture toughness using indirect composite]. Nihon Hotetsu Shika Gakkai zasshi. 2008;52:49-58.

[166] Ruse ND, Troczynski T, MacEntee MI, Feduik D. Novel fracture toughness test using a notchless triangular prism (NTP) specimen. Journal of biomedical materials research. 1996;31:457-63.

[167] Scherrer SS, Denry IL, Wiskott HW. Comparison of three fracture toughness testing techniques using a dental glass and a dental ceramic. Dental materials. 1998;14:246-55.

[168] Glidewell Dental Laboratories. Obsidian® Ceramic Restorations - Product Information; 2017 [Cites Sept 17th, 2018]. Available from: https://glidewelldental.com/services/all-ceramics/obsidian-ceramic-restorations.

[169] Prismatik Dentalcraft Inc. Material Safety Data Sheet OBSIDIAN Milling Blocks; 2018 [Cited Sept 17th, 2018]. Available from: http://glidewelldental.com/wp-content/uploads/2016/02/msds-obsidian-milling-blocks.pdf.

[170] Thornton I, Ruse ND. Characterization of nanoceramic resin composite and lithium disilicate blocks. Journal of dental researsh 93 (Spec Iss). Available from: https:// iadr.confex.com/iadr/14iags/webprogram/Paper188234.html (IADR abstract)

[171] van Belle G. Statistical rules of thumb.Hoboken, NJ:Wiley; 2008.

[172] Quinn JB, Quinn GD. A practical and systematic review of Weibull statistics for reporting strengths of dental materials. Dental materials. 2010;26:135-47.

[173] Michalske TA, Freiman SW. A molecular mechanism for stress-corrosion in vitreous silica. Journal of the american ceramic society. 1983;66:284-8.

[174] Lee YK, Park HY, Shim JS, Kim KN, Lee KW. Effect of water content on the mechanical strength of dental porcelain. Journal of non-crystalline solids. 2004;349:200-4.

[175] Eldafrawy M, Ebroin MG, Gailly PA, Nguyen JF, Sadoun MJ, Mainjot AK. Bonding to CAD-CAM Composites: An Interfacial Fracture Toughness Approach. Journal of dental research. 2018;97:60-7.

[176] Goujat A, Abouelleil H, Colon P, Jeannin C, Pradelle N, Seux D, et al. Mechanical properties and internal fit of 4 CAD-CAM block materials. Journal of prosthetic dentistry. 2017.

[177] Swain MV, Coldea A, Bilkhair A, Guess PC. Interpenetrating network ceramic-resin composite dental restorative materials. Dental materials. 2016;32:34-42.

[178] Coldea A, Fischer J, Swain MV, Thiel N. Damage tolerance of indirect restorative materials (including PICN) after simulated bur adjustments. Dental materials. 2015;31:684-94.

[179] Sonmez N, Gultekin P, Turp V, Akgungor G, Sen D, Mijiritsky E. Evaluation of five CAD/CAM materials by microstructural characterization and mechanical tests: a comparative in vitro study. BMC oral health. 2018;18:5.

[180] Lim K, Yap AUJ, Agarwalla SV, Tan KBC, Rosa V. Reliability, failure probability, and strength of resin-based materials for CAD/CAM restorations. J Appl Oral Sci. 2016;24:447-52.

[181] Al-Amleh B, Lyons K, Swain M. Clinical trials in zirconia: a systematic review. Journal of oral rehabilitation. 2010;37:641-52.

[182] Okada R, Asakura M, Ando A, Kumano H, Ban S, Kawai T, et al. Fracture strength testing of crowns made of CAD/CAM composite resins. Journal of prosthodontic research. 2018;62:287-92.

[183] Palin WM, Fleming GJ, Marquis PM. The reliability of standardized flexure strength testing procedures for a light-activated resin-based composite. Dental materials. 2005;21:911-9.

[184] Della Bona A, Corazza PH, Zhang Y. Characterization of a polymer-infiltrated ceramic-network material. Dental materials. 2014;30:564-9.

[185] Ramos Nde C, Campos TM, Paz IS, Machado JP, Bottino MA, Cesar PF, et al. Microstructure characterization and SCG of newly engineered dental ceramics. Dental materials. 2016;32:870-8.

[186] Elsaka SE, Elnaghy AM. Mechanical properties of zirconia reinforced lithium silicate glass-ceramic. Dental materials. 2016;32:908-14.

[187] Quinn JB, Quinn GD, Sundar V. Fracture Toughness of Veneering Ceramics for Fused to Metal (PFM) and Zirconia Dental Restorative Materials. Journal of research of the National Institute of Standards and Technology. 2010;115:343-52.

[188] Kumar N. Inconsistency in the strength testing of dental resin-based composites among researchers. Pakistan journal of medical sciences. 2013;29:205-10.

[189] Front Matter. In: Campo EA, editor. Selection of Polymeric Materials. Norwich, NY: William Andrew Publishing; 2008. p. 41-101.

[190] Belli R, Wendler M, de Ligny D, Cicconi MR, Petschelt A, Peterlik H, et al. Chairside CAD/CAM materials. Part 1: Measurement of elastic constants and microstructural characterization. Dental materials. 2017;33:84-98.

[191] Cesar PF, Della Bona A, Scherrer SS, Tholey M, van Noort R, Vichi A, et al. ADM guidance-Ceramics: Fracture toughness testing and method selection. Dental materials. 2017;33:575-84.

[192] Behin P, Stoclet G, Ruse ND, Sadoun M. Dynamic mechanical analysis of high pressure polymerized urethane dimethacrylate. Dental materials. 2014;30:728-34.

[193] Feng X-Q, Mai Y-W, Qin Q-H. A micromechanical model for interpenetrating multiphase composites. Computational Materials Science. 2003;28:486-93.

[194] Egilmez F, Ergun G, Cekic-Nagas I, Vallittu PK, Lassila LVJ. Does artificial aging affect mechanical properties of CAD/CAM composite materials. Journal of prosthodontic research. 2017.

[195] Phan AC, Behin P, Stoclet G, Ruse ND, Nguyen JF, Sadoun M. Optimum pressure for the high-pressure polymerization of urethane dimethacrylate. Dent Mater. 2015;31:406-12.